UNIVERSITI PUTRA MALAYSIA

FINITE ELEMENT ANALYSIS ON SLANTED COLUMN UNDER STATIC LOAD

NURWAJIHAH BINTI LAILI

FINITE ELEMENT ANALYSIS ON SLANTED COLUMN UNDER STATIC LOAD

By

NURWAJIHAH BINTI LAILI

174336

Thesis Submitted to the Department of Civil Engineering

University Putra Malaysia, in Fulfilment of the Requirement for the

Degree in Civil Engineering

JUNE 2017

ABSTRACT

This study presents a finite element analysis of slanted column under various angle of 0°, 3°, 5°, 7°, 9° and 15° with 3m length in height. The buckling behaviour of slanted column subjected to maximum principle of bending stress, bending strain and displacement was studied. The critical load or maximum load of slanted column under static load also was studied. The main objective is to investigate the buckling behaviour of slanted column using a complete linear analysis of 3 dimensional finite element analysis under static load. The material of slanted column used in this study is steel with dimensions of I-417x455x30x50. A total of 6 models were analysed using finite element simulations and verification test has been perform to check the reliability and accuracy of simulation results. The finite element package ABAQUS software has been used to perform linear analysis in order to investigate the buckling behaviour in terms of bending stress, bending strain and also displacement under static load. The results show the critical load is increases as the angle of slanted column increases. The column effective length is also changed as the length of slanted column changed due to the changing of angle of slanted column. It has significant influence that the finite element models were able to simulate the behaviour of slanted column under static load.

ABSTRAK

Kajian ini membentangkan analisis unsur terhingga tiang condong di bawah pelbagai sudut iaitu 0°, 3°, 5°, 7°, 9° dan 15° dengan 3m panjang tinggi. Kelakuan lengkokan tiang condong tertakluk kepada prinsip maksimum lentur tekanan, ketegangan dan anjakan lenturan telah dikaji. Beban kritikal atau beban maksimum tiang condong di bawah beban statik juga dikaji. Objektif utama adalah untuk menyiasat tingkah laku lengkokan tiang condong menggunakan analisis linear lengkap 3 dimensi analisis unsur terhingga di bawah beban statik. Bahan tiang condong digunakan dalam kajian ini adalah keluli. Sebanyak 6 model dianalisis dengan menggunakan simulasi unsur terhingga dan ujian pengesahan telah dilaksanakan untuk memeriksa kebolehpercayaan dan ketepatan keputusan simulasi. Pakej perisian unsur terhingga Abaqus telah digunakan untuk melaksanakan analisis linear untuk menyiasat tingkah laku lengkokan dari segi lenturan tekanan, membongkok ketegangan dan juga anjakan di bawah beban statik. Keputusan menunjukkan beban kritikal semakin bertambah apabila sudut kenaikan lajur condong bertambah juga. Lajur panjang berkesan berubah jika panjang turus condong berubah disebabkan oleh perubahan sudut tiang condong. Ia mempunyai pengaruh penting bahawa model unsur terhingga dapat mensimulasikan kelakuan tiang condong di bawah beban statik.

ACKNOWLEDGEMENT

First of all, all praise and gratitude to the Almighty blessed by divine safely to finally completed this thesis successfully. Many thanks to my supervisor, Dr Izian bt Abd Karim for her guidance and advices throughout this long journey. I sincerely appreciate everything together with her huge amount of patience towards me, was indeed a shining guide throughout the preparation of the thesis.

My appreciation also goes to the both of my examiners, Dr Nor Azizi bt Safiee and Dr Farzad Hejazi for their time listening to my presentation and also contributing their ideas, comments and also given their personal suggestion to make the thesis more clear and understandable.

Not forgetting is my family members who had been extremely supportive of me throughout the period in conducting this research and write the thesis. This thesis is dedicated to them especially for my late father. Finally, I would like to express my special appreciation to all my friends that have helped me to the completion of this thesis in any way. Thank you.

TABLE OF CONTENTS

LIST OF FIGURES

LIST OF TABLES

CHAPTER 1

INTRODUCTION

1.1 INTRODUCTION

Nowadays, it is a new trend of architecture and structural engineering that many tall buildings worldwide have a complex shape such as twisted, tapered and tilted. Those buildings are judged as landmarks of a nation and symbols of technological achievement in a country. The complex-shaped tall building disassembles the orthogonality between beams and columns. In addition, such type of structural system can be found frequently in buildings having slanted columns. The new idea mentioned is that columns are no longer vertical. It can be slanted by the standard angle of 0° to 9°. The slanted columns can transmit the gravity and lateral load simultaneously and are necessary to display the architectural complexity. The studies about slanted columns have not been carried as much as those for the normal column,

so it is worth examining the performance or analysis of slanted column by using rigorous computational analysis and experiments.

In a general, slanted column which also known as 'inclined' column is used in many construction works due to theory of art and also architectural requirements. The design, loads and bending moment in slanted columns are discussed. Slanted columns are originated from the category of structural framing member's gravity load loaded columns and can be applied to both rigid as well as braced frames. Figure 1.1 shows the load deflection due to inclined column. There are some of the examples of slanted column constructions which are rafter & struts of an RCC truss, gable beams of a sloped roof, and the top chord of an RCC Virendeel Girder. The top chord (beam) of a Virendeel girder which is a horizontal member is designed as a column and not as a beam as compression is dominant in it.

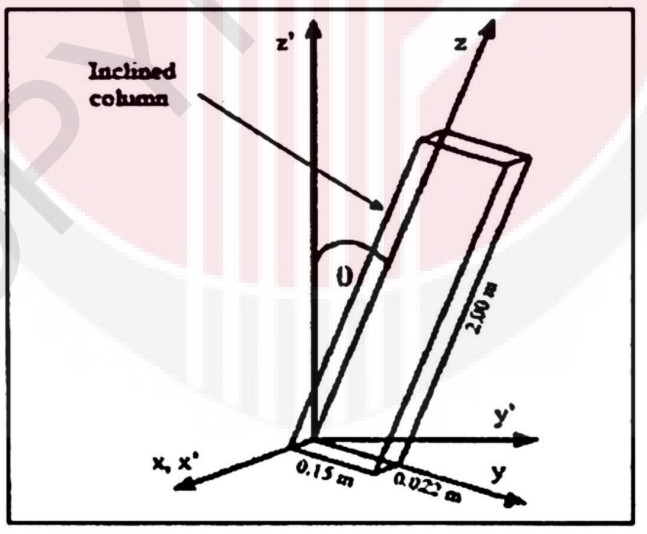

Figure 1.1 A slanted column - Load deflection

A slanted column that possesses a cross-section without symmetry may be subjected to torsional buckling or lateral buckling. Torsional buckling is a sudden twisting of

the column. As the theories say the existence of eccentric loading would decrease in column strength referred to Figure 1.2. The term eccentrically loaded is defined as the situation when the axial load on the column is not concentric or in other words if the line of action of the axial load is not parallel to the central axis of the column. The eccentricity mainly represented by the symbol of 'e', of the load subjects to bending of the column immediately. Hence the combined action of axial and bending would result in reduced load carrying ability.

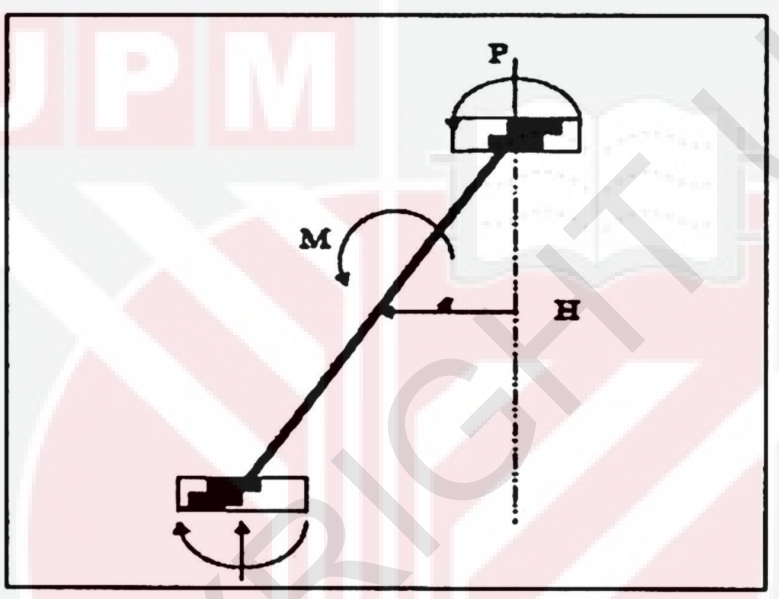

Figure 1.2 Slanted Column Subjected to Eccentric Axial Load

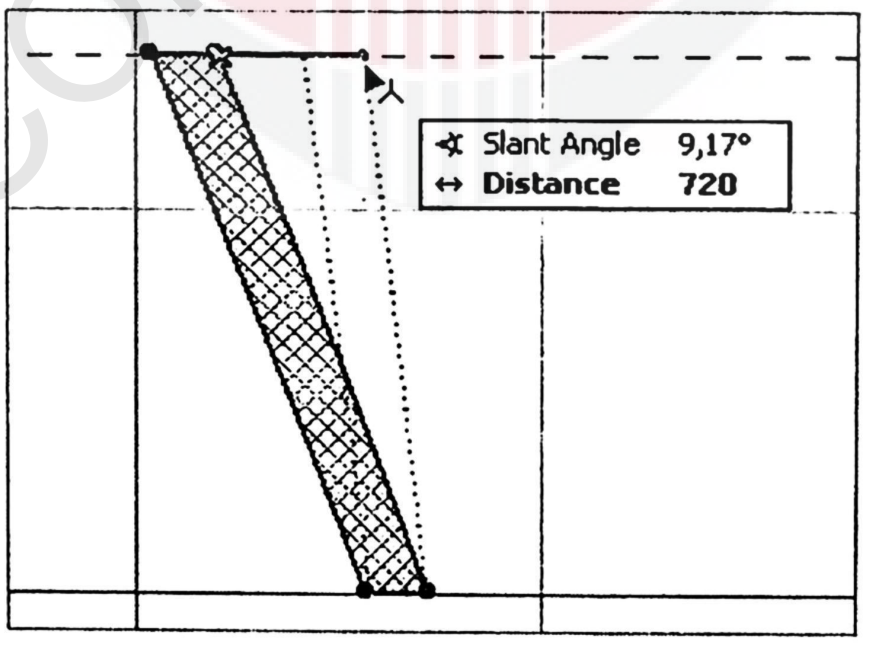

Figure 1.3 Slanted column structure

The design in most of the cases is carried out for axial force and moments by the usual method. In a condition where shear is found predominant (this is the case when the member is inclined appreciably), shear reinforcement should be designed and their provision is made. To solve the fracture potential and local buckling that occur on the slanted column, the predominant approach is use a nonlinear finite element analysis to satisfy with the theoretical analysis using Euler's theory by developing the existing equation of normal column in order to identify the critical load value.

This will show the critical time where the column cannot resist the applied load which is maximum level of load and starts to buckle as well. Usually, the compression members are succeptible to buckling. Figure 1.3 show the picture of slanted column. Buckling is loss of stability where the axial loads caused lateral deformations as the load applied increases slowly and start to buckle as well. Axial forces that causing buckling is called critical load and is associated to the column length. The critical load is depends on the length of column, type of material used and section properties of column itself.

1.2 PROBLEM STATEMENT

There was lack of knowledge research on the finite element modelling and analysis on slanted column under static and dynamic load due to its complexity. Hence, more investigations need to be conducted as to gain more information about the performance of slanted column in a construction area. In this case study, a model structure been modified to have slanted columns at beam-column connection. The

model will be given an axial load on compression to get the critical load which make the slanted column to deform or buckle. The type of model structure chosen is in I-shape and steel material properties. In addition, the Euler's equation been used to satisfy the k factor and determine the critical load that affecting slanted column. Thus, the finite element analysis (FEA) should be conducted in order to identify the behaviour of slanted column more precisely.

1.3 OBJECTIVES

There are three main objectives for this research project: -

1. To identify the critical load, P_{cr} on slanted column of different angle which boundary condition is pinned-fixed condition.
2. To determine the buckling shape of slanted column in terms of deflection, stress-strain relationship and bending moment reaction under static load.
3. To study the relationship between theoretical value k with angle of slanted column using Euler's Formula.

1.4 SCOPE OF WORK AND LIMITATION

In order to achieve the objective of this study, the research implementation begins with finding all the information and references that related to the proposed study. Even though the information regarding to the existing analysis of slanted column is

not much but some of the references are seem to be similar with the proposed study been collected and reviewed. The sources of information are obtained from the journals, papers and also internet.

A literature review on :

1. Buckling of slanted column under static load only.
2. The existing analysis of slanted column or inclined beam in different parametric study.
3. Finite element analysis of structural component.
4. Mathematical solution to calculate buckling of slanted column in different approach using Euler's Formula
5. Linear and nonlinear analysis using finite element analysis

Analysis is done through substructure model of slanted column adapted from beam-column connection with different angle. The properties of substructure model are steel material with the shape of I and the unit will be used as Pascal or kiloNewton per metre square in both elements. The setup of the boundary and loading conditions is fixed as fixed-pinned end condition in order to not allow any rotation and translation at each end condition. Simulation and analytical studies are done by using ABAQUS which this finite element software is capable of modelling, analysing 2-D dimensional column with interactive graphical outputs. The results might be useful to develop the performance of slanted column due to strain and local buckling and fulfil the criteria for design process. The nonlinear analysis is focus on the critical

load applied to the slanted column varies with time and the analysis data is presented by using graph.

1.5 REPORT OUTLINE

In this project, there are five chapters included; the first chapter is the introduction with problem statement, objectives and scope of work. Meanwhile, the second chapter is literature review which focus on discussion regarding the behaviour of slanted column and calculation related to the slanted column. The third chapter is methodology which describes the derivation of Euler's equation for critical load, the software used, the application of material linear and nonlinear analysis on ABAQUS and some theoretical issues. After that, chapter four is the complete analysis and results present in tabulated and graphical data with the discussions based on the result obtained. Lastly, chapter five is the summary and conclusion of the entire project, discussion of the results briefly and analysis of the findings obtained.

CHAPTER 2

LITERATURE REVIEW

2.1 INTRODUCTION

The Finite Element Analysis (FEA) is a numerical method to obtain approximate solutions for solving problems of engineering and mathematical physics. This method subdivides a structure or a body into smaller elements of finite dimensions that called as finite elements. This analysis useful in solving the complicated geometries, loadings and material properties where complicated analytical solutions. Besides that, the simple equations are developed for these finite elements which then assembled into a larger system of equations that models the entire problem. In order to predict the performance and behaviour of the design where to identify the safety factor, strength and weakness of the design accurately. A typical finite element analysis begins by the studying the nature of the problem and creating a domain for the

problem after which the domain is discretised into elements of a regular geometry. These elements are connected at a finite number of joints called "Nodes" or "Nodal points". Finite element method is a matrix oriented method which combining theory of elasticity, theory of plasticity and numerical techniques. Some of the advantages of the FEM are model complex is shaped bodies easily, able to handle several load conditions without difficulty, able to handle different kind of boundary conditions and model bodies composed of several different materials.

2.2 SLANTED COLUMN UNDER STATIC LOAD

The slanted column possesses the following two unique features which are the top end is only deformable in vertical direction and the buckling strength is affected by the angle change from α to α' due to the deformation. In the present study, by using the derivation method incorporated with Euler's equation to account for the constraint condition a set of nonlinear equations is derived. The exact solutions for the linear and nonlinear analysis are obtained for inclined columns with various end conditions. The buckling behaviours of an inclined column with various type of restraint condition which are two ends simply supported, fixed-pinned simply supported and fixed-roller simply supported are determined in detailed which include an axial to lateral bending configurations. In this study, we have two types of loading which are static load and dynamic load. For static load, we only apply the load in vertical direction on slanted column and investigate the buckling effect to the slanted column. The value of critical load to apply on slanted column is going to be compared between the literature values and analytical from the software. Meanwhile, the fracture and

strength degradation of the slanted column were studied to obtain sufficient information of the column behaviour over the time period in years. If a static load test appears to be the best option, load cases can be developed to simulate critical conditions. During the static load test, data can be continuously recorded with data "snapshots" taken at prescribed loading increments (Dayton, 2016). Dimensional inspections can be conducted to quantify any permanent deflections or set either pre-static loading and/or post-static loading (Dayton, 2016).

Static Load Tests can be performed to validate foundation design assumptions regarding the axial compression or axial tension resistance provided by a deep foundation element, or its deflected shape under a lateral load. The most important records needed in column testing are the applied load and the corresponding lateral displacements about the minor and major axes, strains at characteristic points, end rotations, angles of twist, and over-all shortening (Negussie Tebedge, 2002). The applied loads and measured strains during a static load test provide a stress-strain relationship for the deep foundation element from which a strain-dependent composite-section secant modulus can be determined. (Fellenius, 2016). Three of the phases, the study of full-scale beam-columns laterally loaded in a principal direction, the model frame study, and the study of obliquely loaded full-scale beam-columns, are concerned with the investigation of static resistance. (Howland, Egger, Mayerjak, & Munz, 2009). The effect of the axial load is readily predicted by the elementary theory if the influence of strain hardening is included and if failure by lateral deflection and twisting does not occur (Howland, Egger, Mayerjak, & Munz, 2009).

2.3 BUCKLING OF SLANTED COLUMN

A deformation is termed "elastic" if, upon removal of all external forces, the undeformed reference shape restores itself completely. The basic assumption underlying the constitutive laws of classical elasticity theory is that the restoring force (stress) in a body is a single-valued function of the deformation (strain) of the body and, moreover, that it is independent of the history of the deformation (Demetri Terzopoulos). A slanted column may represent an inclined member of a truss, a frame, or a meridional element of an asymmetrically deformable conical shell with rigid edges (Chang, 1974). Such a structure has a unique constraint condition. A set of nonlinear equations for buckling of elastic slanted columns is derived by the variation method in corporation with the Lagrange multiplier to deal with the constraint condition (Atay, 2011). The bifurcation of such columns with simply supported ends is considered along with results obtained from conventional methods. No bifurcation will occur for columns with other end conditions. A set of formulas derived from the linearized eigenvalue method is also presented. The results obtained from the latter are slightly higher than those obtained from the nonlinear theory. The buckling loads may lower further if the change of the inclined angle at the loaded end is taken into consideration during the deformations. In addition, the critical buckling load increase with an increasing initial angle, so does the critical displacement (Jian Zhao, 2008).

Previous study state that the behaviours of an inclined columns with two ends simply supported can be examined in details including the bifurcation from an axial to lateral

bending configurations. They also come out with the exact solutions for the non-linear equation for slanted column with various end condition by using the variation method incorporated with Lagrange's multiplier. The solutions involved are by Eigenvalue method, effect of angle change and comparison with conventional approach.

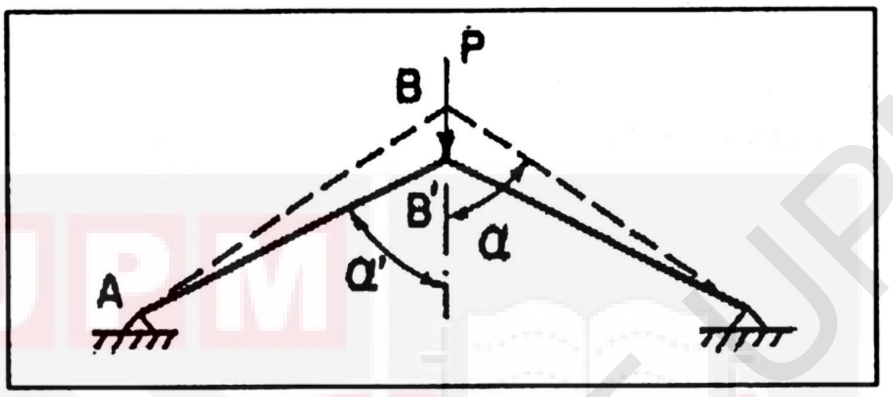

Figure 2.1 Misses Truss *(Chang, 1974)*

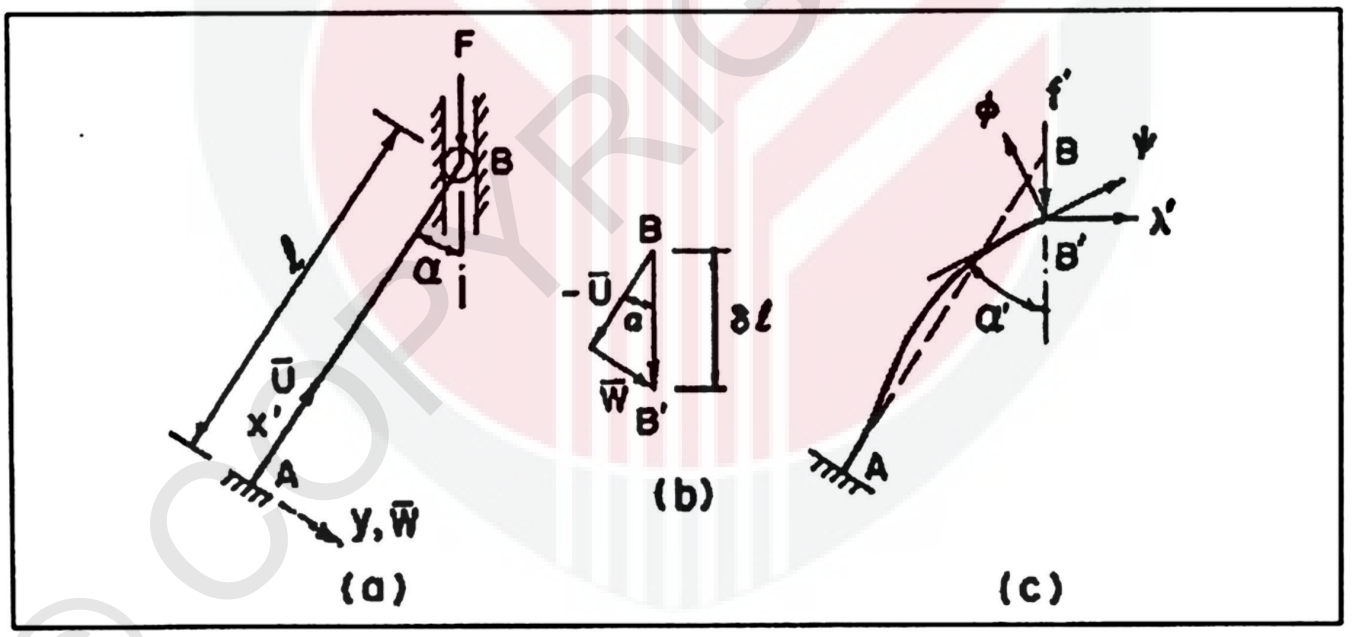

Figure 2.2 Inclined Bar *(Chang, 1974)*

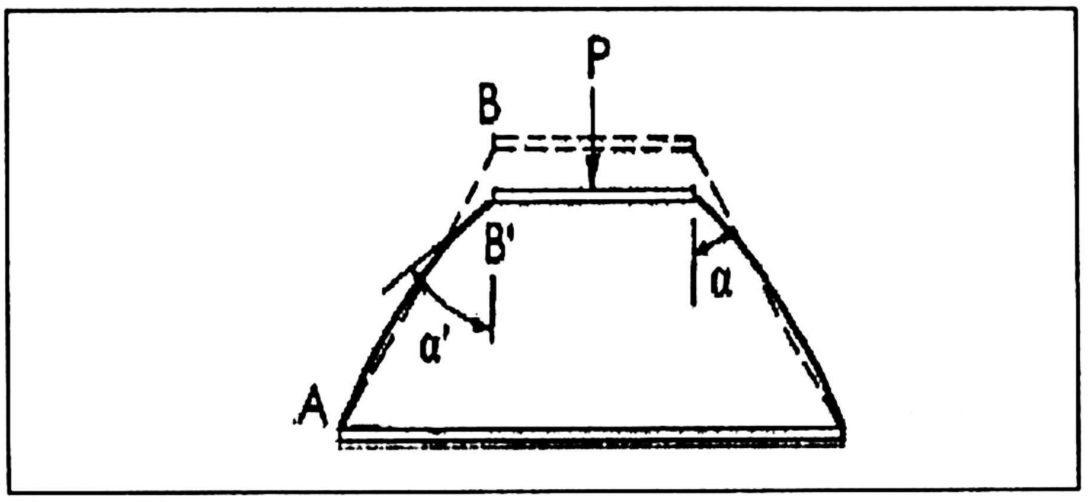

Figure 2.3 Conical frustum *(Chang, 1974)*

In the present study, the effects of both bending and normal thrust are taken into consideration. The simply supported ends are generalized to include other possible end conditions. Thus, in general, this model represents a frame rather than a truss. The frame is subjected to the vertical force, *P*, at the central joint as shown in Figure 2.1. Because of symmetry, the structure may be analyzed by an inclined column as shown in Figure 2.2. This column may also represent the inclined member of a three-bar frame with a rigid horizontal bar subjected to a single force at the center. This three-bar frame may simulate a meridional element of a conical frustum with rigid bulkheads undergoing axisymmetric deformation as shown in Figure 2.3. According to (Lin-Hai Han, 2010), they state that the strength decreased significantly with the increasing of the tapered angle.

This comprehensive study presents the exact solutions of a class of large deflection problems. The buckling loads determined from these solutions are lower than those obtained by the eigenvalue method. Nevertheless, provides the simple equation for the eigenvalue, which in turn yields the buckling value for a given column. In fact,

the eigenvalues are practically applicable for columns with small angle α and large slenderness ratio R. In addition, the larger angle, the differences get bigger, and if the effect of angle change is taken into consideration, the story will be quite different for both ends simply supported inclined columns.. The non-linear buckling loads of shallow arches are much lower than the linear bifurcation buckling loads due to the effect of the pre buckling deformations. (Yong-Lin Pi, 2006)

2.4 FINITE ELEMENT ANALYSIS OF SLANTED COLUMN OR INCLINED BEAM

The finite element method (FEM) is a numerical method for solving problems of engineering and mathematical physics. It is also referred to as finite element analysis (FEA) ABAQUS is used to enable the incorporation of extended finite element capabilities (E. Giner a, 2008). The evaluation of inclined column based on the performance of fully restrained welded connections is carried out by Yong, Jin (2012). The studies on the inclined column and beam connection that appears frequently in the complex-shaped structures are not sufficient in comparison to those on the conventional structures so that the structural safety and the behavior are not clear yet. In this study, the fracture potential and local buckling which can occur around the connection are examined and the results will be applied to investigate the connection capacity.

According to (Yong-Wan Kim, 2012), there exists a tensile or compressive stress in the beam connected to the inclined column exists increasing with respect to the

inclined angle. The axial force that distributed horizantally from the inclined column affects the stress and strain distribution in the beam directly which cause the resisting capacity of beam against the flexural deformation changes. Although the amplified amount of force was applied to the model, which means that the inclined angle of column is unrealistic, the results of this study proved that the horizontal distribution of the axial force in the inclined column affects the potential of fracture at the connection by causing early yielding, and that it also delays or facilitates flange local buckling. Therefore, it is possible to conclude that the extra check for the inelastic behavior, local failure and buckling shall be considered when the inclined column-beam connection is designed (A.M Tarbia, 2014).

Since this study deals only with the strain distribution and local buckling of beam flanges, it is still necessary to check fatigue at the connection, because they are also crucial for the seismic performance of structural members, and sensitive to the amount of axial stress around the welded connection joint. Furthermore, a full scale experiment shall be performed to prove the prediction of behavior from finite element analysis. A crucial step in any implementation of the X-FEM is the definition of the nodes to be enriched as a result of the crack and mesh geometries. (E. Giner a, 2008). The FE model is also applied to analyze the effect of moment gradient on distortional buckling. It is found that the distortional buckling strength of beams is increased due to the presence of moment gradient (Cheng Yua, 2006). The boundary conditions applied vary widely, generally producing excessive femoral deformation, and although it has been shown that the muscle forces influence femoral deflections and

loading, little consideration has been given to the displacement constraints (Speirs, 2006). The locations for the maximum deflections are obviously dependent upon the boundary conditions; while the maximum deflection obviously occurs at the center of the simply supported plate, its locations will not be so clear for other boundary conditions. (Henry Khov, 2009).

2.5 BUCKLING OF SLANTED COLUMN USING EULER'S THEORY

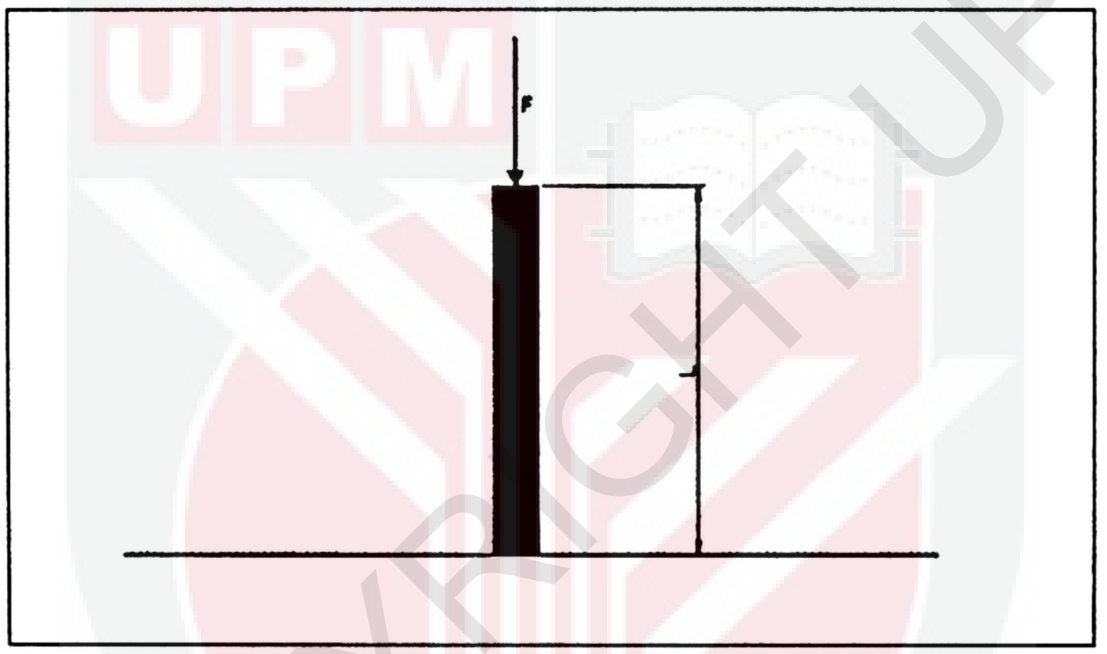

Figure 2.4 Long column with load applied *(Apostol, 1973)*

Columns fail by buckling when it reach their critical load. Long column can be analysed using Euler's Formula.

$$P = \frac{\pi^2 EI}{(kL)^2}$$

The 'L' in this equation symbolizes length and 'P' symbolizes the allowable load before buckle. As the length increases, the allowable load decreases. With shorter

columns compared to its thickness, one can infer from the same equation above that the allowable stress on a column before buckling increases as length decreases. The type of end connections for the column is another important factor in determining buckling stress.

From pinned-pinned to fixed-fixed to fixed-pinned connection, they are each represented in the Euler equation with different values of 'k' The fixed-fixed connection increases the allowable stress before buckling more than any of the other end connections. In construction, it occurs differently for different materials.

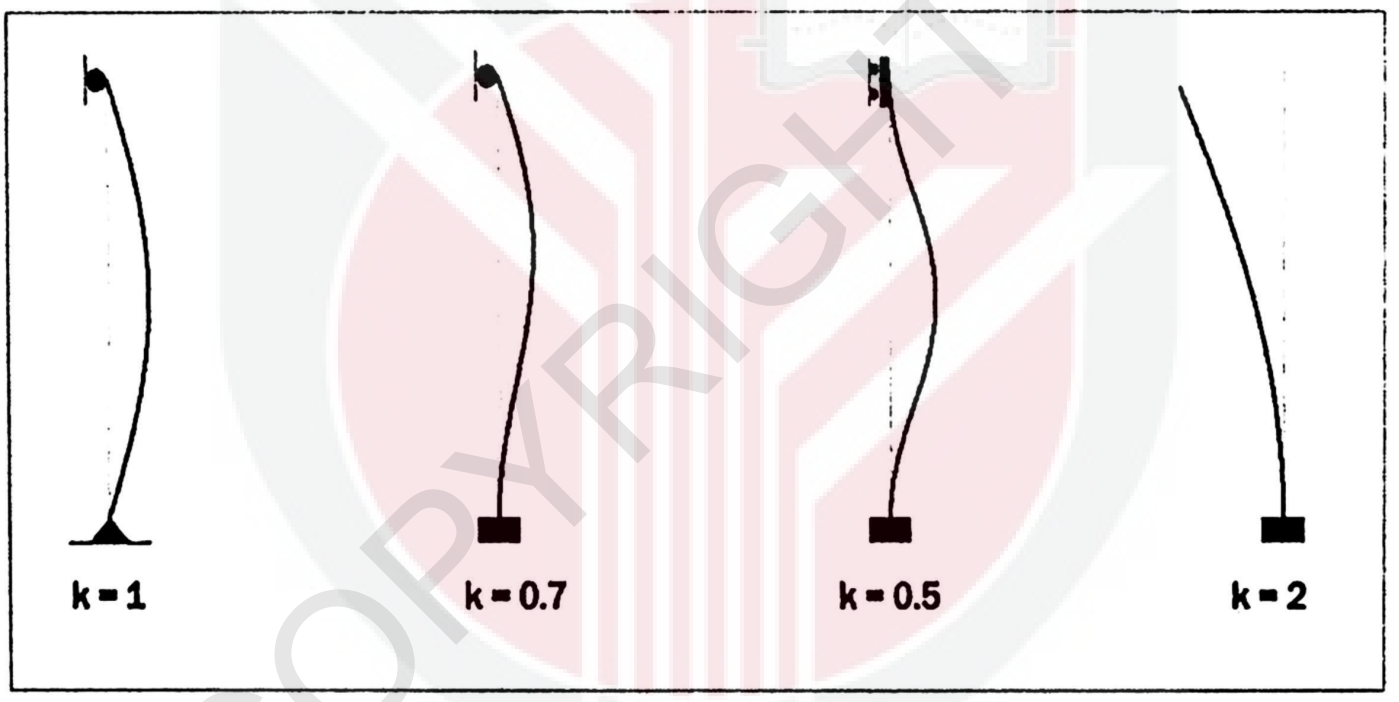

Figure 2.5 The effective length factors

This factor of material is captured in the Euler's equation with 'E" and 'I,' different material properties. In steel columns, this occurs elastically. This differs for reinforced concrete.

CHAPTER 3

METHODOLOGY

3.1. INTRODUCTION

In this chapter, it shows that the study of slanted column can be termed as inclined beam-column theory which incorporating the inclination of long column. The basic theory of mathematical and analytical methods is presented and detailed description of slanted steel column modelled is explained. The mathematical solution has been carried out by developing the equation of Euler's method in order to determine the critical load will be applied on slanted column. After that, the comparison is made based on the of theoretical value of critical load which cause buckling to the slanted column. The analysis is conducted to predict the buckling effect on slanted column by using the finite element software which is ABAQUS software. Nonlinear analysis

is to study the performance of the slanted column in 5 years onwards. The data represented in form of graph.

3.2 PRELIMINARIES STUDY ON THEORETICAL APPROACHES

First of all, the new equation of critical load, Pcr has been developed which satisfy the slanted column condition using Euler's equation.

Basically, general equation is :-

$$\frac{d^2y}{dz^2} + \frac{P}{EI}y = 0$$

Where, $y = Asin(kz) + Bcos(kz)$,

$$and \quad k^2 = \frac{P}{EI} \quad \rightarrow \quad k = \sqrt{\frac{P}{EI}}$$

By applying boundry conditions, where z = 0 and y = 0, then B = 0. After that, subtitute the value of z = L, B = 0, then y = A sin (kL).

Assuming no deflection occurs, then A=0,

$$kL = n\pi \quad \rightarrow \quad \sqrt{\frac{P}{EI}}L = n\pi$$

$$\therefore P_{cr} = \frac{\pi^2 EI}{L^2}$$

Therefore, the new equation been developed as to determine the critical load for slanted column by the general Euler's equation. The cases to be focus on is when then column has pinned-fixed boundary condition.

3.2.1 Pinned-pinned boundary condition

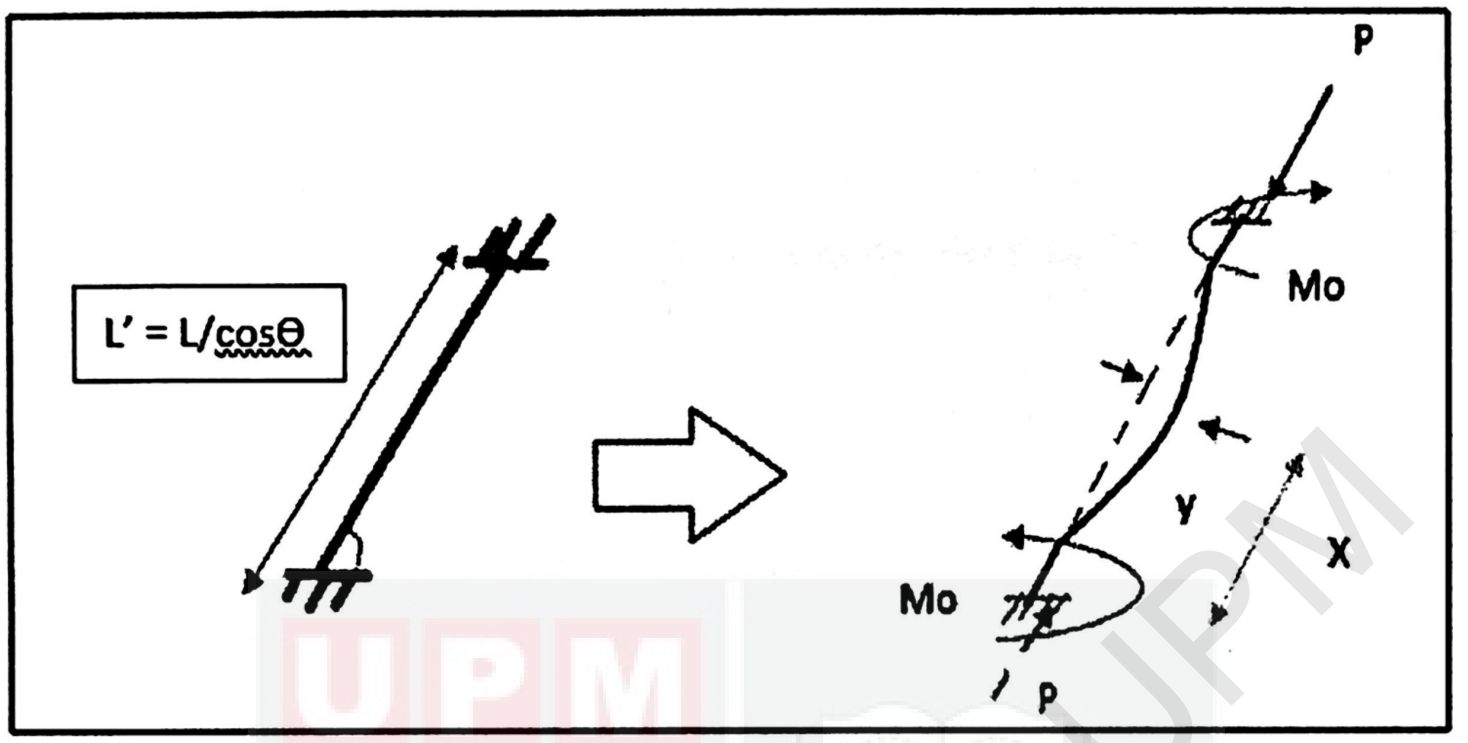

Figure 3.1 Structure with fixed end support condition

By taking Moment due to P at X ;

$$M = M_o - Py$$

$$EI\frac{d^2y}{dx^2} = M_o - Py$$

$$\frac{d^2y}{dx^2} = \frac{M_o}{EI} - \frac{Py}{EI}$$

$$\text{Let, } \frac{P}{EI} = k^2$$

$$\frac{d^2y}{dx^2} + k^2y = \frac{M_o}{EI}k^2$$

$$\text{From } y = CF + PI,$$

$$CF = A\cos(kx) + B\sin(kx) \quad , \quad PI = \frac{M}{P}$$

$$y = A\cos(kx) + B\sin(kx) + \frac{M_o}{P}$$

If x = 0, y = 0 ; ~~$A \rightarrow$~~ $-\frac{M_o}{P}$.

Differentiate, $y = A\cos(kx) + B\sin(kx) + \frac{M_o}{P}$

$$\frac{dy}{dx} = -Ak\sin(kx) + Bk\cos(kx)$$

If x = 0, dy/dx = 0 ; ~~$Bk \rightarrow$~~ 0

$$\therefore y = \frac{-M_o}{P}\cos(kx) + \frac{M_o}{P}$$

$$= \frac{M_o}{P}(1 - \cos(kx))$$

When x = L, y = 0 ; which L = L/cosθ

$$0 = \frac{M_o}{P}(1 - \cos(kL))$$

$$\cos(kL) = 2n\pi$$

$$kL = 2\pi\,, \quad k = \sqrt{\frac{P}{EI}}$$

$$\sqrt{\frac{P}{EI}}(L) = 2\pi$$

$$\frac{P}{EI} = \frac{2^2\pi^2}{L^2}$$

$$P_{cr} = \frac{4\pi^2 EI}{(L')^2} \;, sub\; L' = \frac{L}{\cos\theta}$$

$$\therefore P_{cr} = \frac{4(\cos\theta)^2\pi^2 EI}{(L)^2}$$

3.2.2 Both Pinned end

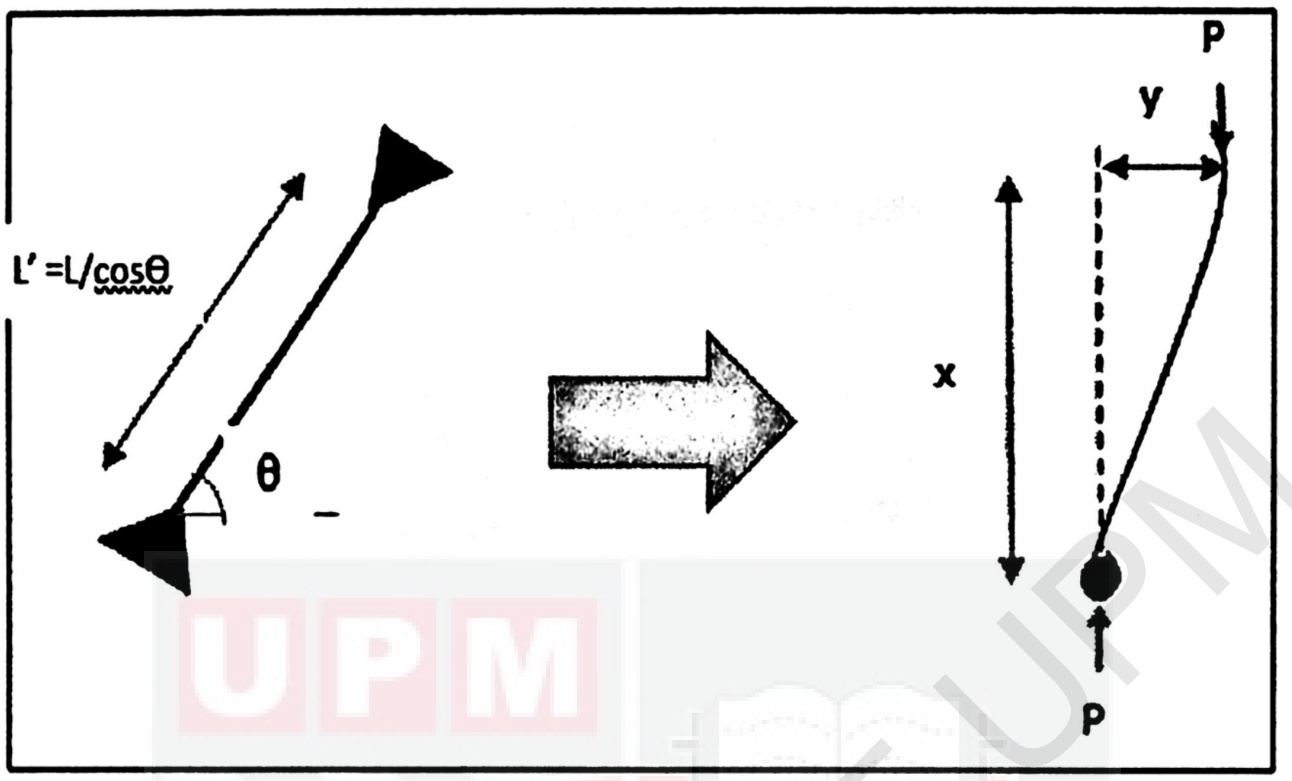

Figure 3.2 Structure with pinned end support condition

By taking Moment due to P at X ;

$$M = -Py$$

$$EI\frac{d^2y}{dx^2} = -Py$$

$$\frac{d^2y}{dx^2} + \frac{Py}{EI} = 0$$

If, $\frac{P}{EI} = k^2$; $\frac{d^2y}{dx^2} + k^2EI = 0$

CF = Acos(kx) + Bsin(kx)

FI = 0

Then, y = A cos(kx) + B sin(kx)

When x = 0, y = 0; ~~A = 0~~

If x = L, L = L/cosθ, and y = 0 ;

$$0 = B \sin (kL)$$

$$\text{Sin } (kl) = 0$$

$$kl = n\pi \quad , k = \sqrt{\frac{P}{EI}}$$

$$\sqrt{\frac{P}{EI}}(L) = \pi \qquad since\ L' = L/cos\theta$$

$$\therefore P_{cr} = \frac{\pi^2 EI}{(L')^2} \quad \rightarrow \quad P_{cr} = \frac{(cos\theta)^2 \pi^2 EI}{(L)^2}$$

3.2.3 Fixed-pinned End condition

Euler buckling theory,

$$EIy'' = M = -Py$$

$$EIy'' + Py = 0$$

$$y = Asin\left(\sqrt{\frac{P}{EI}}\right)x + Bcos\left(\sqrt{\frac{P}{EI}}\right)x$$

A and B are constants, determined from the boundary conditions,

The boundary conditions are y=0 at x=0, and gives x=L,

The first boundary conditions are y=0 at x=0, and x=L. The first boundary condition leads the conclusion that B=0, so

$$y = Asin\left(\sqrt{\frac{P}{EI}}\right)x$$

Then, insert the second boundary condition, where x=L, thus

$$y(L) = 0 = Asin\left(\sqrt{\frac{P}{EI}}\right)L$$

$$\sin(\pi) = 0 \; then, \sqrt{\frac{P}{EI}}L = \pi$$

$$solve\ P \quad \therefore P_{cr} = \frac{\pi^2 EI}{L^2}$$

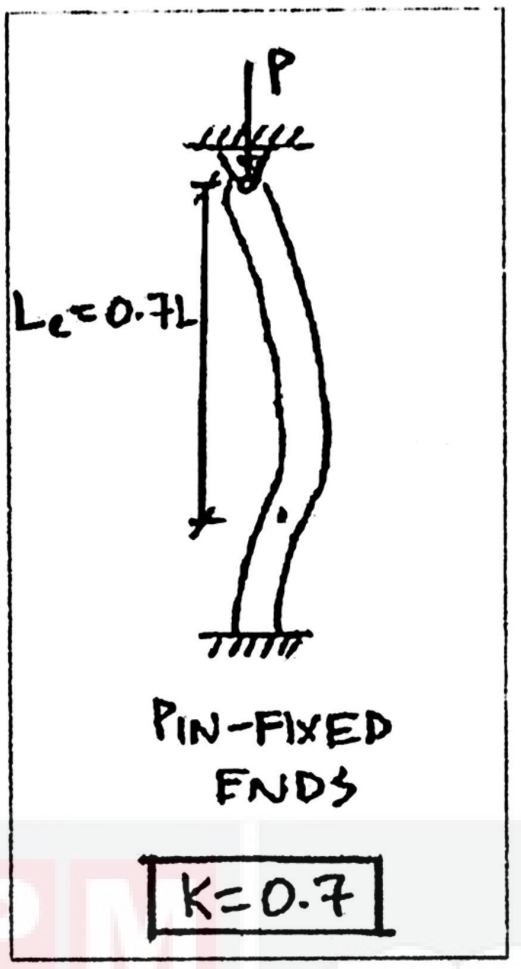

Figure 3.3 k factor due to pinned-fixed condition

It gives new equation for critical load,

$$P_{cr} = \frac{\pi^2 EI}{(KL)^2} = \frac{\pi^2 EI}{(0.7L)^2} = \frac{\pi^2 EI}{(\frac{L}{\sqrt{2}})^2} = \frac{2\pi^2 EI}{L^2}$$

Due to slanted column, existence of angle is taken into account, new k is determined.

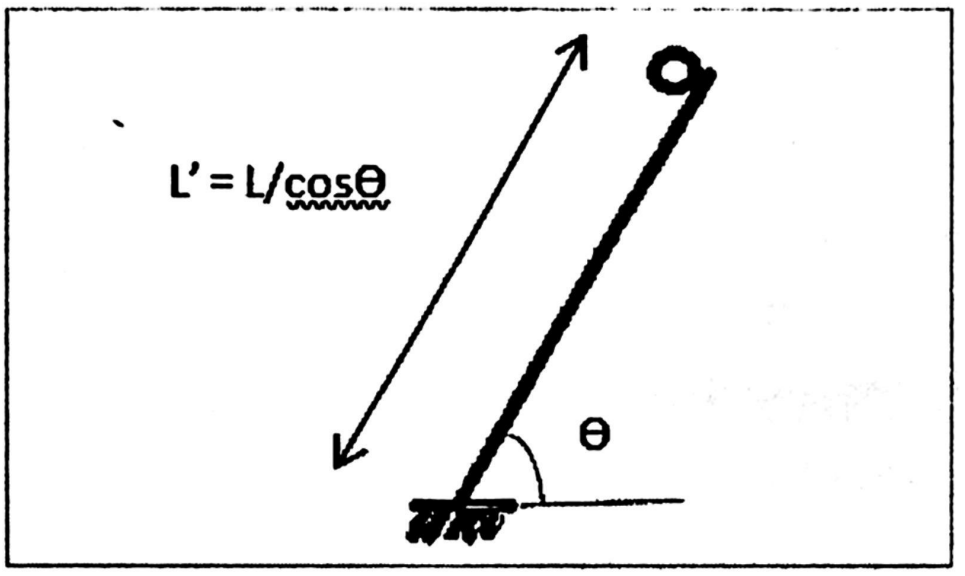

Figure 3.4 Structure with pnned-fixed end condition

By substitute new L into critical equation,

$$Pcr = \frac{2\pi^2 EI}{L^2} = \frac{2\pi^2 EI}{\left(\frac{L}{cos\theta}\right)^2}$$

$$= \frac{2(cos\theta)^2 \pi^2 EI}{L^2}$$

$$\therefore k_{new} = \frac{0.7}{cos\theta}$$

3.2.4 Case Study

In this study, the model structure is designed as the slanted column placed at the lower column and connect with tie connection only. For the Finite Element Analysis, slanted column substructure with different angle are developed so that different inclined angles of column could be compared to the normal slanted column. The substructure will be analysed for various angles of the slanted columns which are 3°, 5°, 7°, 9° and 15° from vertical respectively. The analysis done in 2-Dimensional by using ABAQUS modelling software.

The proposed model building that will evaluate in this study as shown in Figure 3.5 below.

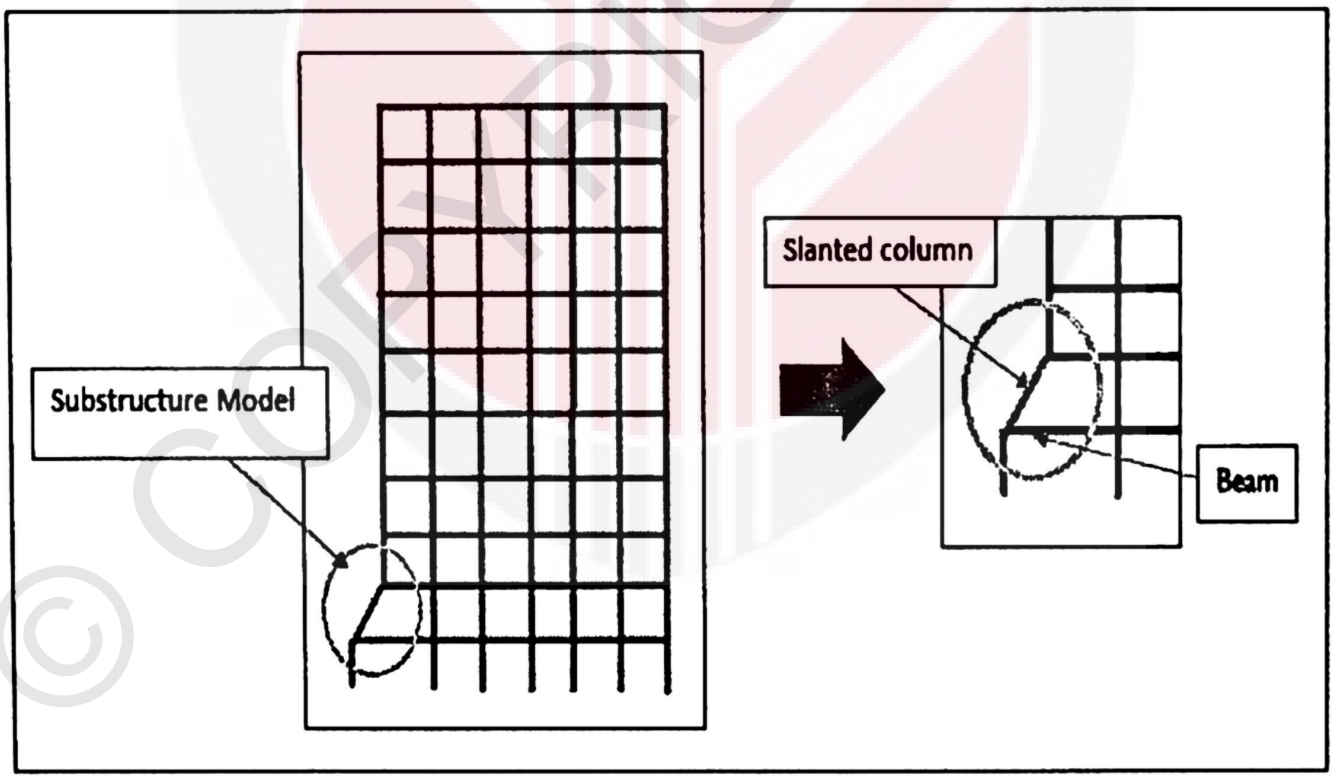

Figure 3.5 Model Building Frame

3.3 ABAQUS FINITE ELEMENT SOFTWARE

Abaqus is a software suite for Finite Element Analysis (FEA) developed by Dassault Systèmes. The Abaqus Unified FEA product suite is part of the SIMULIA brand and offers powerful and complete solutions for both routine and sophisticated engineering problems covering a vast spectrum of industrial applications.

The Abaqus product suite consists of four core software products:-

- Abaqus/CAE - Known as 'Complete Abaqus Environment'. This is the interactive GUI for analysis pre- and post-processing.
- Abaqus/Standard – A solution package that utilises implicit integration schemes, ideal for static and low-speed dynamic events.
- Abaqus/Explicit – A solution package that utilises an explicit integration scheme to solve highly nonlinear problems, well suited to simulate brief transient dynamic events such as crash analysis, ballistic impact and drop-testing.
- Abaqus/CFD – Provides advanced Computational Fluid Dynamics capabilities. The scalable parallel CFD simulation capabilities address a broad range of nonlinear coupled fuid-thermal and fluid-structural problems.

3.3.1 Modelling in ABAQUS software

SIMULIA Abaqus software is the best non-linear Finite Element Analysis and Computational Fluid Dynamics Solvers. ABAQUS System uses finite element analysis techniques to provide accurate solutions for all types of linear and nonlinear stress, strain, dynamic, displacement and fractural problems. A substructure model of the column-beam connection was developed for Finite Element Analysis (FEA). For the substructure model, a typical inclined column-beam connection on the second floor was chosen to be used.

3.3.2 Loading

Loading datasets describe the external influences to which the model is subjected. All types of loading in ABAQUS software are features based except for discrete loads. ABAQUS element library lists the loading available for each particular element

3.3.3 Support condition

Support conditions describe the way in which the model is supported or restrained. A support dataset contains information about the restraints applied to each degree of freedom. By restraint certain axial, the requested conditions support can be obtained.

3.3 VERIFICATION STUDY

It is important to know whether the model can comprehensively represent the behaviour of structure. Thus, the ability and reliabilty of the model must be check through verification phase. The main objective of the verification study is to verify the reliability and ability both of the model and software used. For the purpose of the verification process, the result and analysis from the computer modelling will be compared with the result from the manual calculation of simple normal column. The model used for verification process is 2-Dimensional modelling. The dimension and cross section of the model used is shown in Figure 3.6.

The percentage of difference is calculated between the critical load obtained from the ABAQUS software and one calculated by using Euler's formula. The difference between these two values should not over 30% otherwise the values obtained from the ABAQUS will not acceptable and should be redesign the model. The simple column with fixed-end boundary condition is been designed and the profile of the model is a circular column. Column has dimensions of 3m in length and 0.25m in radius. The base feature used in ABAQUS is circular which the surface area is equivalent with I steel.

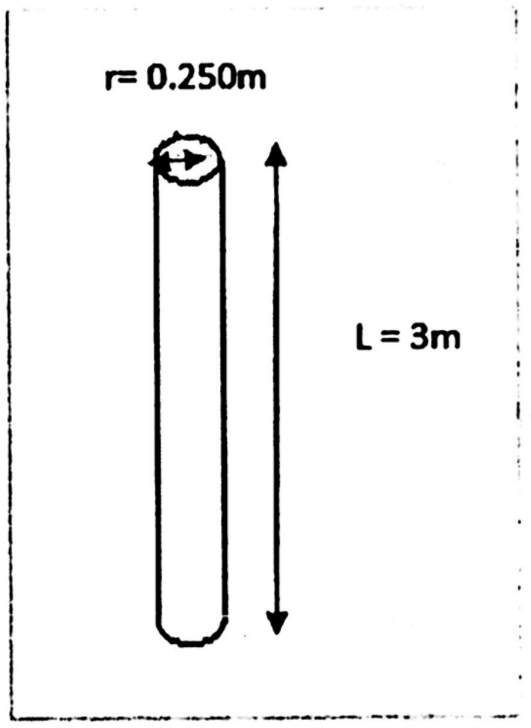

Figure 3.6 Cross section and dimension of column

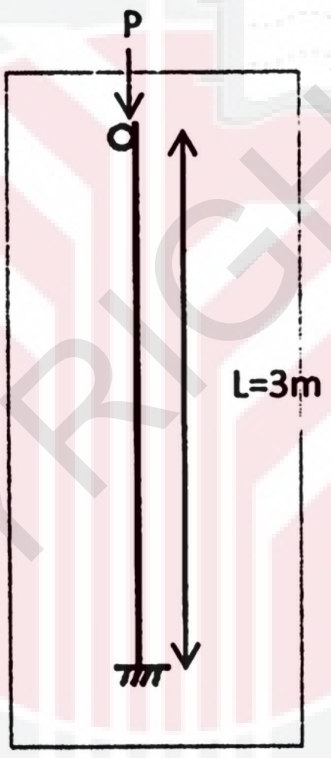

Figure 3.7 Idealisation of 2D modelling for verification study

3.4 2-DIMENSIONAL MODELLING OF SLANTED COLUMN

3.4.1 Geometric modelling

Geometric modelling is to prepare an underlying geometry for the intended model, which is very important in the subsequent step for meshing. In ABAQUS software, the geometry of 2D modelling is basically consisted of point, line, surface and profile.

The geometry of column has been defined using ABAQUS software, shown in Figure 3.8 and lower column is slanted with different angle. The angle chose from 3°, 5°, 7°, 9° and 15°. The substructure model for 2D view of various angle shown in Figures 3.8. All the dimensions in meter.

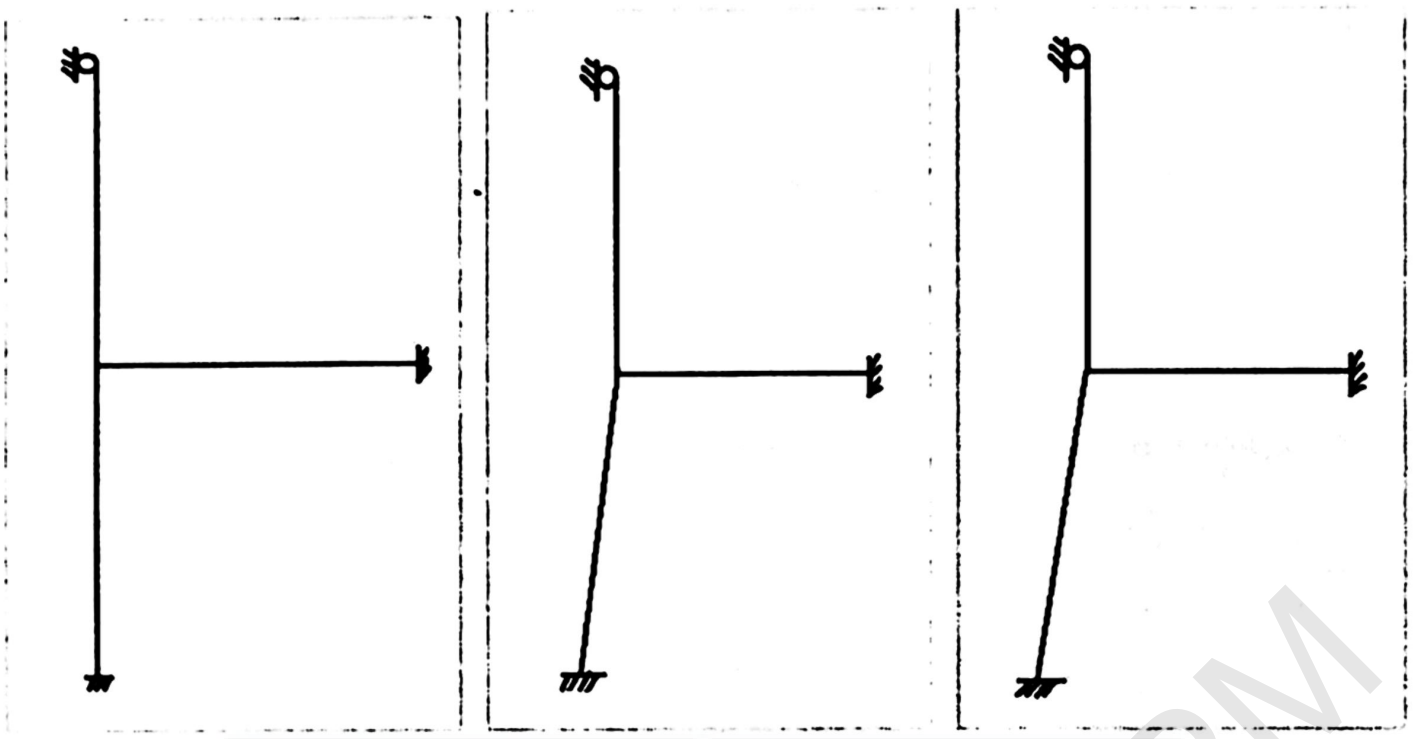

Figure 3.8 Model of substructure in 2-D view where the slanted column at (a) 0° angle (b) 3° angle (c) 5° angle (d) 7° angle (e) 9° angle (f) 15° angle

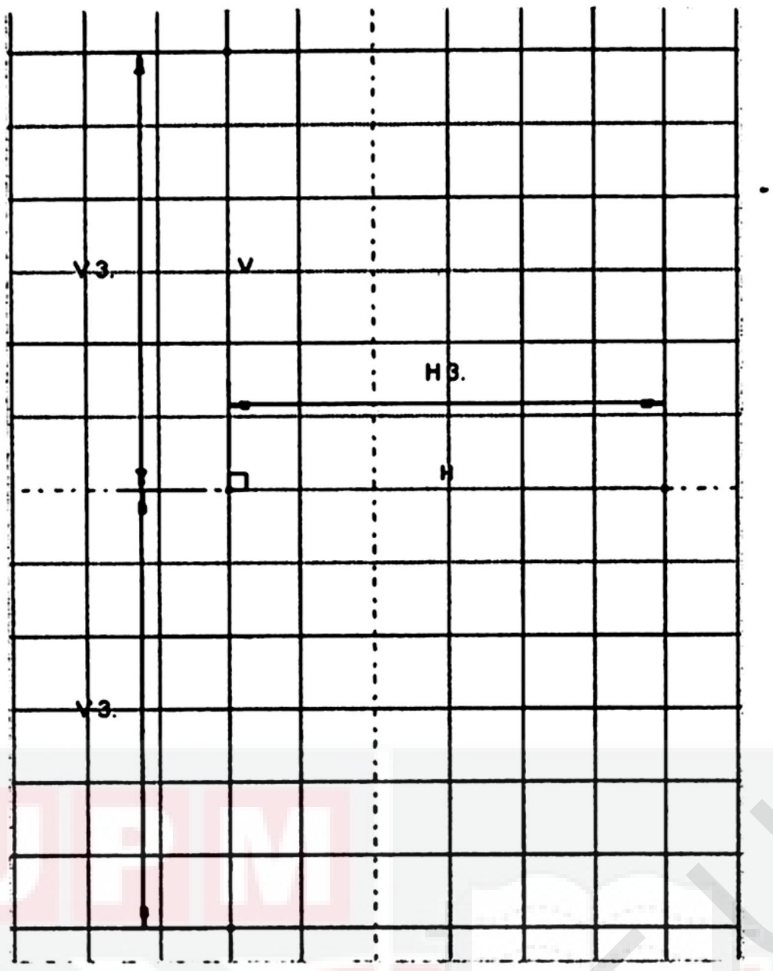

Figure 3.9 The idealization of column and beam in ABAQUS software

3.4.2. Material properties

The material properties for the structure for column and beam components is shown in Table 3-1.

Table 3-1 Material properties for column and beam components

Components	Young's Modulus (kN/m^2)	Shear Modulus (kN/m^2)	Poisson's ratio
Column and beam	$200x10^6$	$77x10^6$	0.3

3.4.3. Meshing

During this process, the model was discretized into finite elements with volumes in ABAQUS software. The overall view of the structure after meshing is shown in Figure 3.10.

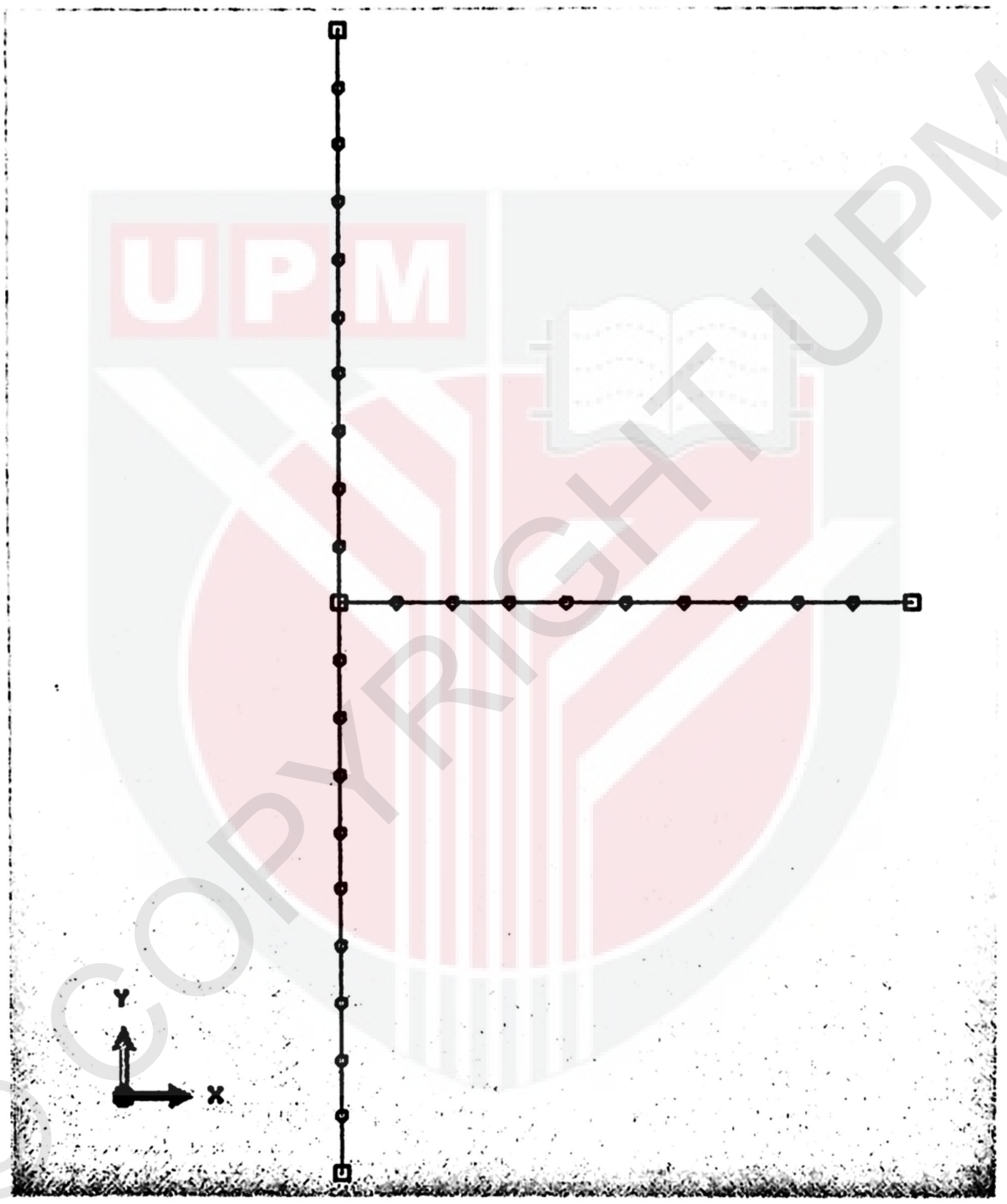

Figure 3.10 Meshing of the 2D model of structure

3.4.4. Boundary condition and loading

ABAQUS software allows all input of restraints or load at individual nodes and elements to be done directly to the selected entities. The restraints were applied at the end of both upper and lower column and beam which is restrained laterally and no rotation or translation are allowed at the end of column and beam. Besides that, tie connection also been used in this case of study.

Static load, P is applied as concentrated force on the top of the slanted column which is equal to 1kN and distributed equally over the upper column in opposite y-direction. The directions of restraints and loading are shown in Figure 3.11

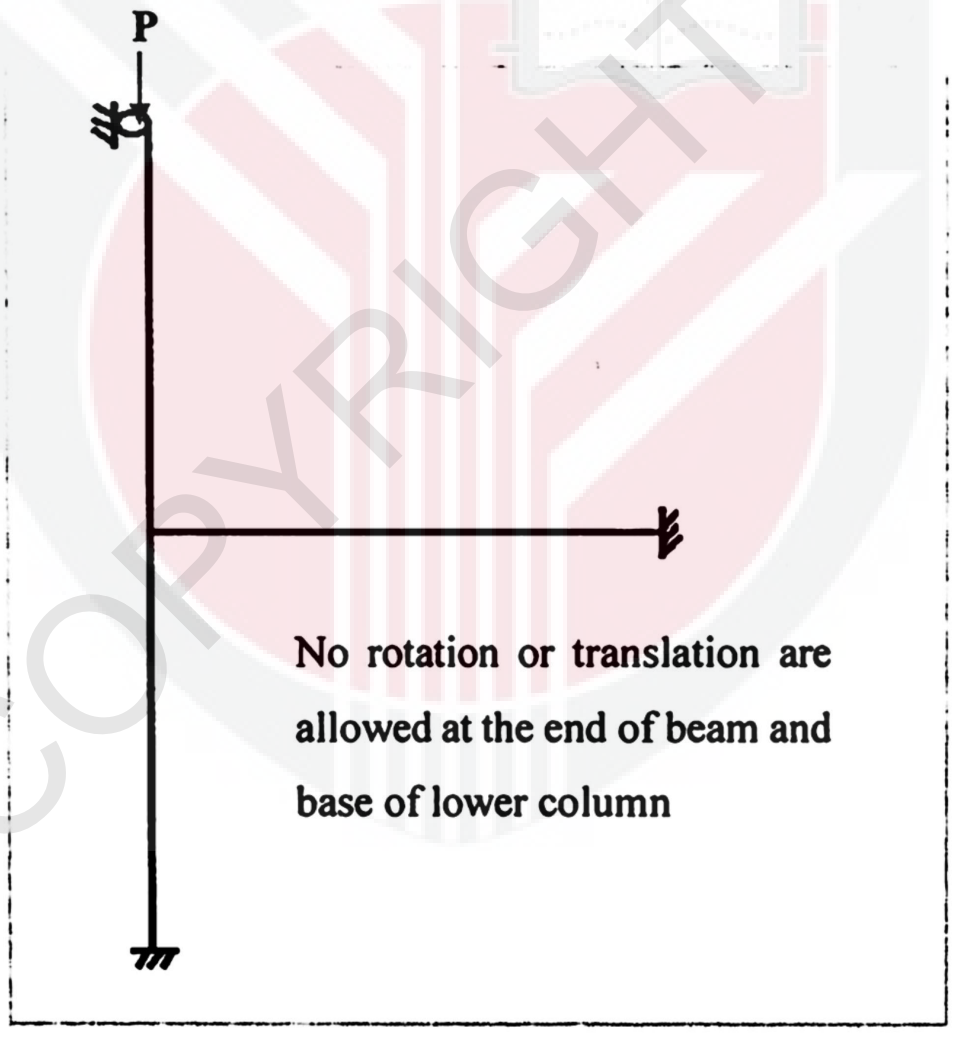

Figure 3.11 Boundary condition and loading of the 2D model of substructure

CHAPTER 4

RESULTS AND DISCUSSION

4.1 INTRODUCTION

Once the linear finite element analysis is successfully computed, the results can be obtained in ABAQUS software in various form, such as buckling shape, contour plot, and listed values in result report. Buckling shape are performed to give clear view of the model to examine its deformations due to stresses or displacement. All the results in a specific element can be checked in the list of the results obtained. For this study, the behavior of slanted column that be investigated are deflection, bending stress and strain and also the critical value that affect the slanted column to buckle due to different angle of slanted column.

This chapter begins with result verification by comparing between manual and analytical results. There will be a discussion about the percentage of increment value on the deflection, bending stress and strain and also the critical load that affect the

slanted column to buckle due to different angle of slanted column subjected to compression loading. The verification study would give an idea of how accurate the computer models in comparison with manual work. This also would be followed by parametric study on proving the k-factor of effective length in Euler's formula equal to 0.7 since the model is modelled as fixed-pinned boundary condition in 2-dimensional modelling. This section also would give us clear picture on how the differences of the different parameters could affect the model respond to the different angle of slanted column.

4.2 VERIFICATION STUDY

The percentage of difference is calculated between critical load calculated using Euler's formula and the critical load obtained from the ABAQUS software to determine whether the k factor is equivalent with 0.7. The percentage of difference should not exceed 30% so that the simulation analysis is reliable and accepted. The verification study on 2-dimensional element conducted as the value much approximate and easy to design as well. The angle of slanted column that been analyzed are 0°, 3°, 5°, 7°, 9° and 15° degree of angle. The simple column with fixed-end boundary condition is been designed and the profile of the model is a circular column with radius of 0.25m. Here is the manual calculation performed by implementing the Euler's formula in order to determine the critical load of column to buckle subjected to its effective length.

Given,

Radius, r = 0.250m

Effective Length, L = 3.0m

Young's Modulus, E = 200×10^6 kN/m^2

P = 1.0 kN

Calculation:

Second moment of inertia, $I = \frac{\pi}{4} r^4$

$$= \frac{\pi}{4}(0.250)^4$$

$$= 3.068 \times 10^{-3}\ m^4$$

$$Critical\ load, P_{cr} = \frac{2\pi^2 EI}{L^2}$$

$$= \frac{2\pi^2(200 \times 10^6)(3.068.\times 10^{-3})}{(3)^2}$$

$$= 1.346 \times 10^6\ kN$$

Meanwhile, the analysis from the software shown in Figure 4.1. The deformed shape of the column presented in 3 types of mode shapes for every cases. The results shown in Figures 4.3, 4.4, 4.5, 4.6 and 4.7.

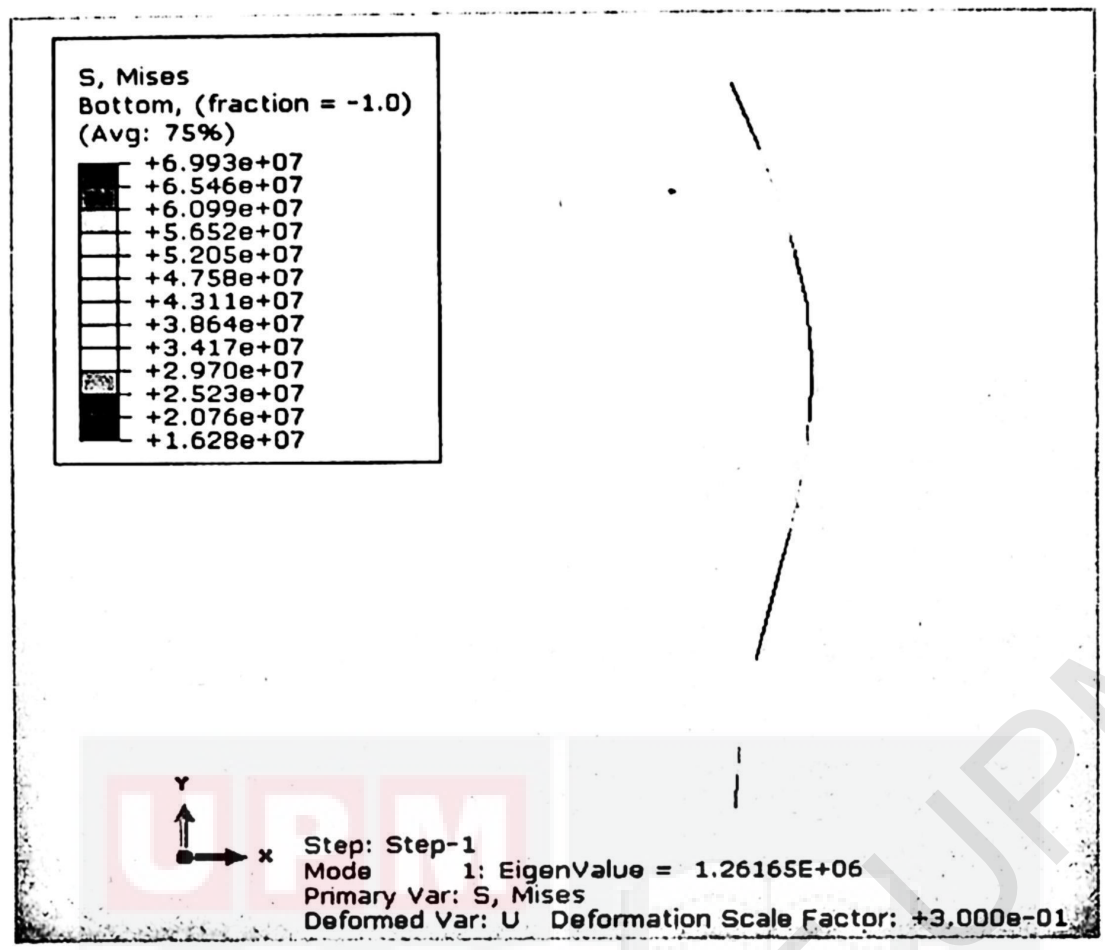

Figure 4.1 Deformed shape of finite element in 2D modelling for $\Theta=0^{\circ}$

Based on the simulation result, the mode 1 gives critical load equal to 1.262×10^6 kN.

Therefore, the ratio of difference between ABAQUS and manual calculation is:

$$\%\, difference = \frac{P_{cr,manual} - P_{cr,abaqus}}{P_{cr,manual}} \times 100\%$$

$$= \frac{(1.346 - 1.262) \times 10^6}{(1.346) \times 10^6} \times 100\%$$

$$= 6.24\% < 30\%$$

Based on the calculation, it shows the differences between manual and computer analysis only 6.24%. Thus, it shows that the good agreement between model in ABAQUS and manual calculation. The verification study is carry on with different angle of slanted column. Figure 4.1 shows the deformed shape of finite element in

2D modelling when the column is in normal column. The effective length is fixed to 3m. The verification study is continued with the various angle of slanted column to study the differences of critical load value due to various angle.

Table 4-1 Summary of result for verification study of various angle of slanted column

Angle (Θ)	Abaqus software, $x10^6$ (kN)	Manual calculation, $x10^6$ (kN)
0°	1.262	1.346
3°	1.257	1.342
5°	1.248	1.336
7°	1.236	1.326
9°	1.219	1.313
15°	1.145	1.256

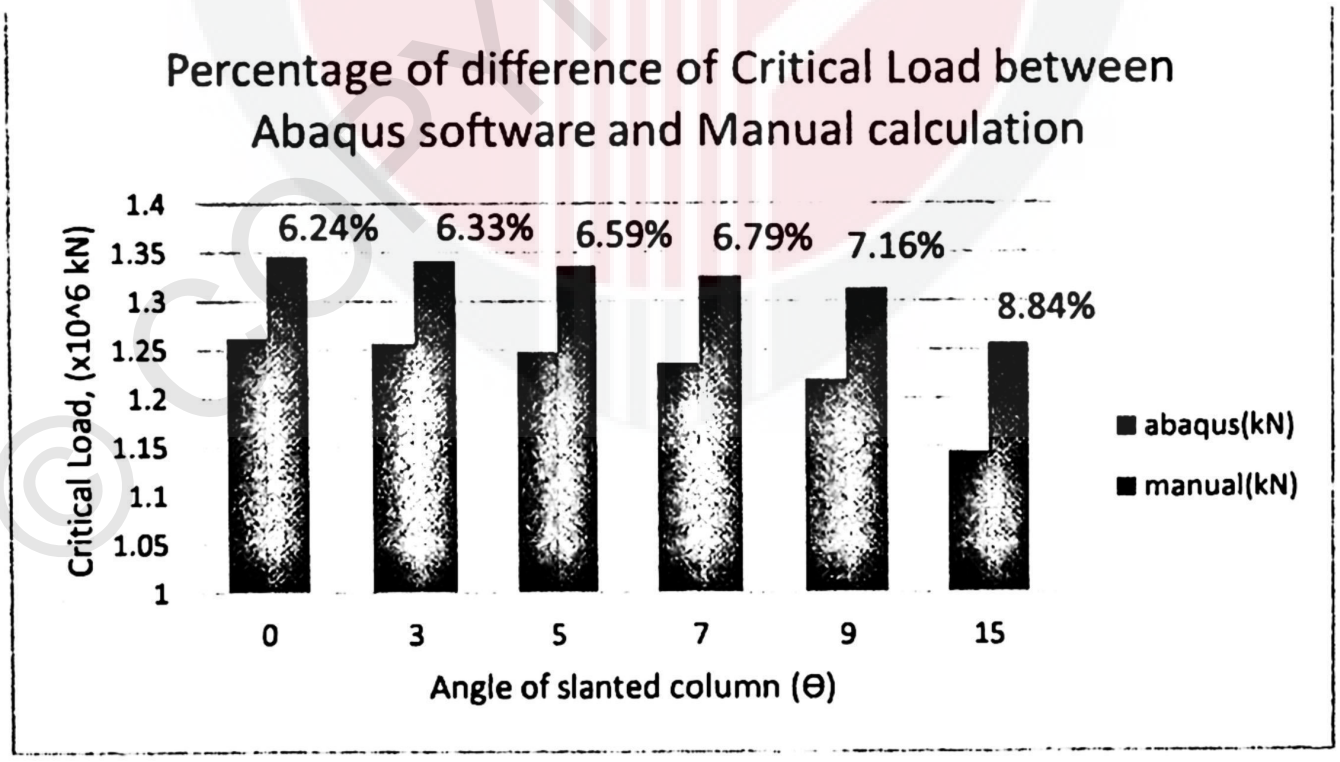

Figure 4.2 The bar chart of percentage of difference of critical load between ABAQUS software and Manual calculation

Based on the bar chart in Figure 4.2, it shows that the highest percentage of difference given by angle 15° which equal to 8.84%. Even though, the result still acceptable as it not exceeds 30% of difference and the value of maximum load can be used in analysis. The graph also show that the critical load is decrease as the angle of column increases. This is due to the strength and tensile strength that exist due to the static load applied during the simulation of the structure. The difference of maximum load between angle is slightly small because the angle of slanted column used also very small in value. That is the reason why the difference of critical load is small respect to different angle.

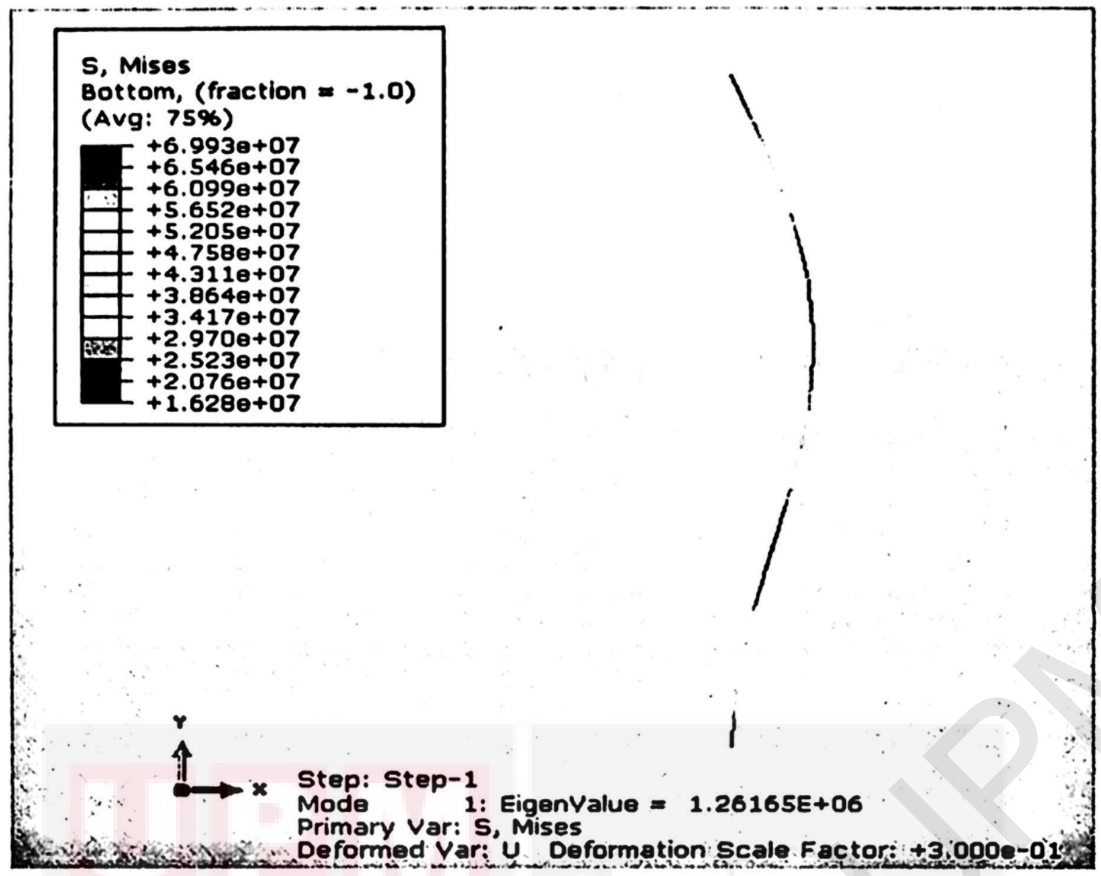

(a)

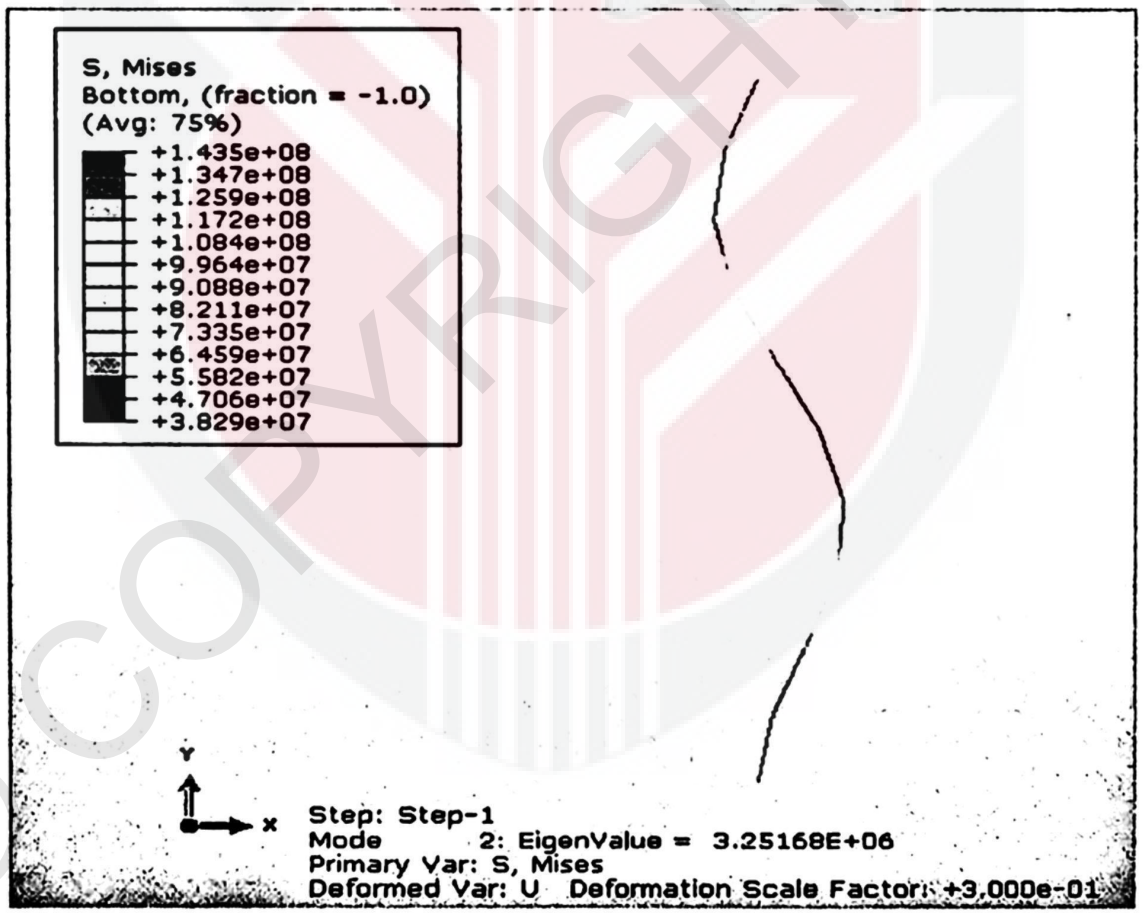

(b)

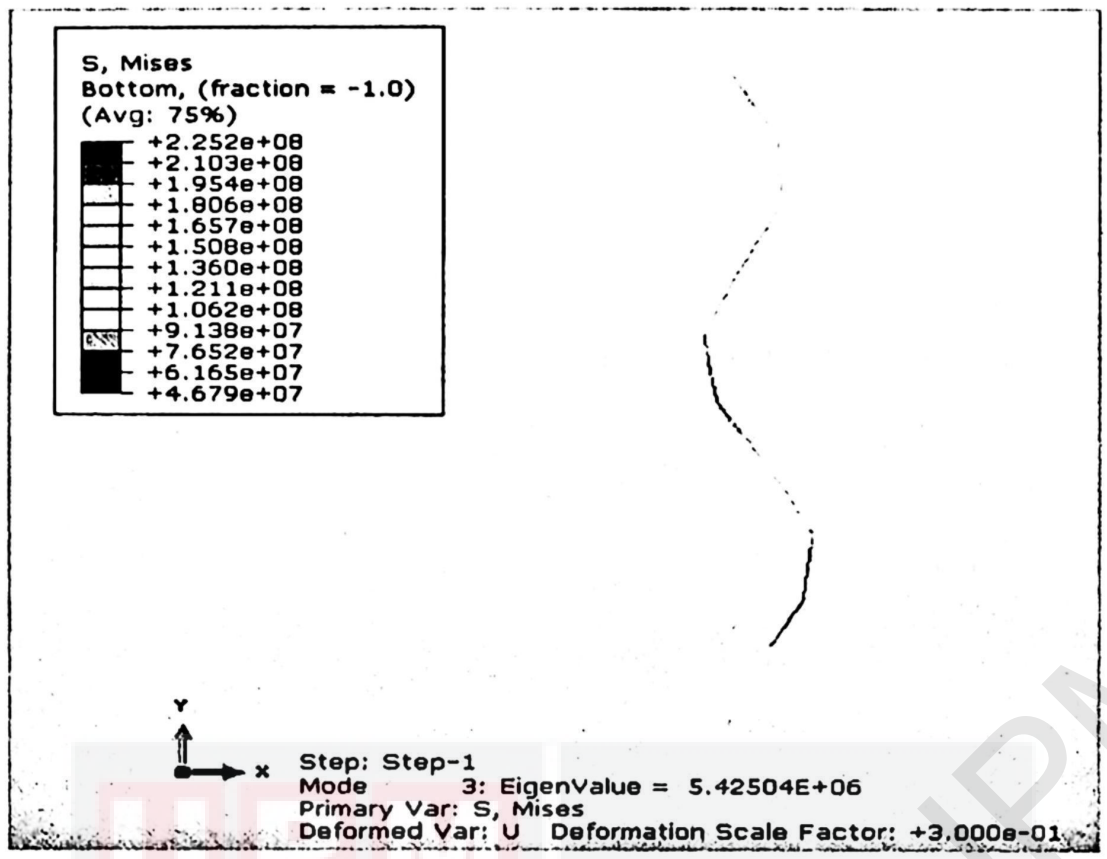

(c)

Figure 4.3 Deformed shape of finite element in 2D modelling for Θ=0° where (a) Mode 1 (b) Mode 2 (c) Mode 3

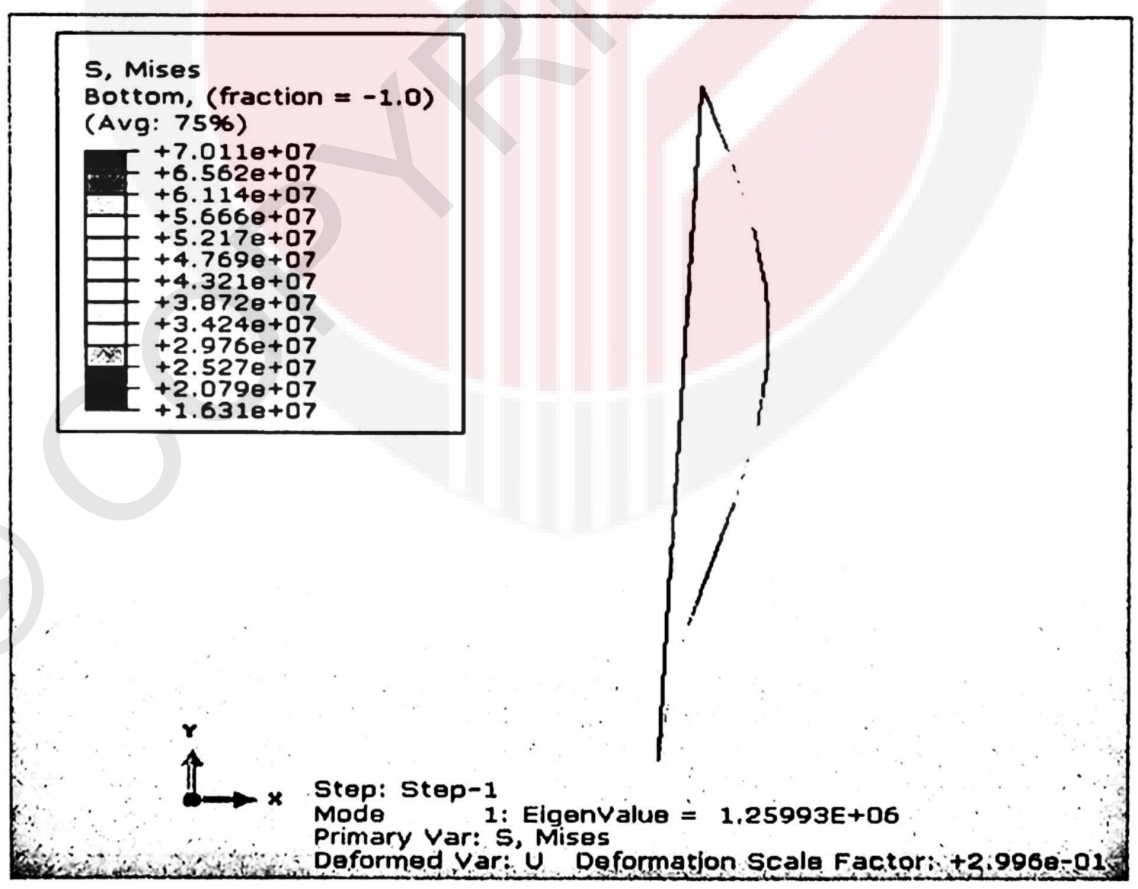

(a)

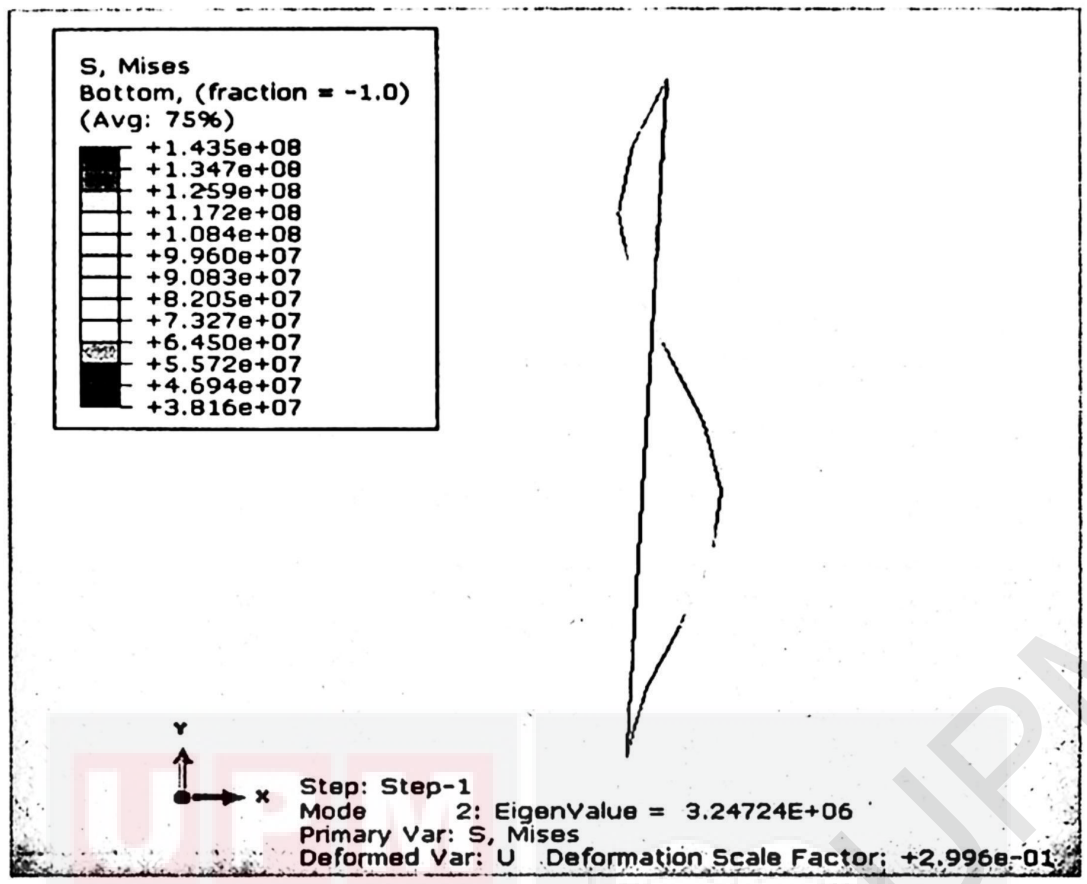

(b)

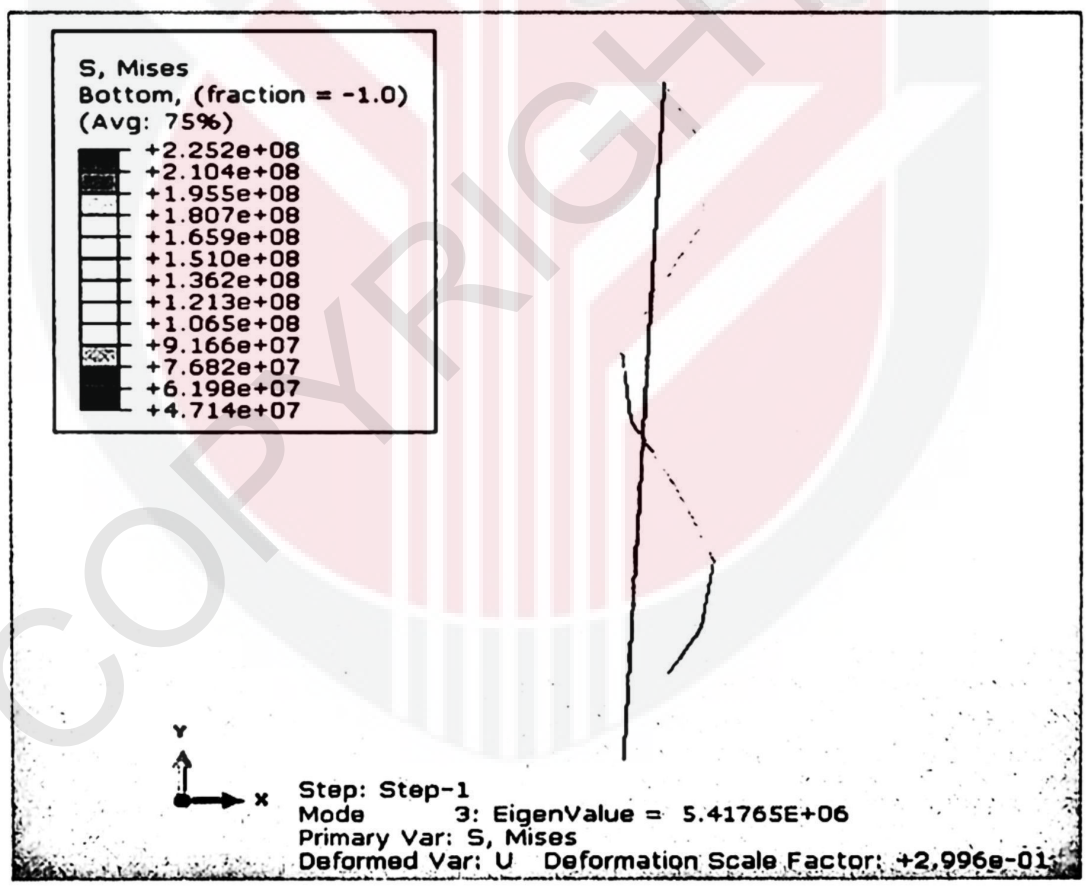

(c)

Figure 4.4 Deformed shape of finite element in 2D modelling for Θ=3° where (a) Mode 1 (b) Mode 2 (c) Mode 3

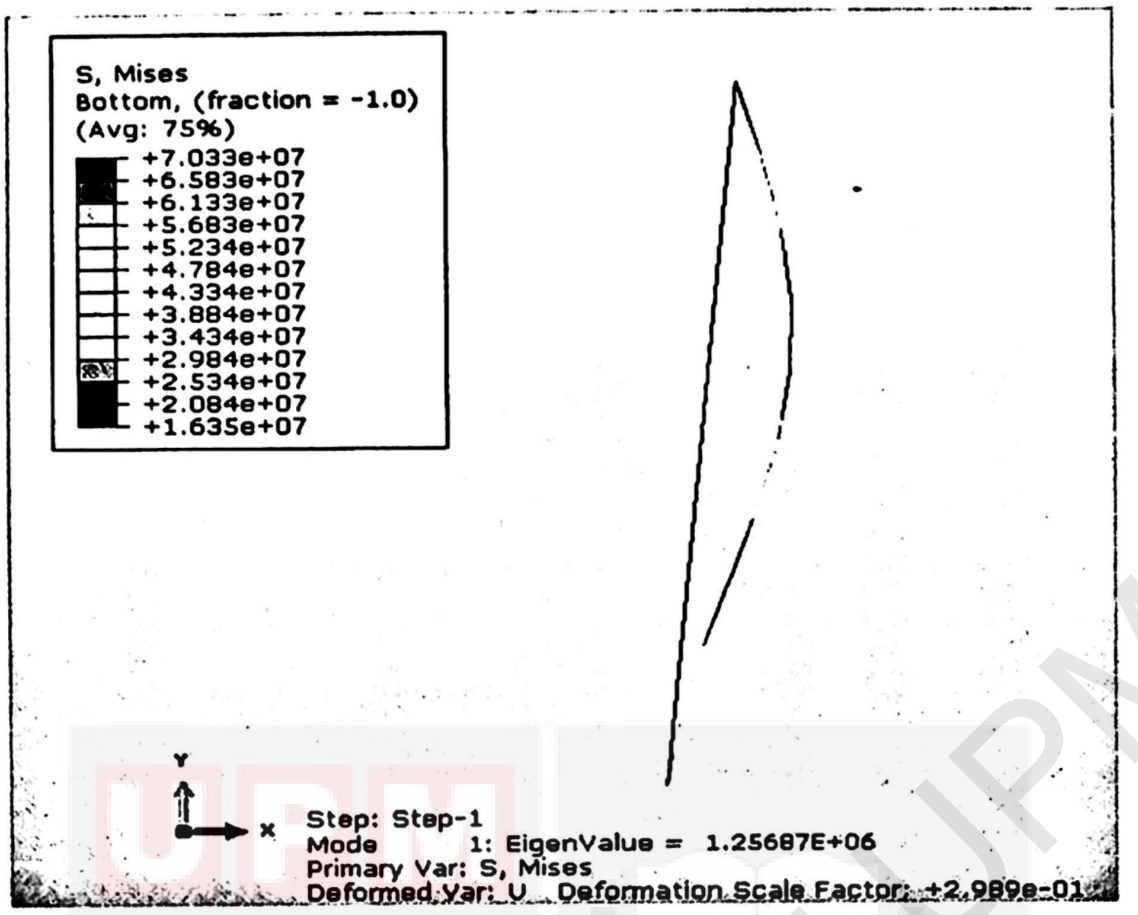

(a)

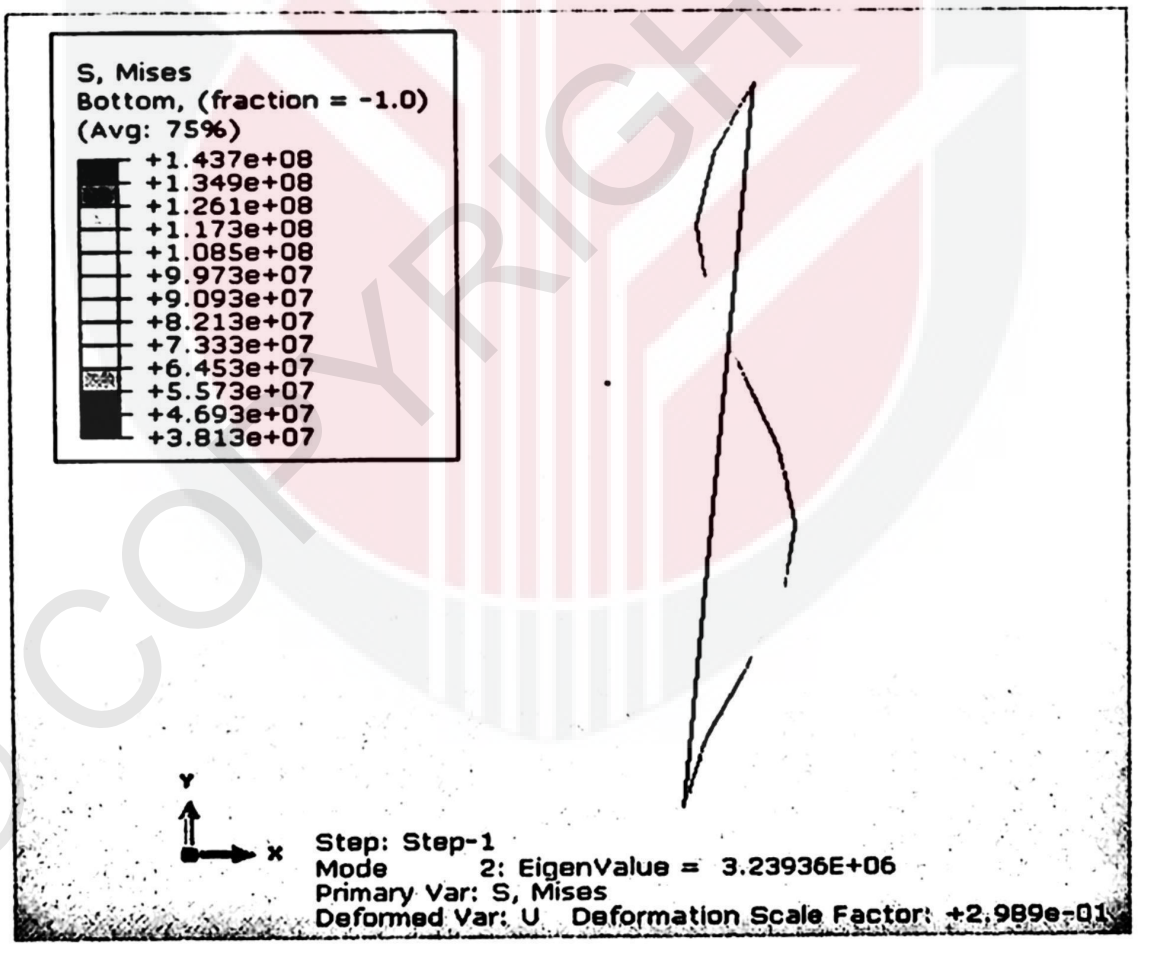

(b)

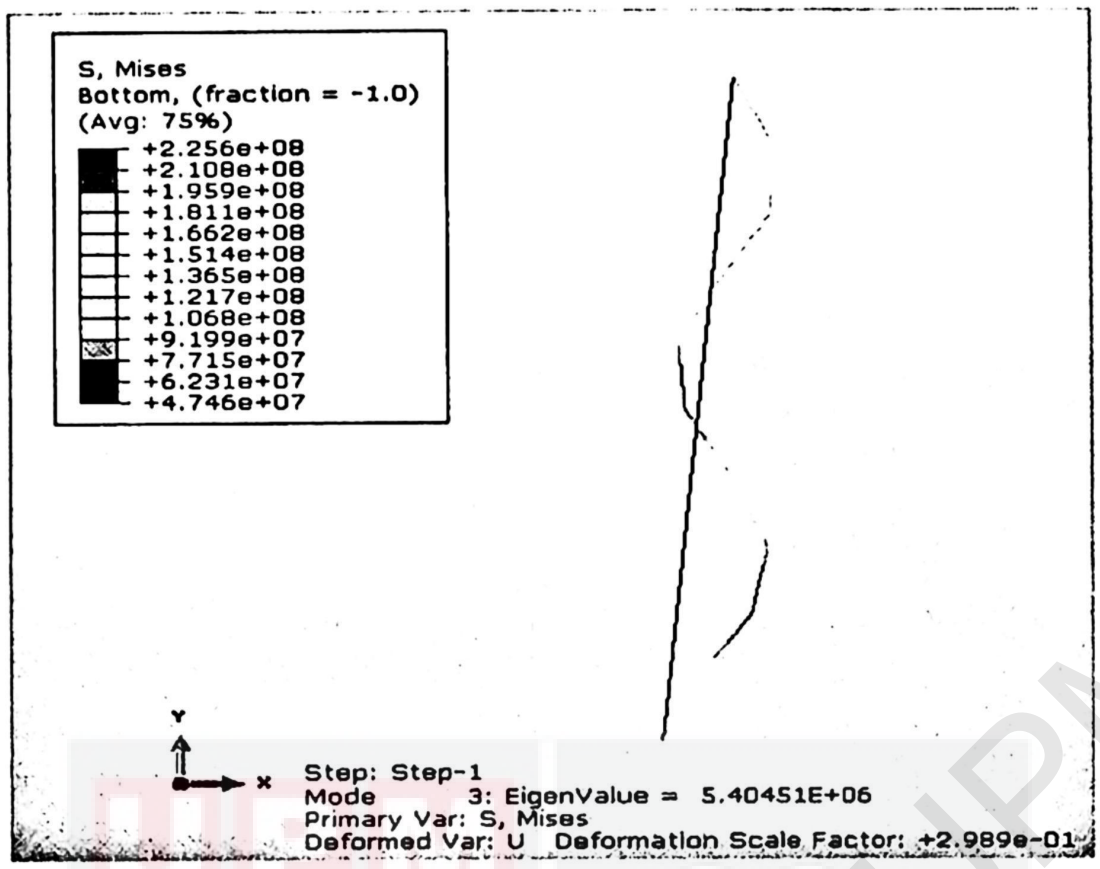

(c)

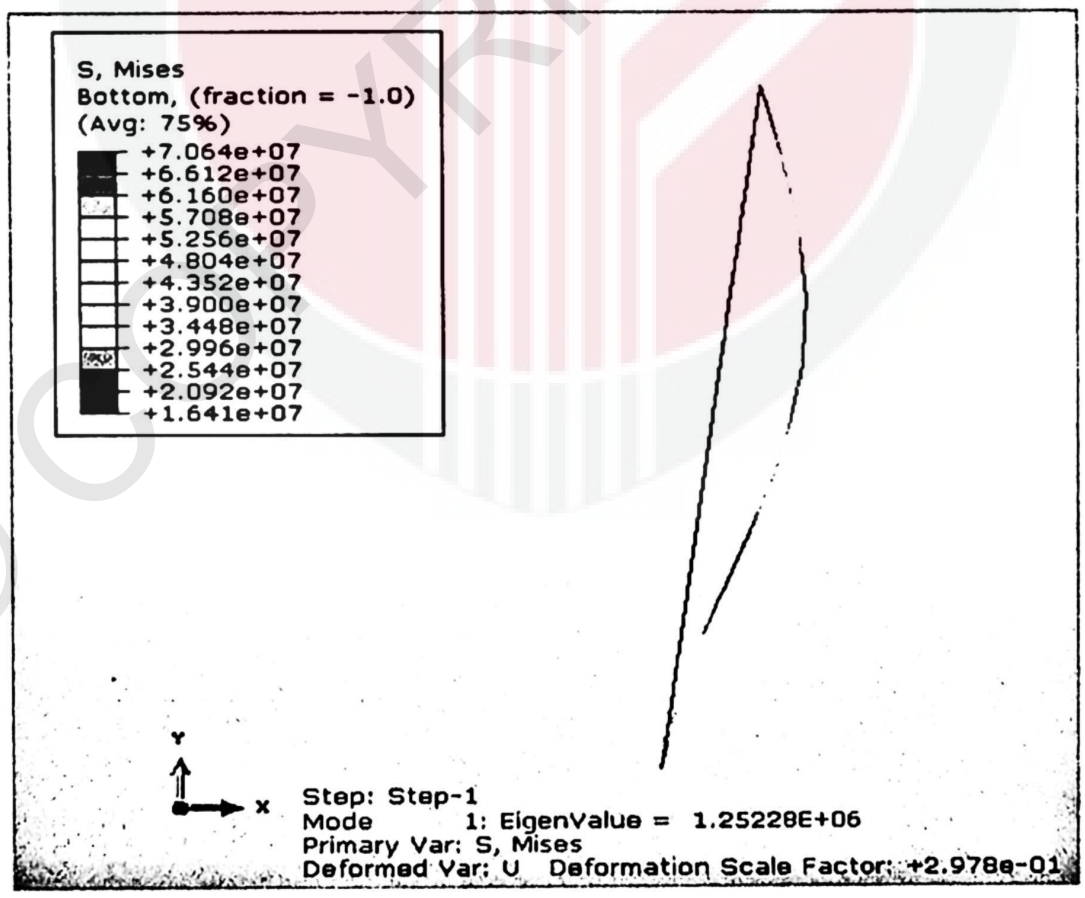

(a)

Figure 4.5 Deformed shape of finite element in 2D modelling for Θ=5° where (a) Mode 1 (b) Mode 2 (c) Mode 3

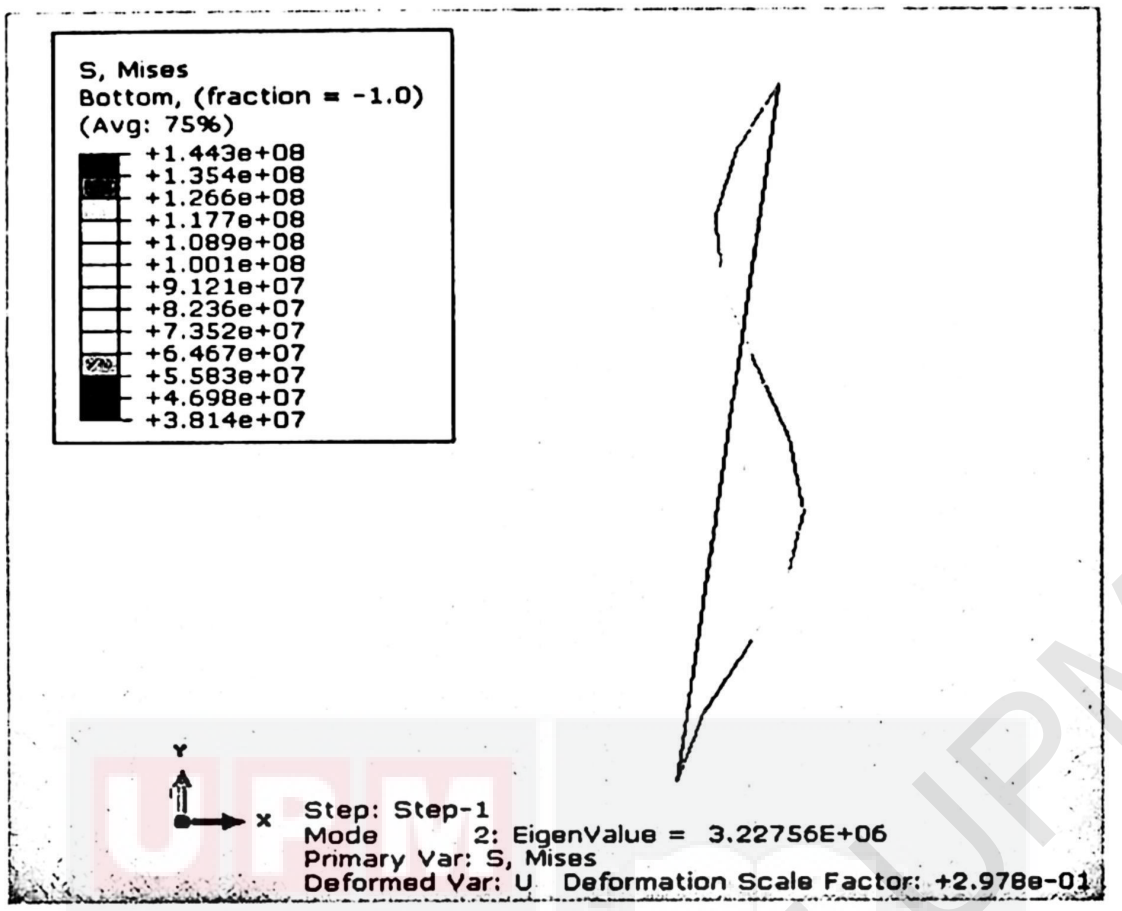

(b)

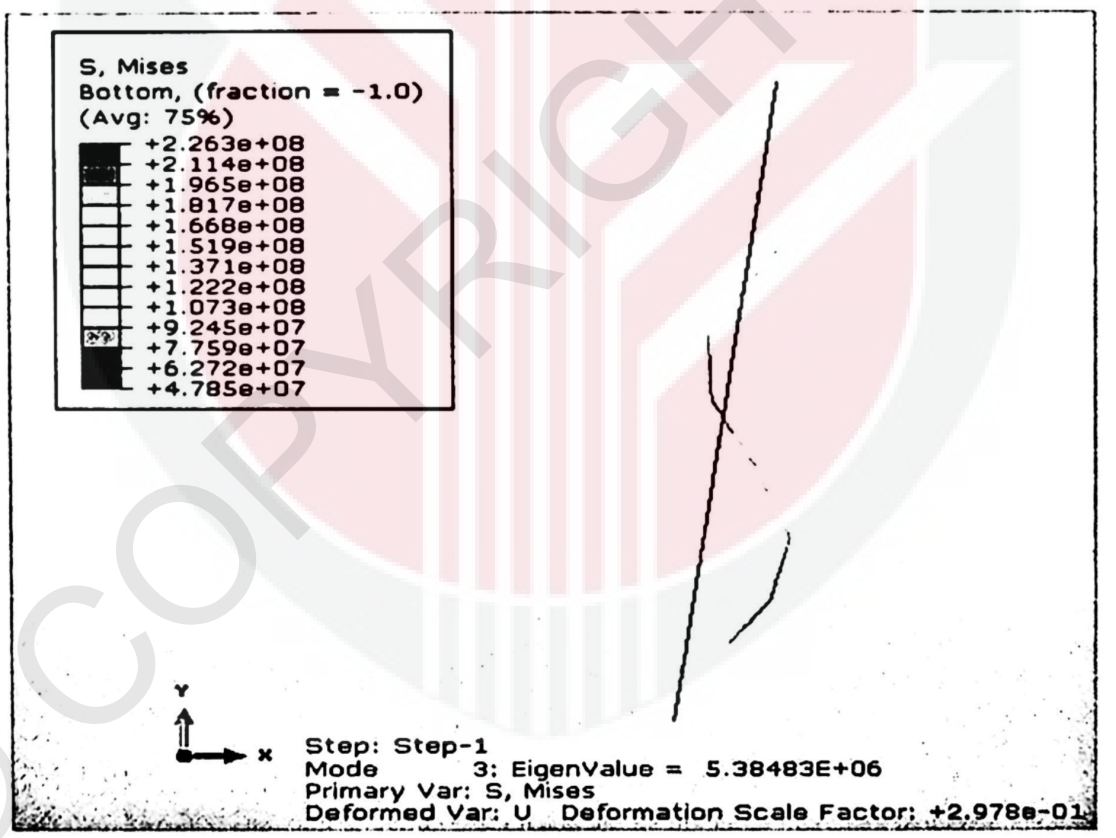

(c)

Figure 4.6 Deformed shape of finite element in 2D modelling for Θ=7° where (a) Mode 1 (b) Mode 2 (c) Mode 3

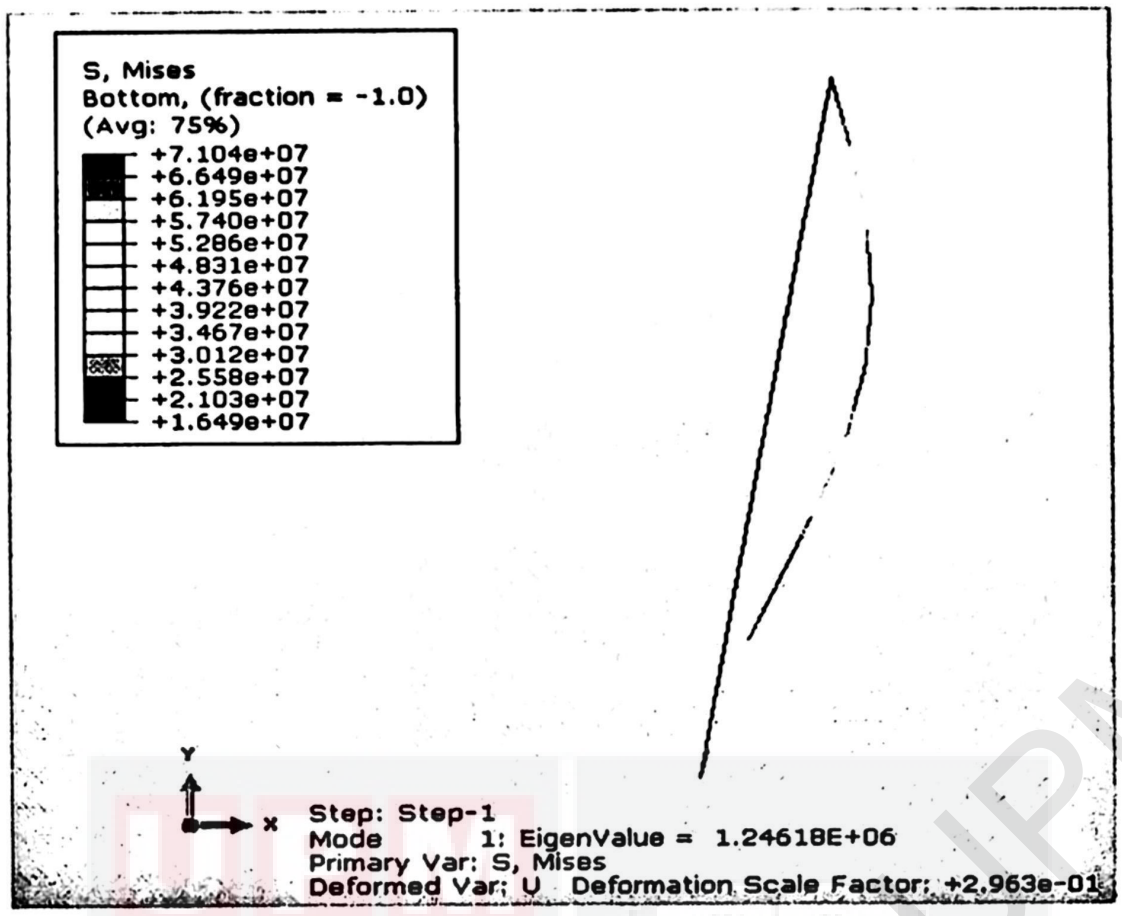

(a)

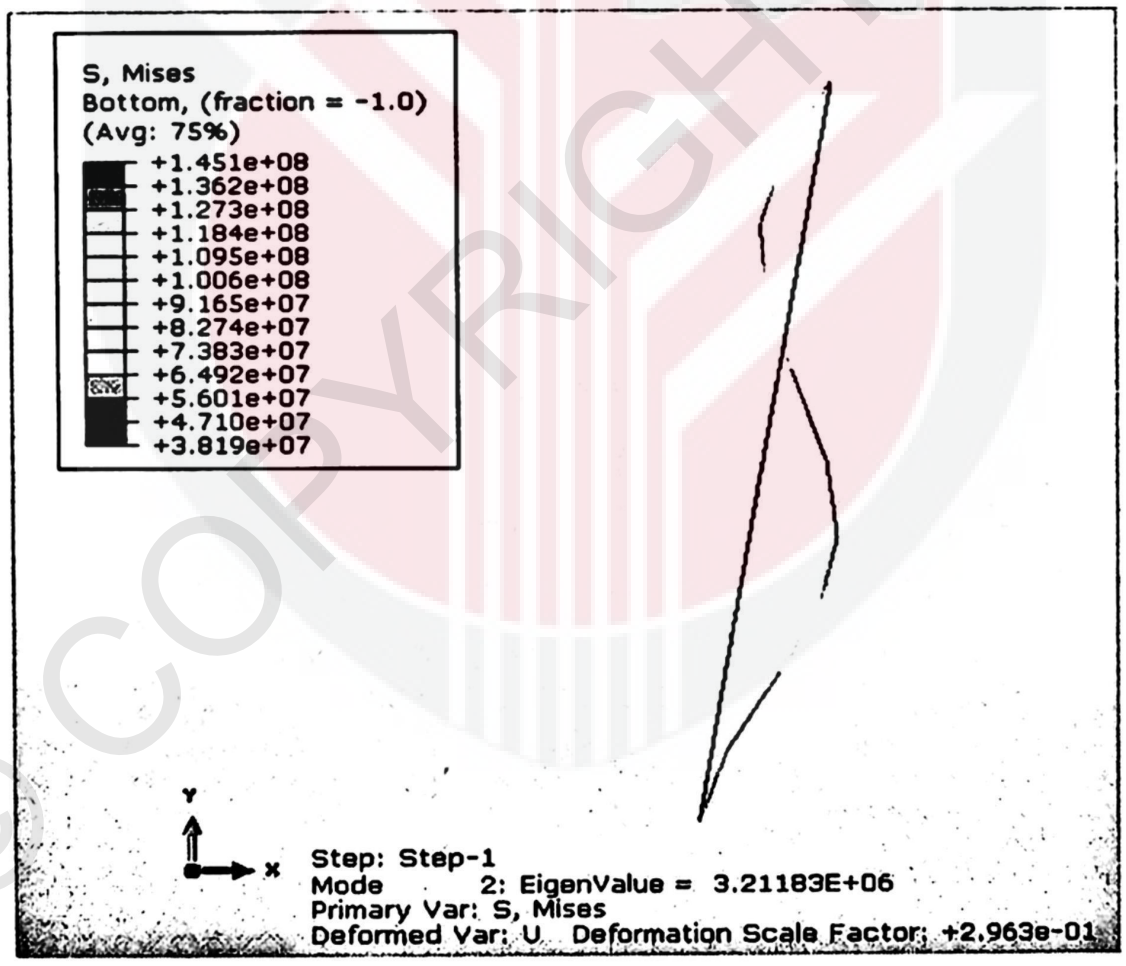

(b)

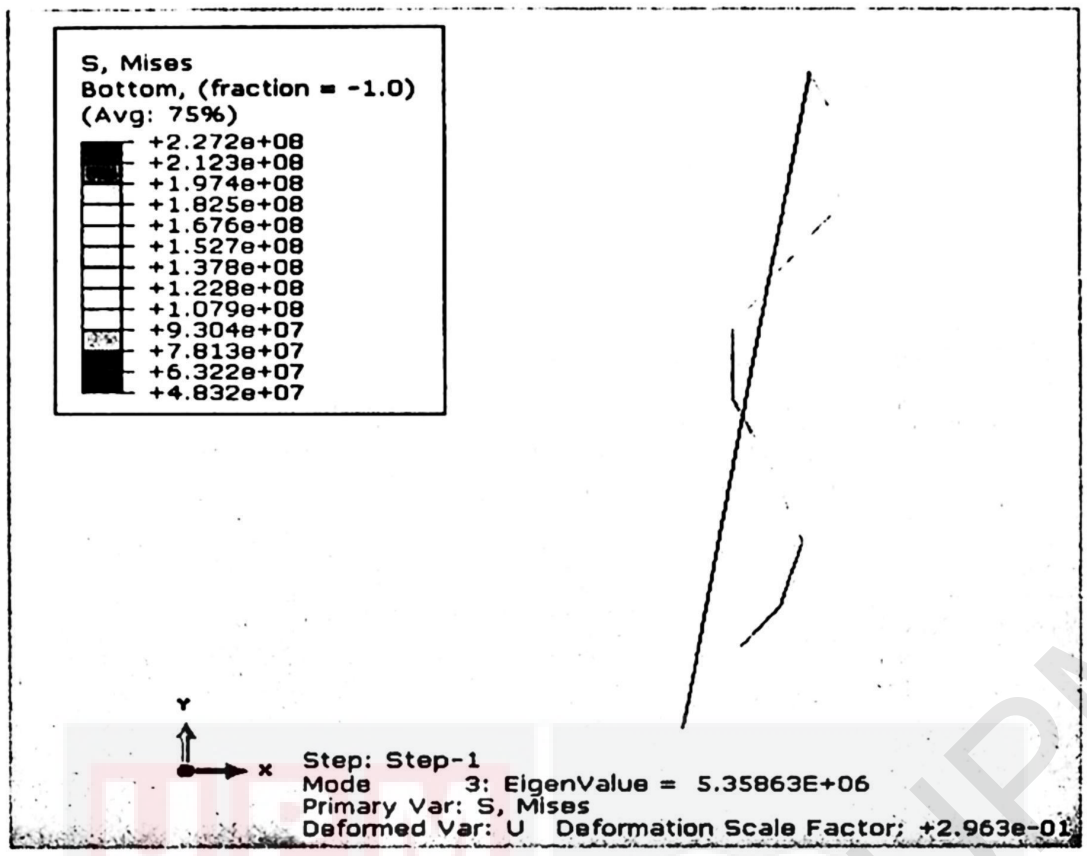

(c)

Figure 4.7 Deformed shape of finite element in 2D modelling for Θ=9° where (a) Mode 1 (b) Mode 2 (c) Mode 3

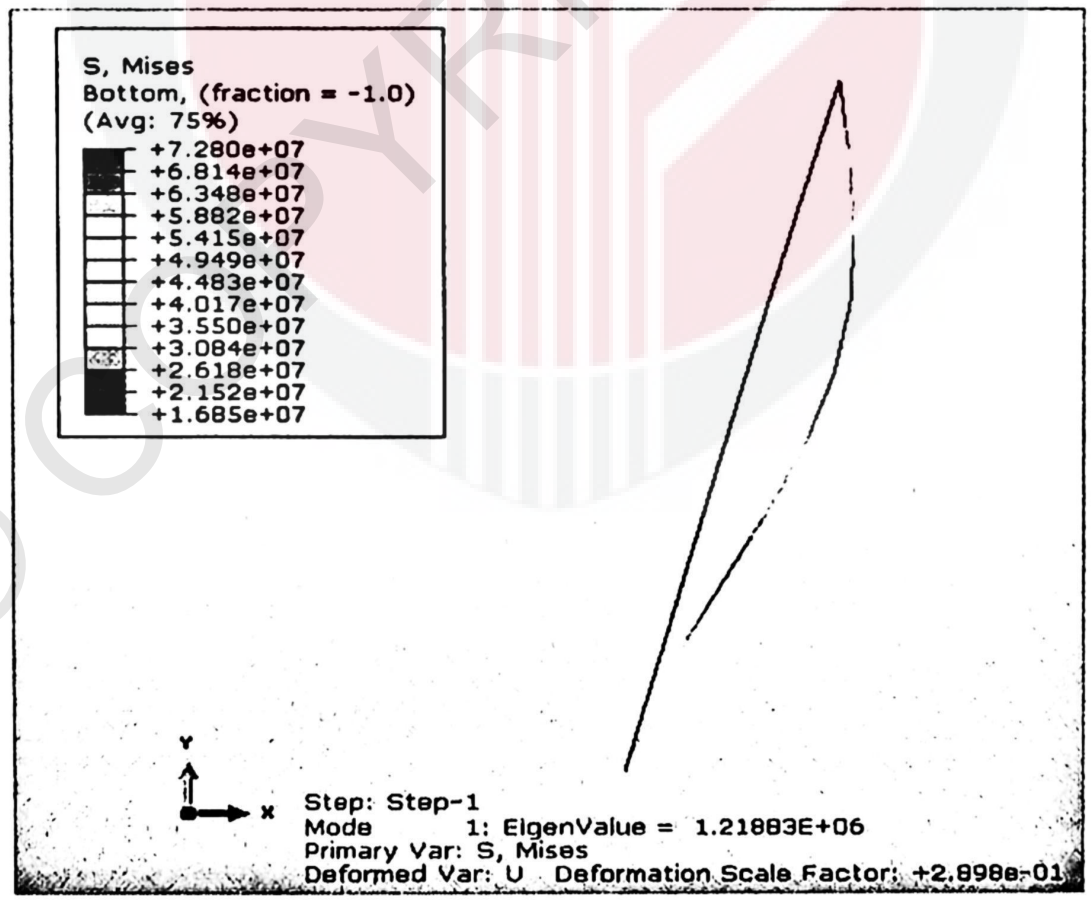

(a)

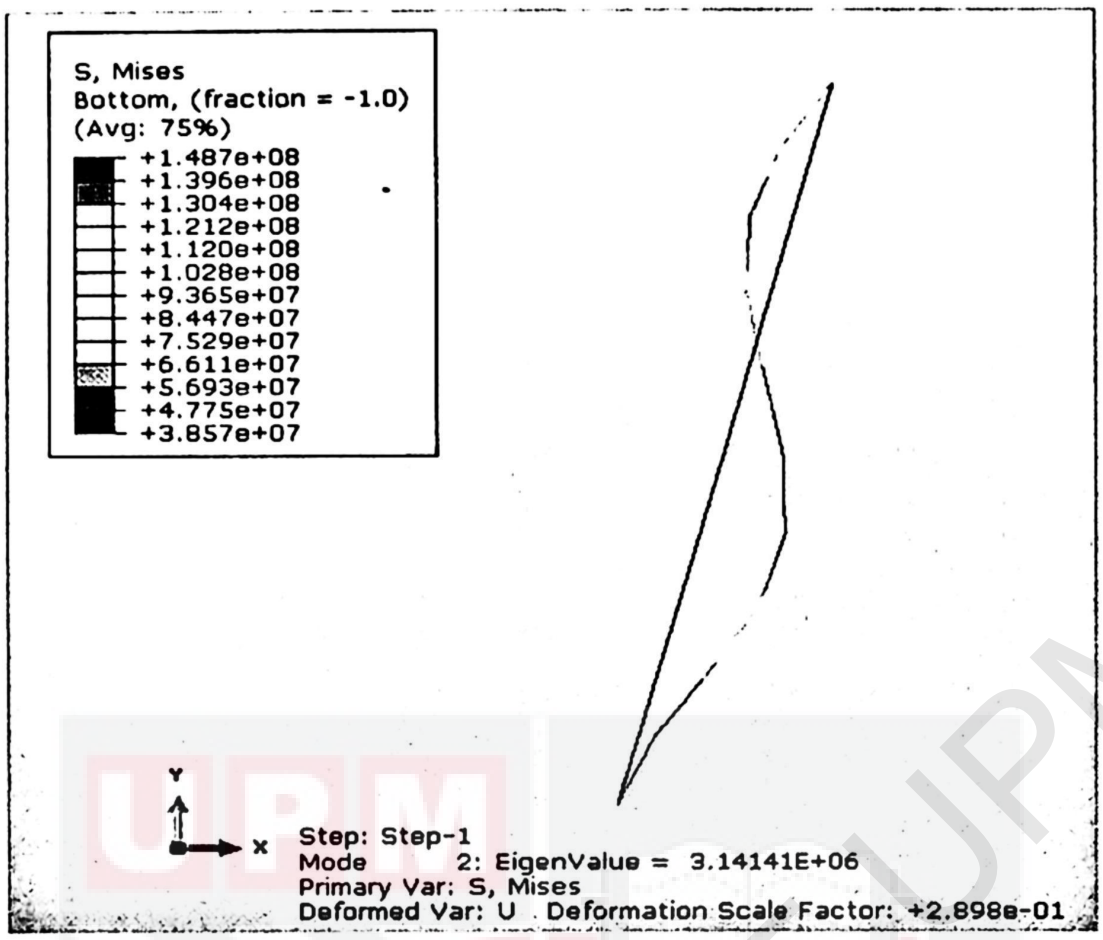

(b)

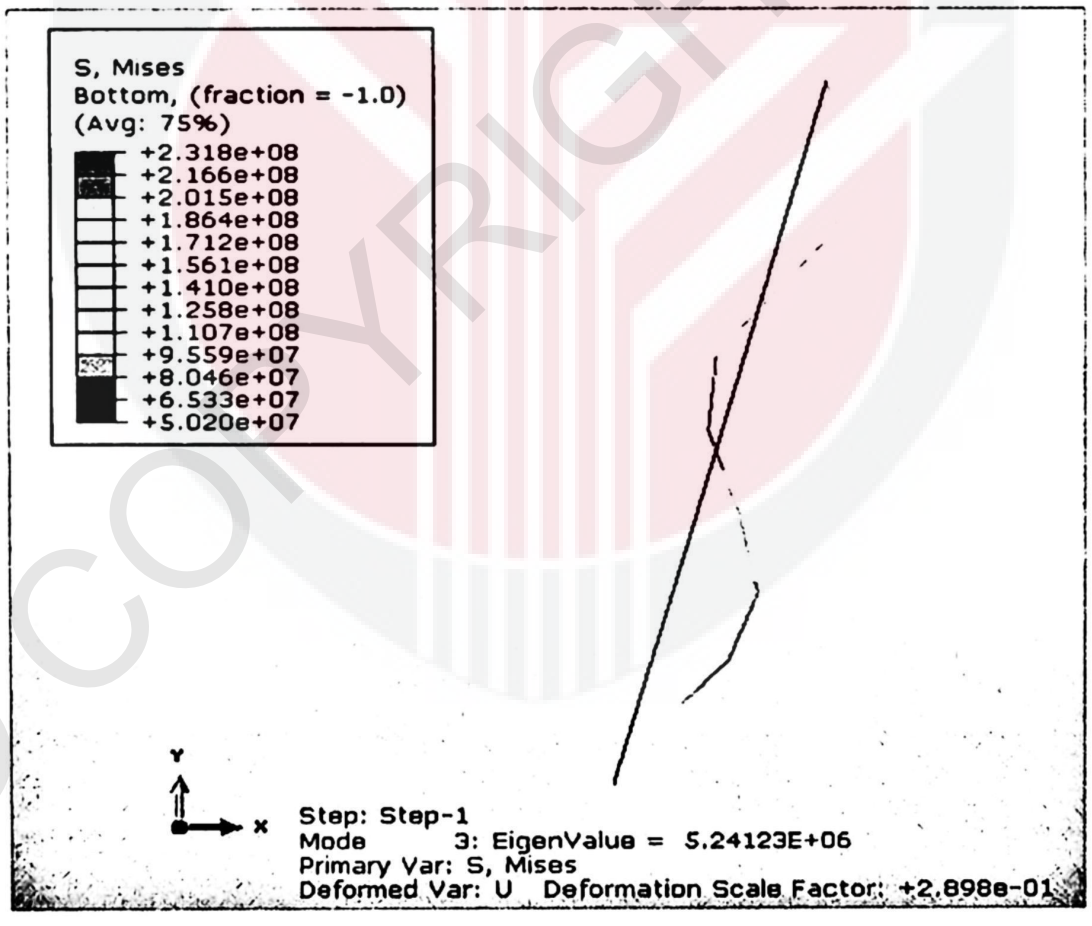

(c)

Figure 4.8 Deformed shape of finite element in 2D modelling for Θ=15° where (a) Mode 1 (b) Mode 2 (c) Mode 3

Figures 4.3, 4.4, 4.5, 4.6, 4.7 and 4.8 show the deformed shape obtained from the simulation in ABAQUS software for angle 3°, 5°, 7°, 9° and 15°. The results from these figures represent the deformed shape of the slanted column at different angle in 3 different types of mode. The mode explains the critical value for the column at different effective length. Based on the result of analysis, the critical load due to increases angle for mode 2 are 3.25×10^6 kN, 3.24×10^6 kN, 3.23×10^6 kN, 3.21×10^6 kN and 3.14×10^6 kN respectively. Meanwhile, 5.42×10^6 kN, 5.41×10^6 kN, 5.38×10^6 kN, 5.36×10^6 kN and 5.24×10^6 kN are the critical load values for mode 3. From these figures of different type of modes, it can be concluded that the reduction in effective length gives the higher value of critical load but still as the lowest angle gives the higher value of critical load than the wider angle of slanted column.

4.3 PARAMETRIC STUDY

4.3.1 Relationship of new k factor due to angle of slanted column

During Chapter 3, new k for inclined column has been determined in the preliminaries study. Based on the critical load obtained in verification study, the values used to find the new k-factor that influence the load due to angle of slanted column is going to verified. The calculation shown below.

$$For\ \theta = 0^{\circ}, \quad P_{cr} = 1.262 \times 10^{6} kN$$

$$1.262 \times 10^{6} = \frac{2\pi^2 EI}{(kL)^2}$$

$$k = \sqrt{\frac{2\pi^2 EI}{1.262 \times 10^{6}(3^2)}} = \sqrt{\frac{2\pi^2 (200 \times 10^{6})(3.068x10^{-3})}{1.262 \times 10^{6}(9)}} = 0.73$$

From Chapter 3, it gives

$$k = \frac{0.7}{cos\theta} = \frac{0.7}{\cos 0} = 0.7$$

$$\therefore k = 0.7 \approx 0.73\ (proved)$$

Based on the calculation above, the relationship of k value with Euler's formula gives significant role to the critical load obtained. This is because, new k influenced by the changing in length of column. Since $L_{new} = \frac{L}{cos\theta}$, thus, new equation for critical load or maximum load is success developed by considering k factor due to various angle of slanted column.

4.3.2 2-Dimensional Modelling Analysis and Result

4.3.2.1 Critical Load

Critical load was determined through the analysis done by using ABAQUS modelling software. Table 4-2 show the result of critical load obtained and tabulated. The critical loads were 83343kN, 83059kN, 82823kN, 82531kN, 82195kN, and 80849kN respectively. The maximum load decreased as the angle of slanted column increased due to the stiffness of column which is decreasing. The critical load results been illustrated in the bar chart shown in Figure 4.8. The pattern of critical load decreases due to angle of slanted column uniformly. It because the tensile strength decreases as the angle increases and the stiffness of slanted column decreases.

Table 4-2 The critical load value of various angle of slanted column

Angle of slanted column (Θ)	Critical Load (kN)
0°	83343
3°	83059
5°	82823
7°	82531
9°	82195
15°	80849

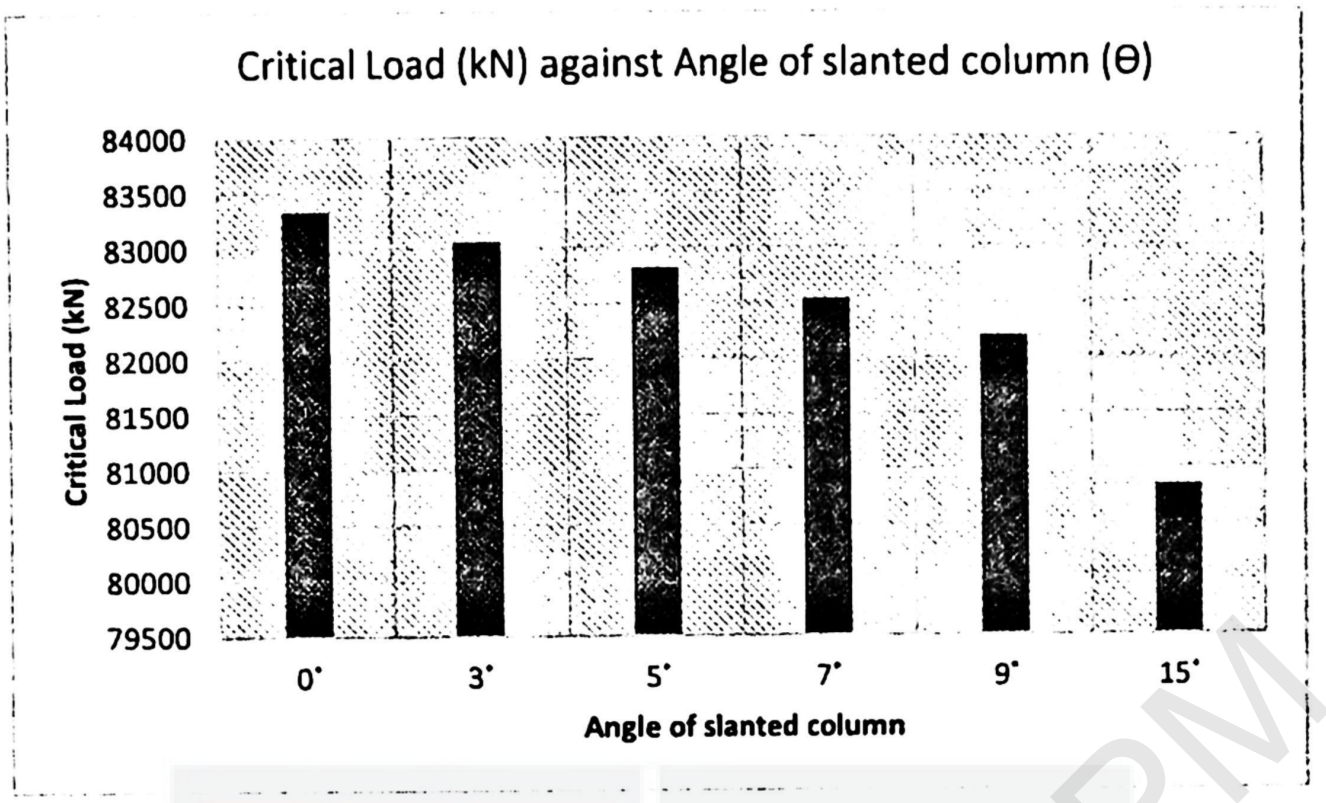

Figure 4.9 Bar chart of the critical load due to various angle of slanted column

Based on the bar chart in Figure 4.9 above, it shows the value of critical load for different angle of slanted column analysed in 3 Dimensional modelling using ABAQUS software. The results been tabulated and represented in bar chart, so the pattern of bar chart above show the critical load decreased as the angle of slanted column increased uniformly. Between angle of 9° and 15°, the critical load seems to have maximum difference which about 1,346kN with the percentage of 1.16%. This is because the wider angle of slanted column results less in stiffness. Meanwhile, the other angle only has decrement at small differences uniformly. The results continued with lists of contours for bending stress, bending strain and displacement observed with various angle of slanted column.

4.3.2.2 Bending Stress, S

Shear stress is typical failure modes associated to diagonal cracking. Bending stress of the structure is to see the strength of the structure to resist the load applied on the surface of the structure. The maximum principal stress for both upper and lower columns to differentiate the stress values obtain for those component due to the static load prescribed.

Figures 4.10, 4.11, 4.12, 4.13, 4.14 and 4.15 show the Mises stress contour illustrate at maximum load for the 2D modelling with various angle of slanted column. Based on these figures, it shows the maximum principal stress area occurs at upper column. The slanted column shows the maximum principal stress becomes smaller than upper column because the boundary condition is changed as fixed-fixed end condition. The values of k also decrease as the angle of slanted column increases uniformly due to the effective length of the column.

Based on the result obtained from abaqus software, the maximum principal stress at angle 0°, 3°, 5°, 7°, 9° and 15° gives 3.379×10^7 kN/m^2, 3.374×10^7 kN/m^2 , 3.369×10^7 kN/m^2, 3.363×10^7 kN/m^2, 3.356×10^7 kN/m^2 and 3.321×10^7 kN/m^2 respectively. In the meantime, the lower column gives maximum principal stress equal to 0.948×10^7 kN/m^2, 0.951×10^7 kN/m^2, 0.953×10^7 kN/m^2, 0.955×10^7 kN/m^2, 0.957×10^7 kN/m^2 and 0.962×10^7 kN/m^2 respectively for angle 0°, 3°, 5°, 7°, 9° and 15°.

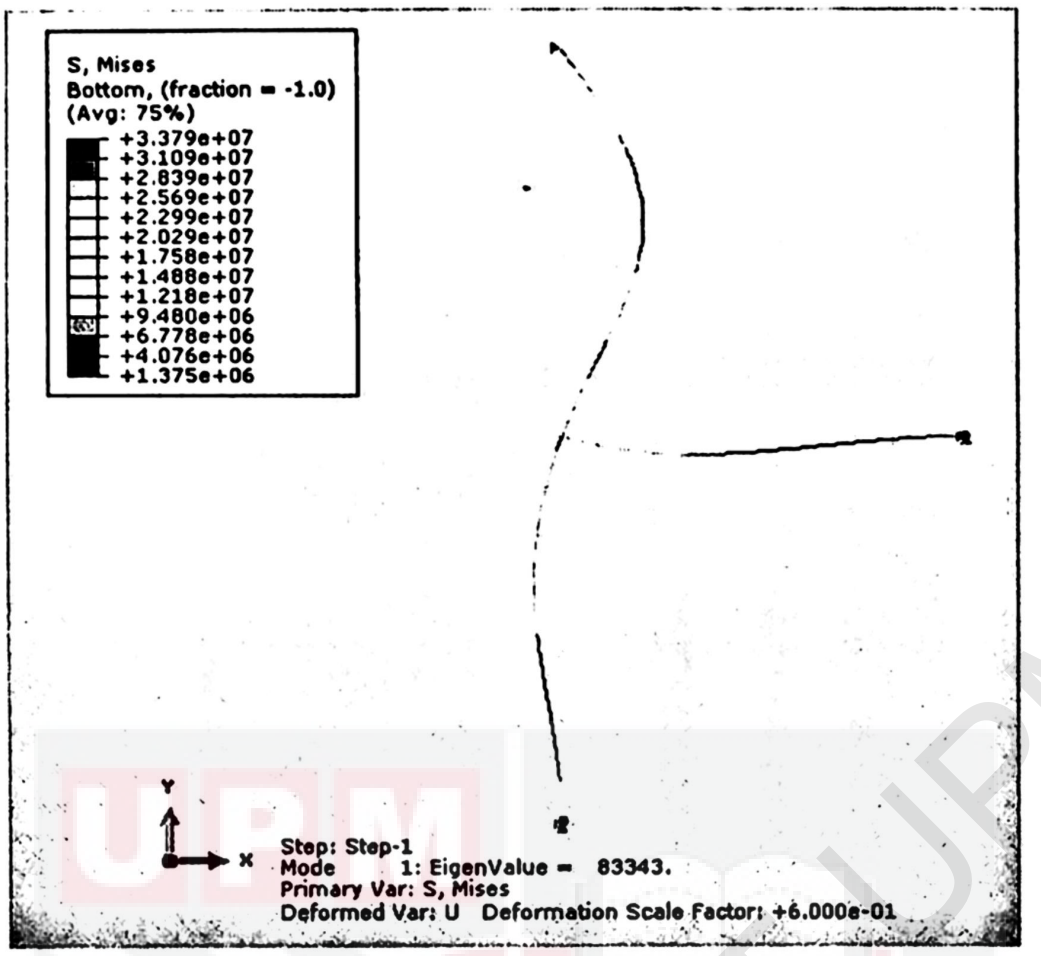

Figure 4.10 Mises Stress contour for 0° angle

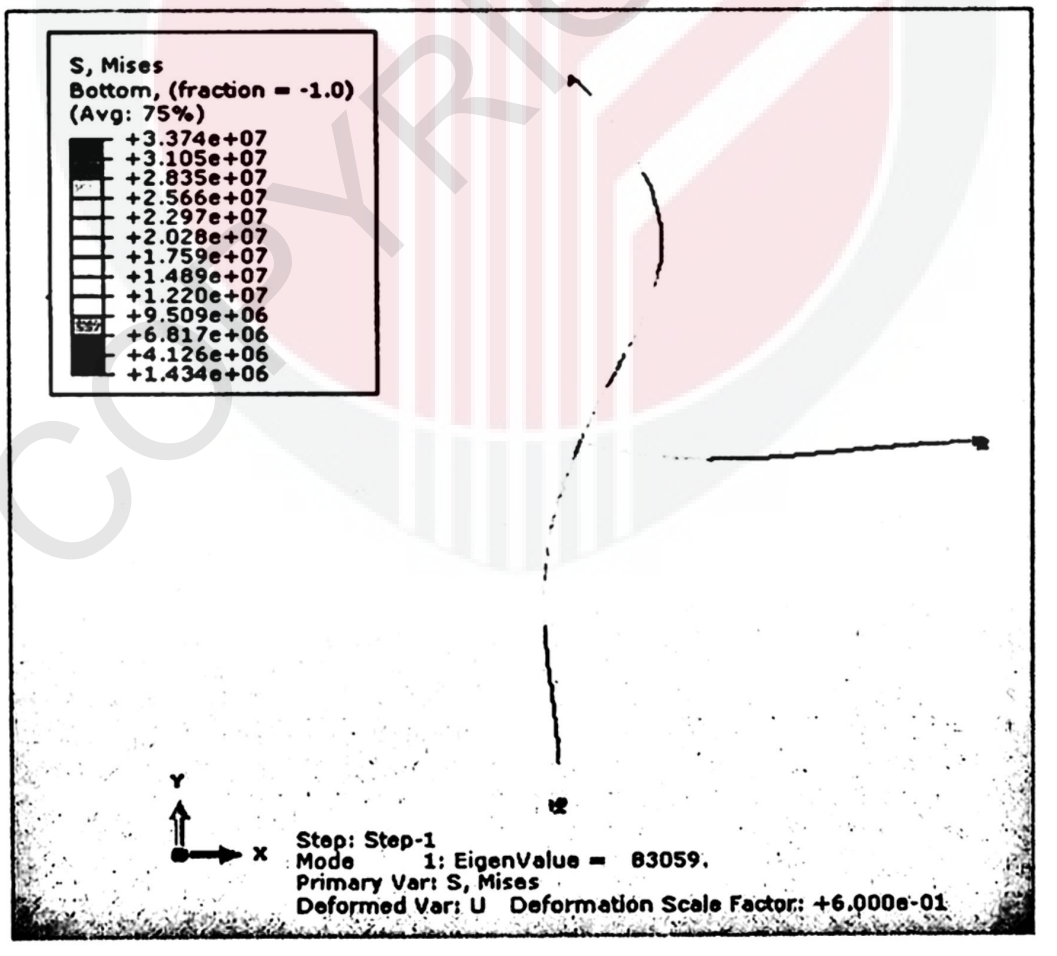

Figure 4.11 Mises Stress contour for 3° angle

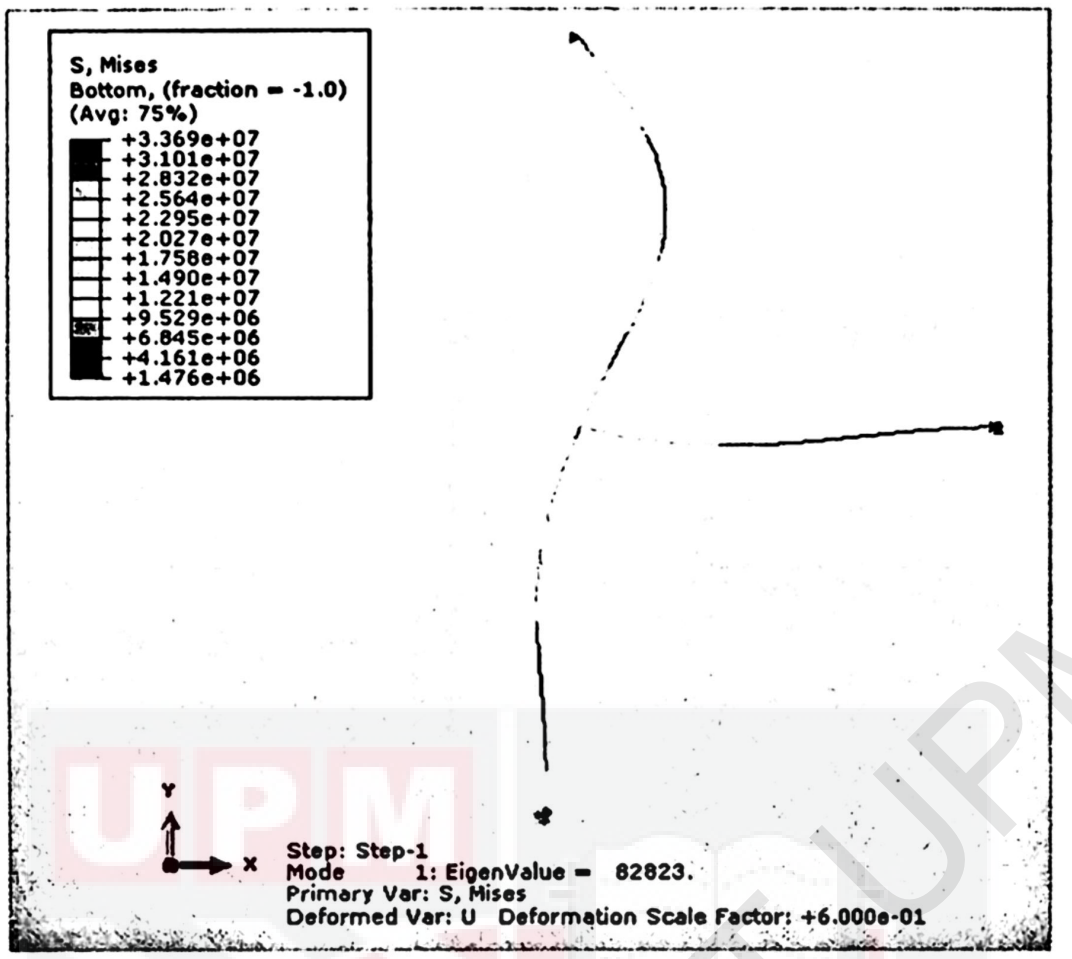

Figure 4.12 Mises Stress Contour for 5° angle

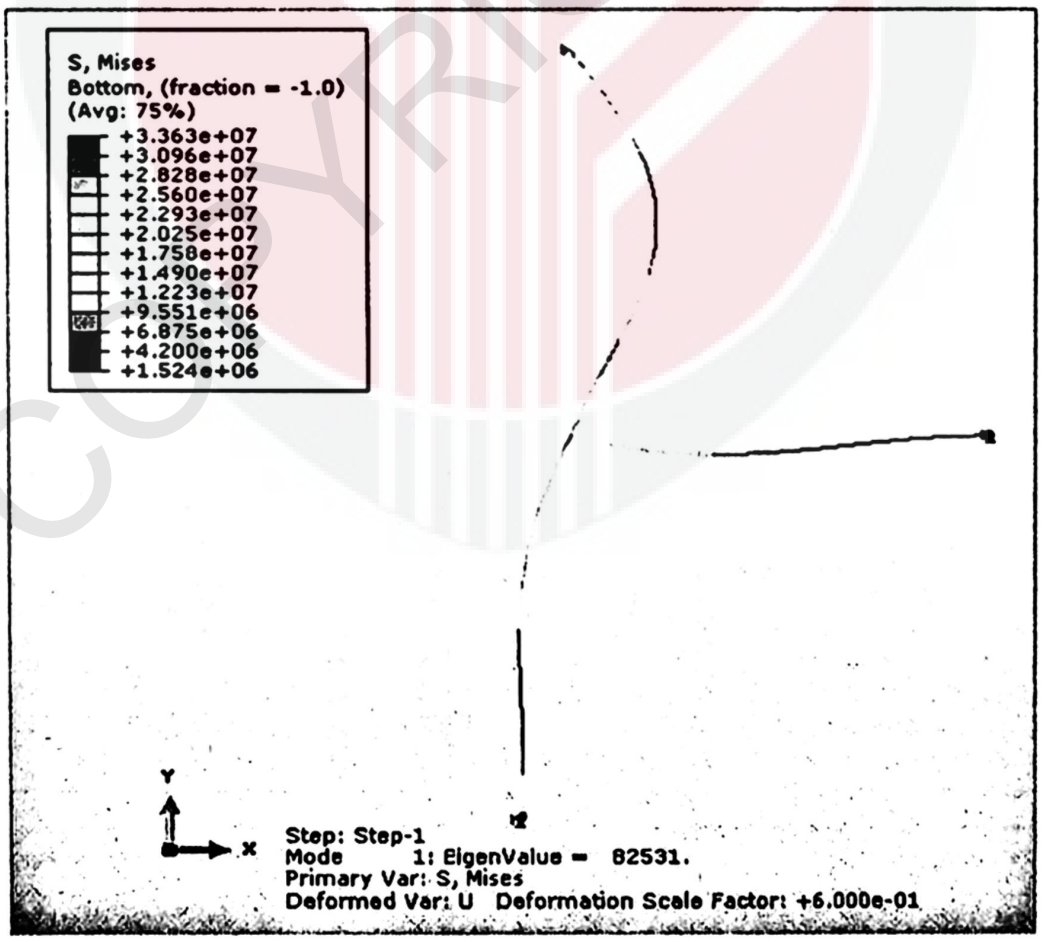

Figure 4.13 Mises Stress Contour for 7° angle

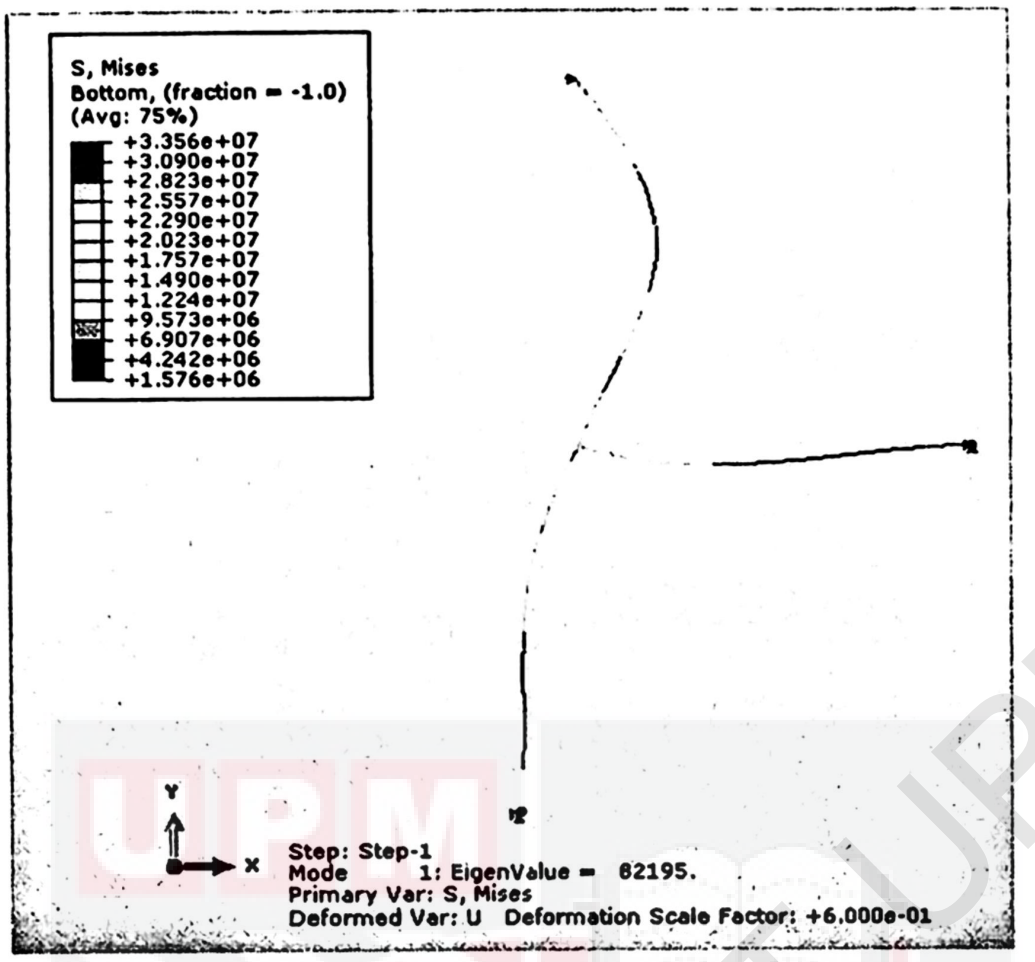

Figure 4.14 Mises Stress Contour for 9° angle

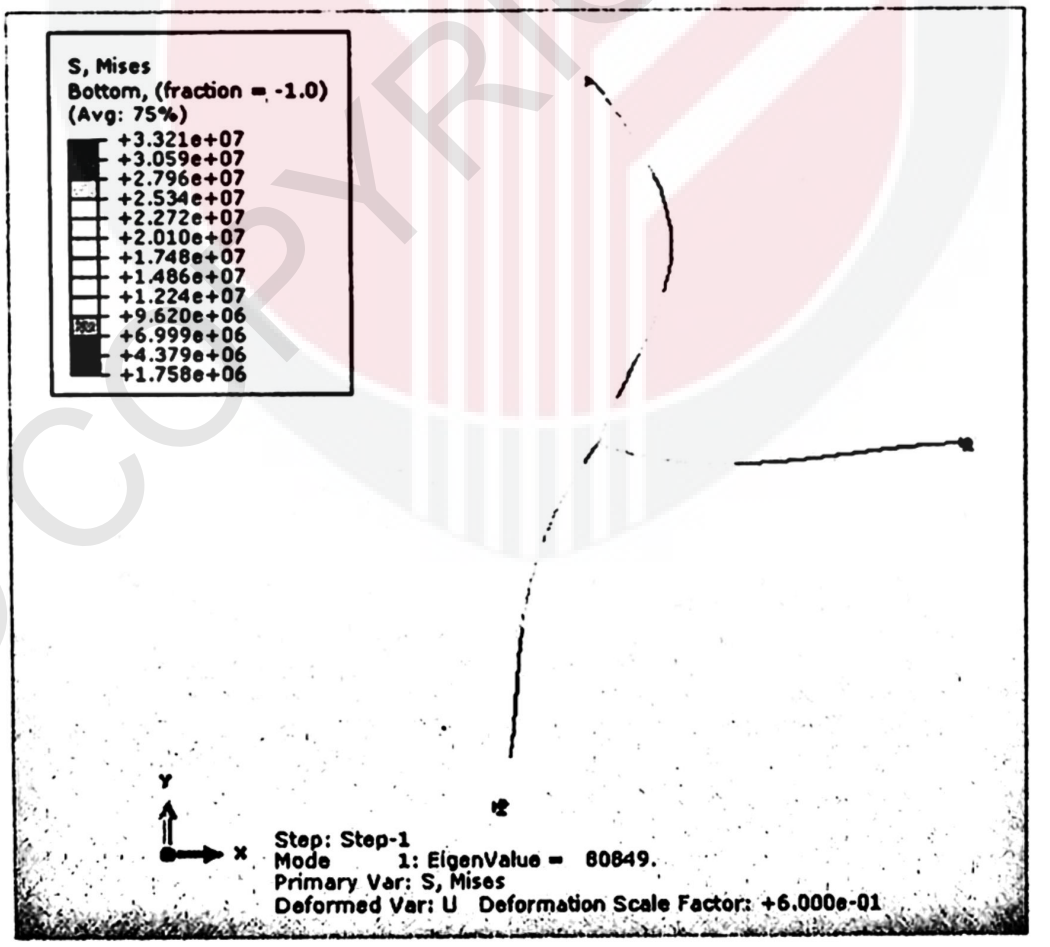

Figure 4.15 Mises Stress Contour for 15° angle

4.3.2.3 Bending Strain, E

Bending strain of the structure is the deformation in terms of elongation of the structure. Strain also is the ratio of the change in length caused by the applied force to the original length. Figures 4.15, 4.16, 4.17, 4.18, 4.19 and 4.20 show the maximum principal contour for strain depicted at the various angle of slanted column. Basically, the bending strain is proportional to the bending stress of structure. Based on Figures 4.15, 4.16, 4.17, 4.18, 4.19 and 4.20, the maximum strain occurs at the connection indicates the red color.

The values for maximum principal strain that occurs at angle 0°, 3°, 5°, 7°, 9° and 15° are 0.0089, 0.088, 0.087, 0.0867, 0.086 and 0.083 respectively. From these figures and results obtained, it can be concluded that the compressive strain is larger at the slanted column on lower part of column and decreased as the angle of slanted column more wider.

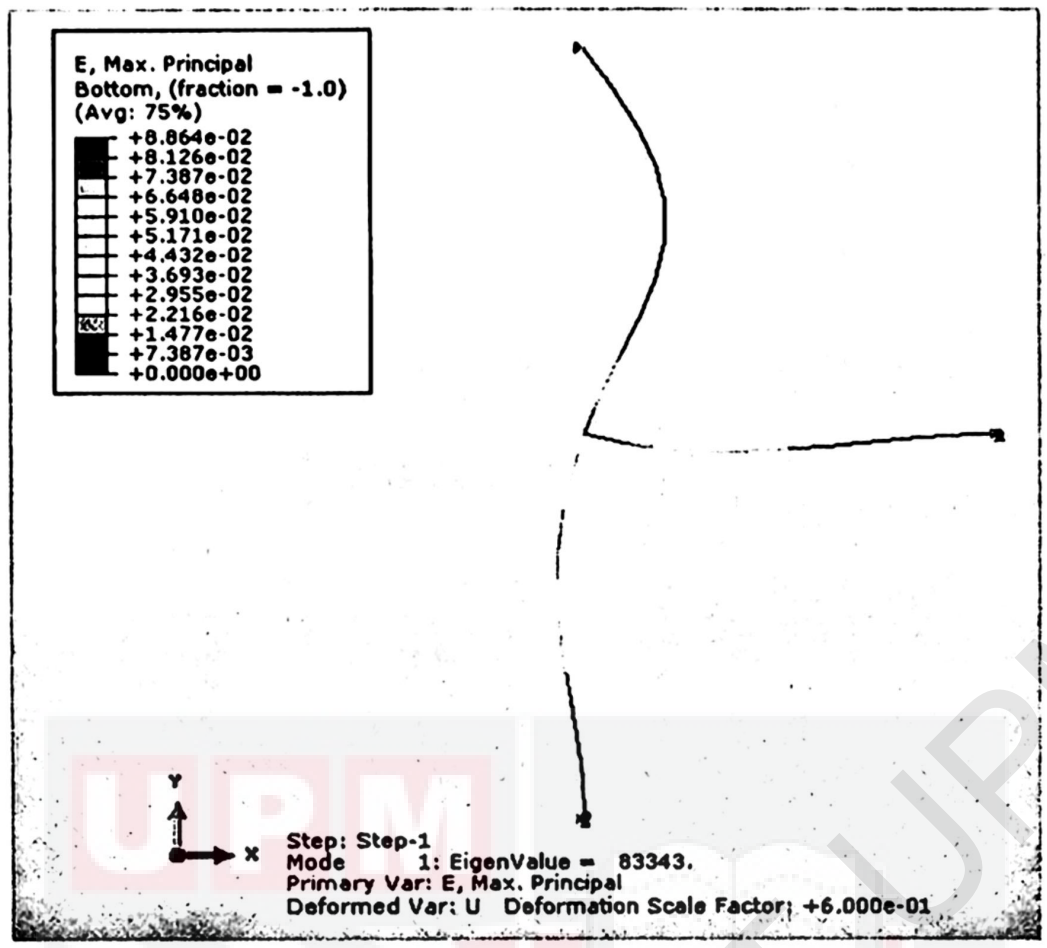

Figure 4.16 Maximum principal contour for strain of 0° angle

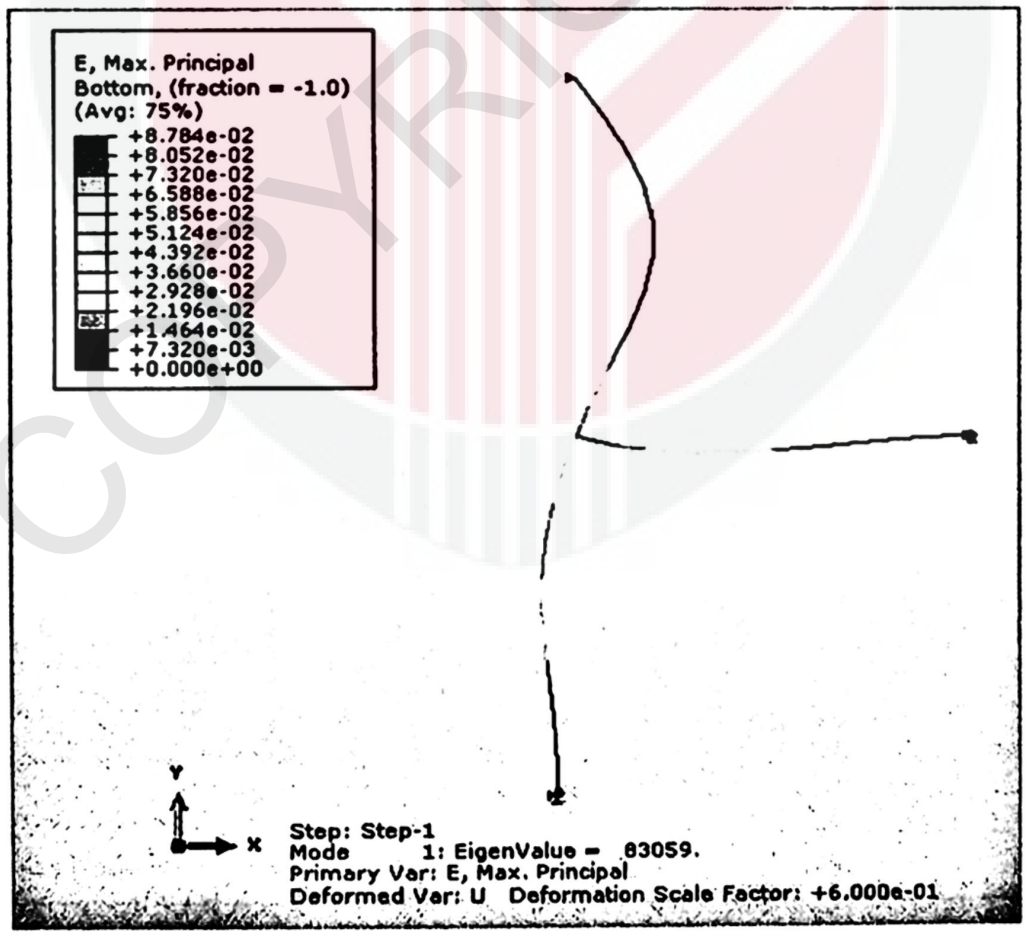

Figure 4.17 Maximum principal contour for strain of 3° angle

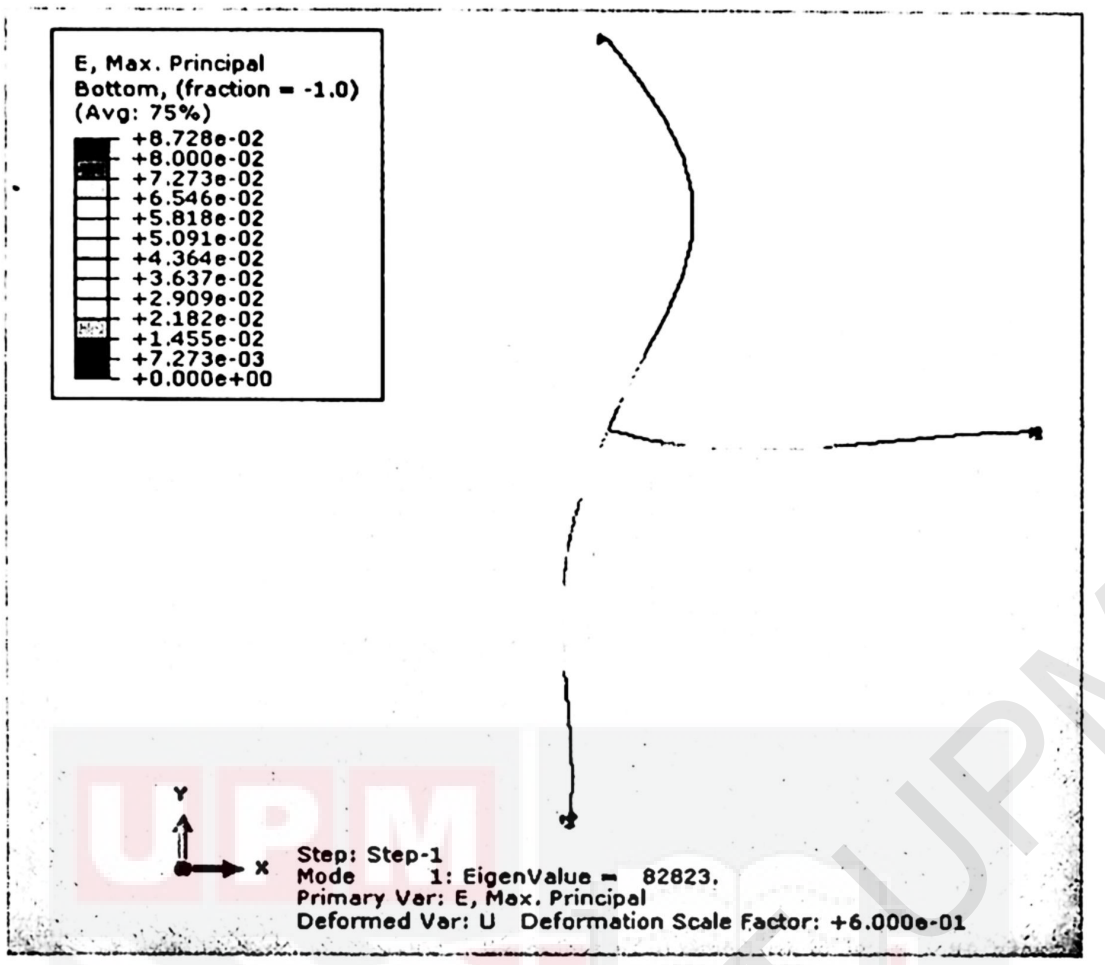

Figure 4.18 Maximum principal contour for strain of 5° angle

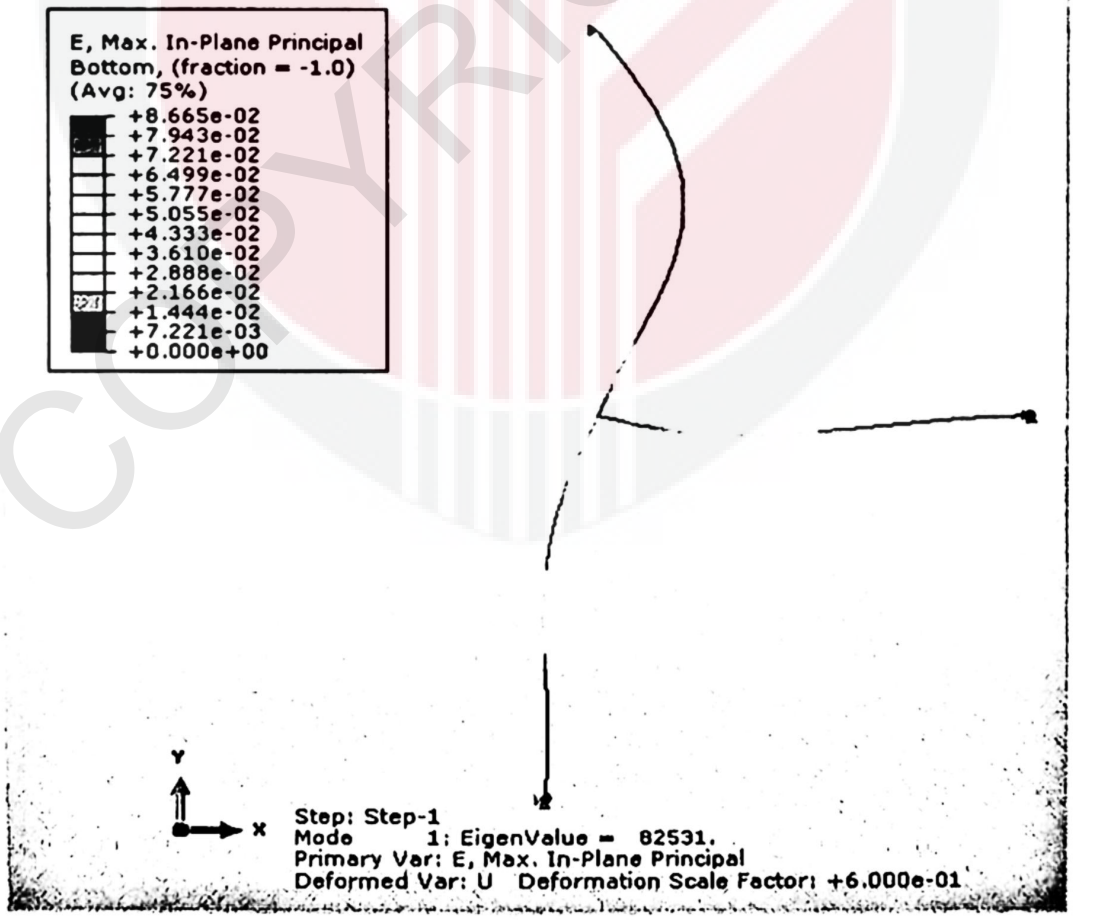

Figure 4.19 Maximum principal contour for strain of 7° angle

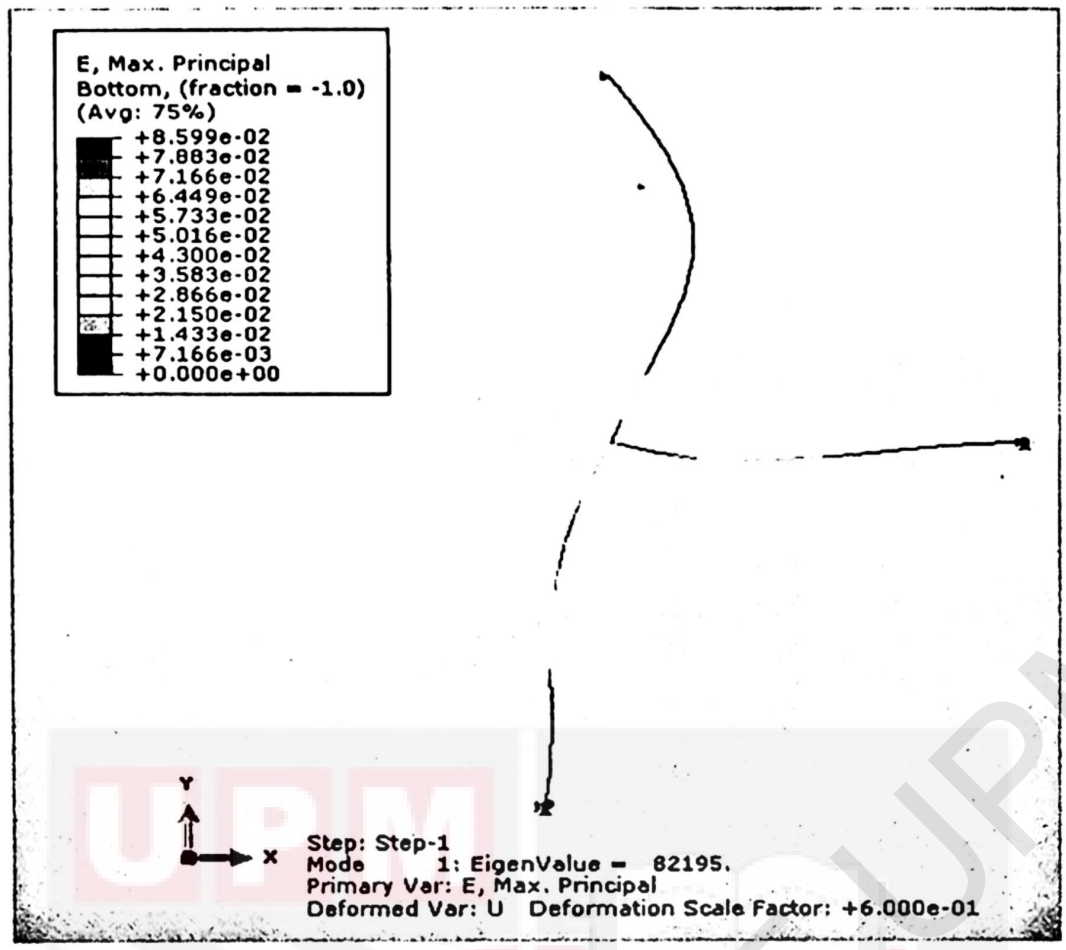

Figure 4.20 Maximum principal contour for strain of 9° angle

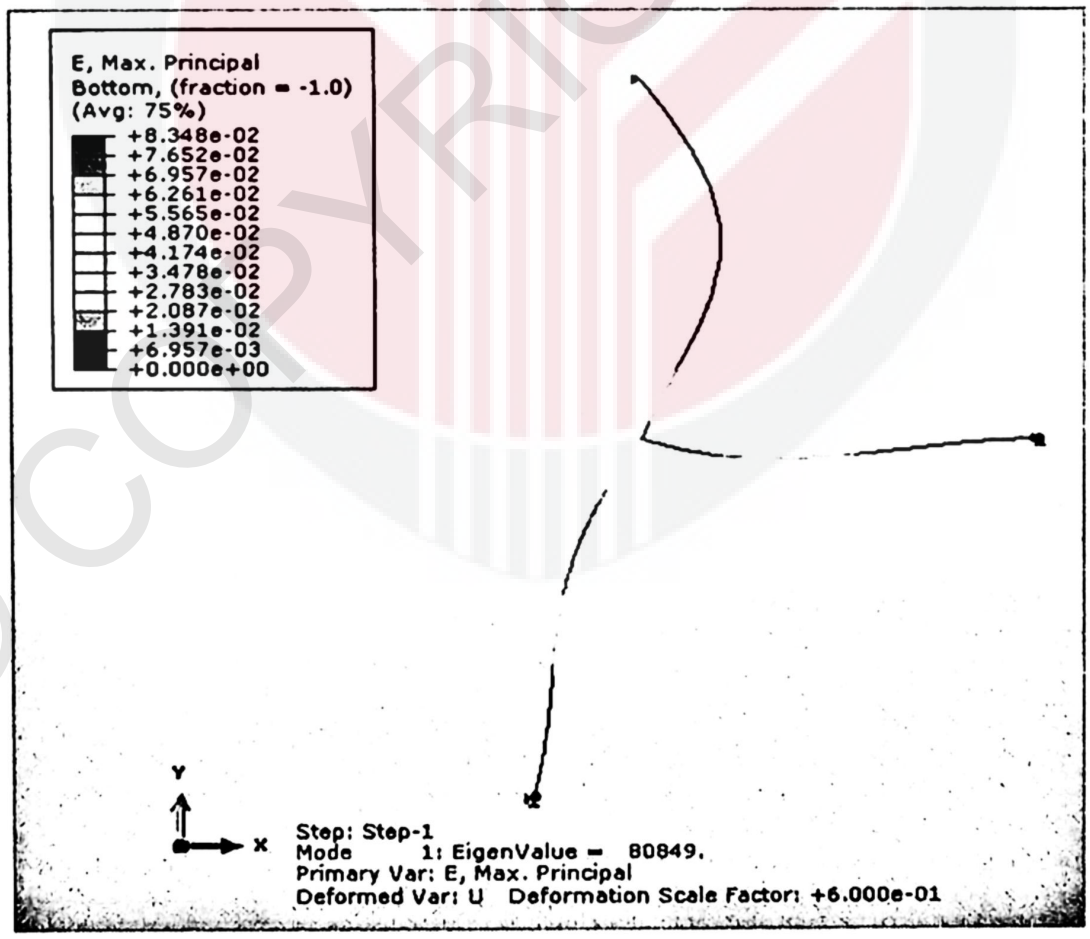

Figure 4.21 Maximum principal contour for strain of 15° angle

4.3.2.4 Displacement, U

Displacement is defined as the distance from which one node or element (beam, column, frame, etc) moved from its original location. The movement could be from a column deflecting, but it could also show result of the entire object moving like a box sliding on a surface with friction. Displacement also can both be measured in terms of distance and in terms of rotation. Figures 4.22, 4.23, 4.24, 4.25, 4.26 and 4.27 show the displacement contour and its deformed shape depicted at maximum load for the different angle of slanted column. The result show maximum displacement area happens at upper column part indicate by red color.

Based on figures 4.22, 4.23, 4.24, 4.25, 4.26 and 4.27, the blue color of contour indicates the minimum displacement which occur at the area near to the boundary condition and also at the connection. This is because, the fixed end condition applied at the base of lower column and also end of the beam component does not allow any rotation and translation to occur. Besides that, the displacement contour at the connection show 0 displacement value so it considering the connection is in fixed condition. Meanwhile, the displacement at slanted column gives small displacement which range from 0.25 to 0.33m. Between figure 4.27 and 4.22, it indicates that the effect of local buckling is quite higher to be happen where the column is slant at angle 15° compare to angle 0° which can be observe in 3D modelling analysis to get the results in details.

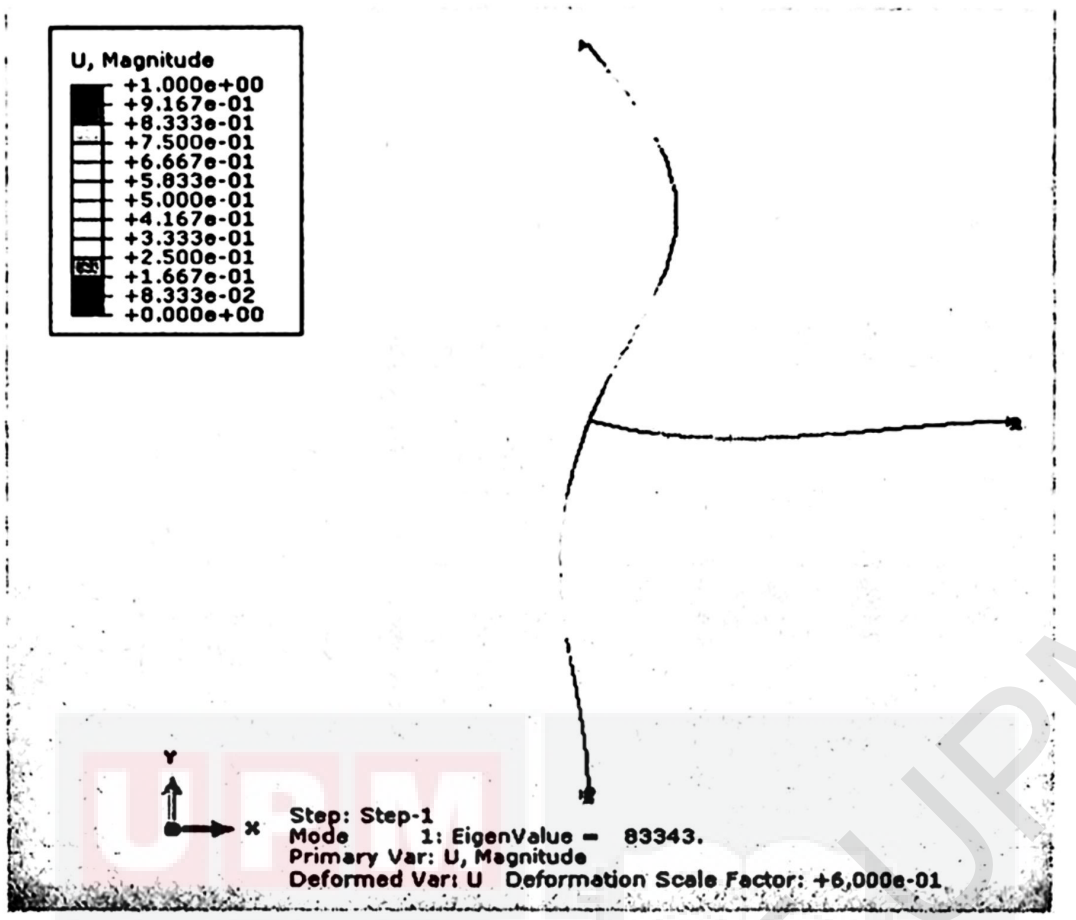

Figure 4.22 Displacement contour for 0° angle of slanted column

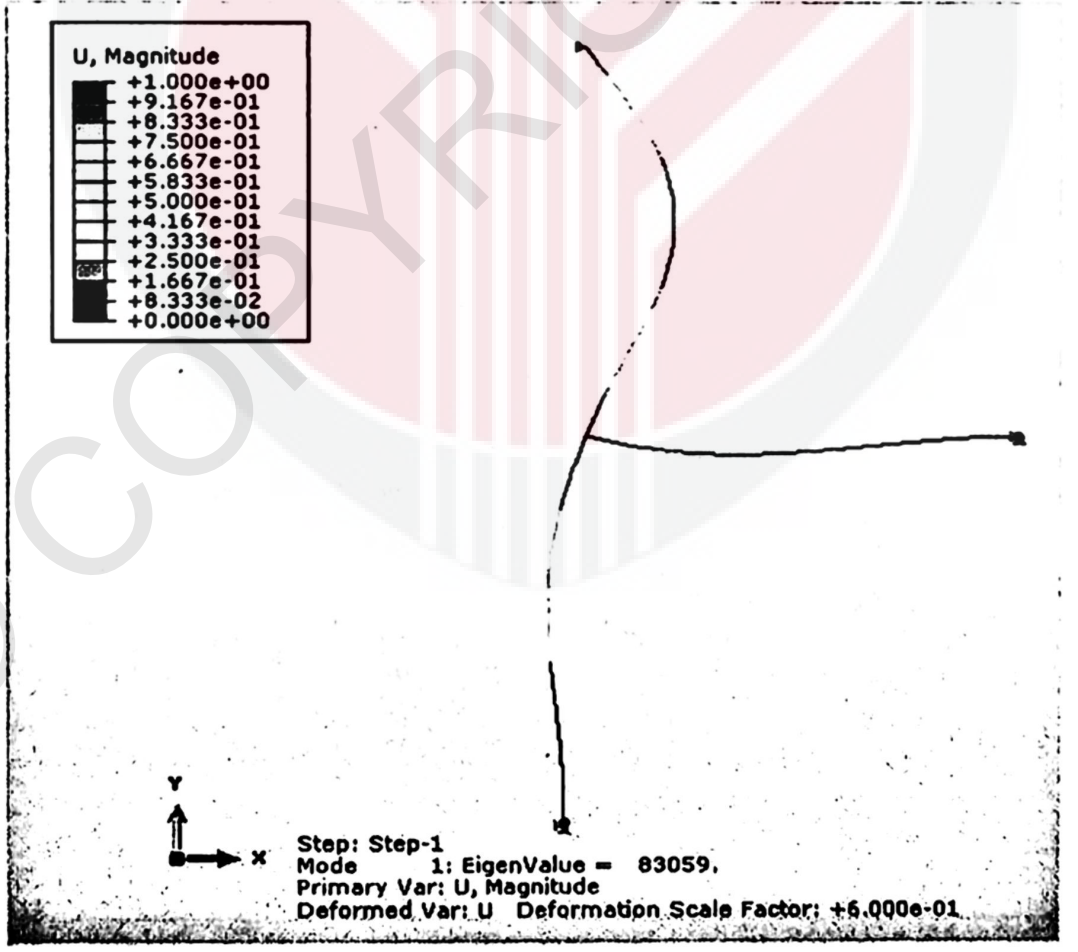

Figure 4.23 Displacement contour for 3° angle of slanted column

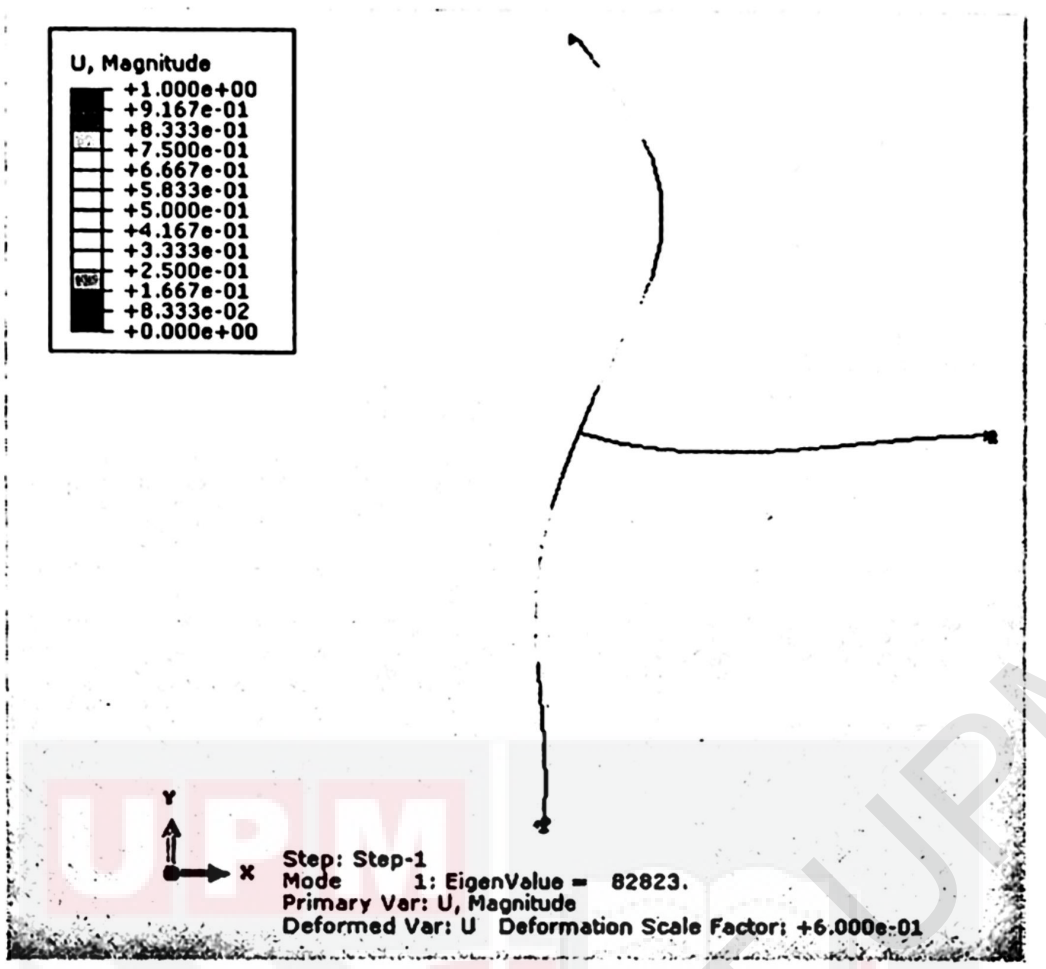

Figure 4.24 Displacement contour for 5° angle of slanted column

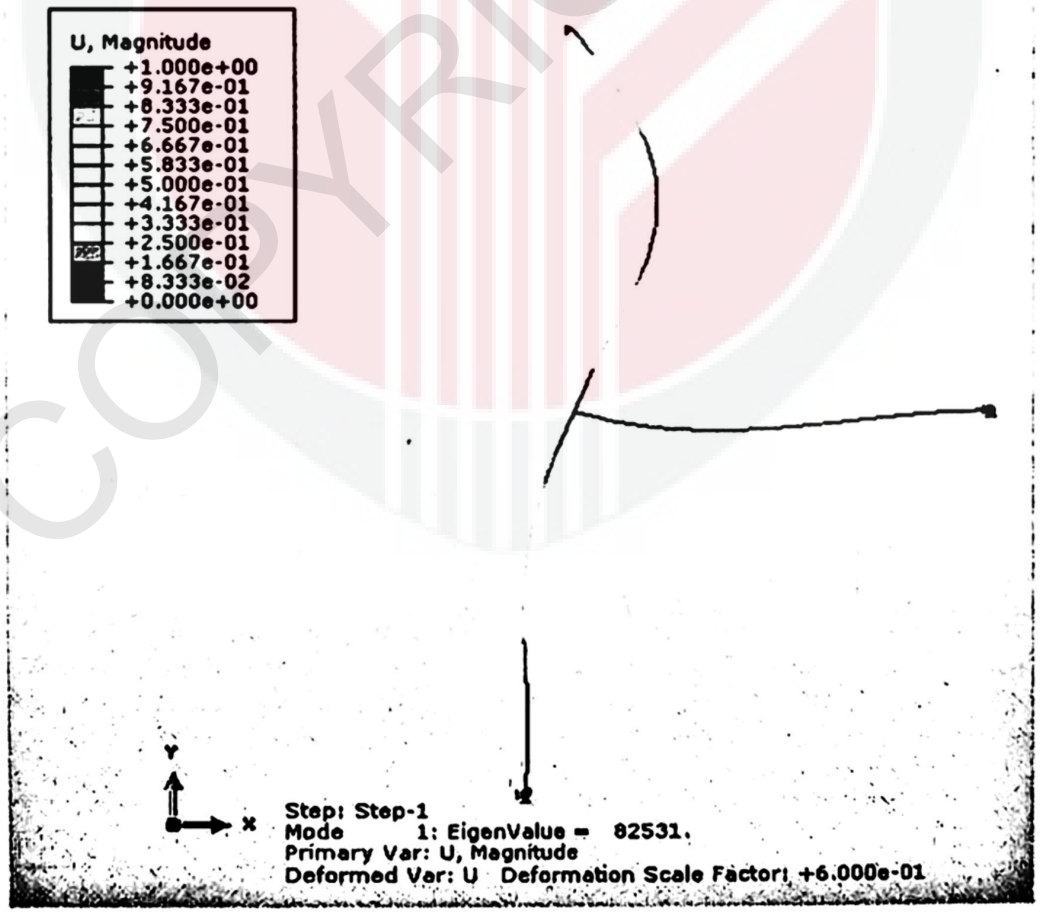

Figure 4.25 Displacement contour for 7° angle of slanted column

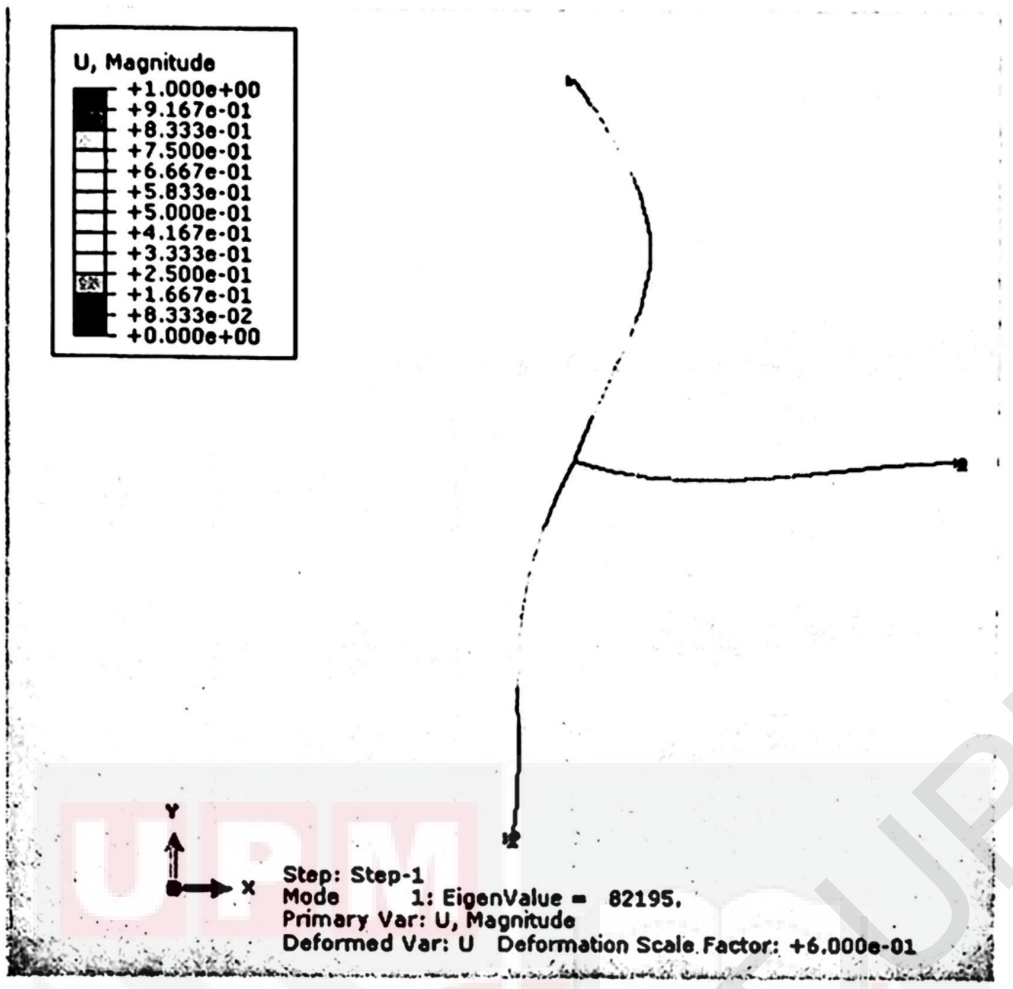

Figure 4.26 Displacement contour for 9° angle of slanted column

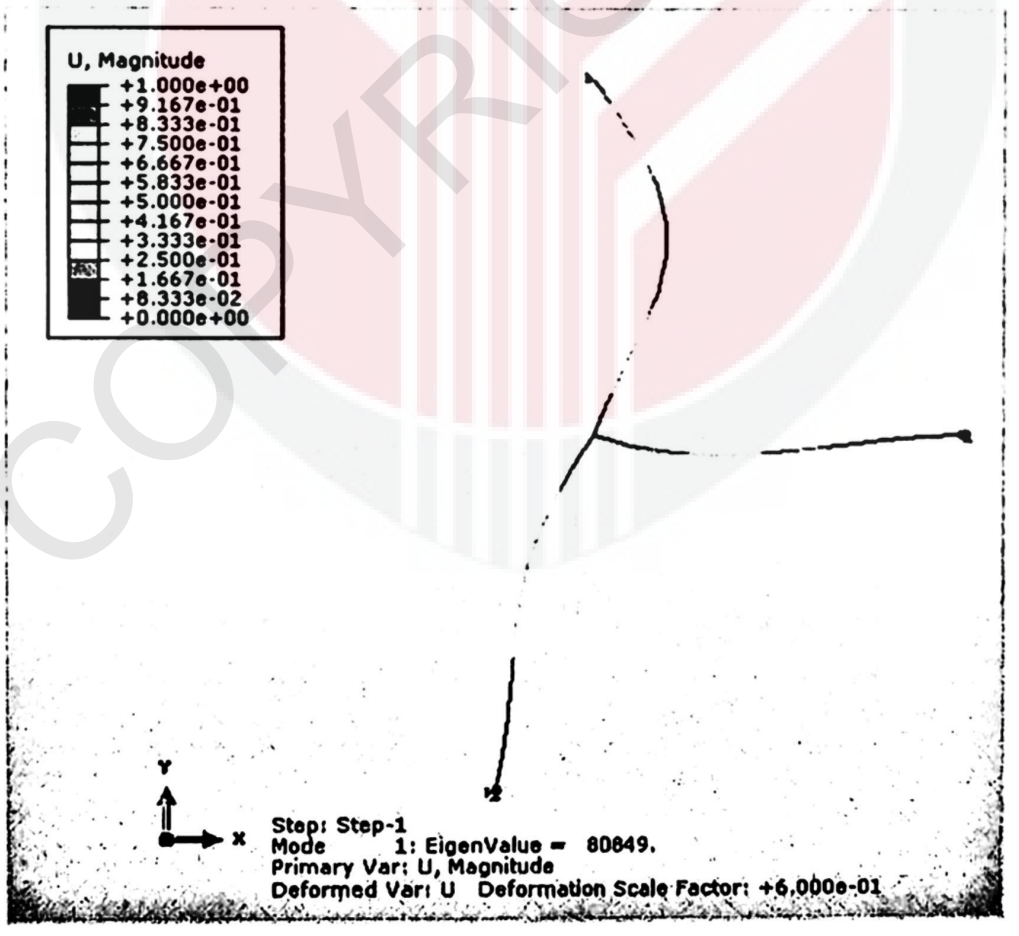

Figure 4.27 Displacement contour for 15° angle of slanted column

CHAPTER 5

CONCLUSION AND RECOMMENDATIONS

5.1 CONCLUSIONS

This study is focused on the structural behaviour of the slanted column under static load in terms of critical load, bending stress, bending strain and displacement. All the objectives for this case of study has been achieved.

ABAQUS software able to simulate the linear behaviour of the slanted column under static column. The proposed model is also capable of predicting the failures in the slanted column. In order to show the reliability of the software, a simple column been simulated and comparison showed that the results are in acceptable range.

6 types of model with various angle of slanted column been simulated in this case study are 0°, 3°, 5°, 7°, 9°, and 15°. Observation on the deformation is observe through

the maximum principle contour of the failures mode of slanted column due to increasing of angle column. Based on the verification study, it shows that the good agreement between the simulation result and manual calculation which the range of difference is not exceed 30%.

After that, the new k-factor which is column effective length factor is developed from Euler's formula. The consideration of angle of slanted column taken into the account so that the k factor is changed as the length of column changed. For this case study, the boundary condition is fixed-pinned end condition which gives $P_{CT} = \frac{2\pi^2 EI}{(L')^2}$, where $L' = \frac{L}{\cos\theta}$. Therefore, new k developed as $k = \frac{0.7}{\cos\theta}$.

The simulation on 3D modelling gives the shape of deflection of structure as expected. Based on the result obtained, it can be concluded that there are tensile strength exists when the angle of slanted column increase. The strength of the column decreases as the angle increase. Besides that, the displacement of the structure increases as the angle increases. Even though the increment in critical load is not so big, it is due to the small amount of inclined prescribed during this study. However, the result show the bending stress and strain show the decrement as the angle of slanted column increases.

5.2 RECOMMENDATION

Due to the time constraints, the model of slanted column discussed in this report is worth to be continued. The research can be extended to cover more detailed analysis with consideration of other factors especially on 3 Dimensional modelling so that can see the local buckling of the structure more details. Besides that, research on the finite element analysis on slanted column under dynamic load after this can be conducted. Another suggestion would be the behaviour of the slanted column under different types of boundary condition with simulation on 3D finite element only. Even though the deformation or buckling analysis was predicted very well by the finite element analysis, the analysis under service condition need in deep study.

REFERENCES

A.M Tarbia, H. A. (2014). Strengthening of RC columns by steel angles and strips. *Alexandria Engineering Journal*.

Andrew D. Speirs, M. O. (n.d.). Physiologically based boundary conditions in finite element modelling. *Journal of Biomechanics*, 2006.

Apostol, T. (1973). Another Elementary Proof of Euler's Formula for ζ(2n). *The American Mathematical Monthly*, 425-431.

Atay, M. T. (2011). Determination of Critical Buckling Loads for Variable Stiffness Euler Columns Using Homotopy Perturbation Method. *International Journal of Nonlinear Sciences and Numerical Simulation*.

Chang, C.-H. (1974). Buckling of Slanted Columns. *Journal of the Engineering Mechanics Division*, 737-756.

Cheng Yua, B. W. (2006). Simulation of cold-formed steel beams in local and distortional buckling. *Journal of Constructional Steel Research*.

Dayton, T. B. (2016). *Static-Dynamic-Load-Test*. Retrieved from http://www.dtbtest.com

Demetri Terzopoulos, K. F. (n.d.). Deformable models. *Visual Computer*.

E. Giner a, N. S. (2008). An Abaqus implementation of the extended finite element method. *Engineering Fracture Mechanics*.

Fellenius, B. (2016). ELASTIC MODULUS DETERMINATION.

Henry Khov, W. L. (2009). An accurate solution method for the static and dynamic deflections of orthotropic plates with general boundary conditions. *Composite Structures*.

Howland, F., Egger, W., Mayerjak, R., & Munz, R. (2009). Static and Dynamic Load Deflection Tests of Steel Structures. *Structural Research Series 092*.

Jian Zhao, J. J. (2008). Post-buckling and snap-through behaviour of inclined slender beam. *Journal of Applied Mechanics*.

Lin-Hai Han, Q.-x. R. (2010). Tests on inclined, tapered and STS concrete-filled steel tubular(CFST) stub columns. *Journal of Constructional Steel Research*.

Negussie Tebedge, L. T. (2002). PROCEDURE FOR TESTING CENTRALLY LOADED COLUMNS. *European Column Studies*.

Yong-Lin Pi, N. S. (2006). Non-linear buckling and postbuckling of elastic arches. *The Centre for Advanced Structural engineering*.

Yong-Wan Kim, J. S. (2012). Performance evaluation of FR welded connection to inclined column. *15 WCEE LISBOA*.

APPENDIX A

ABAQUS FIELD OUTPUT REPORT

```
********************************************************************************
   ODB: D:/Temp/deg0.odb
   Frame: Mode         1: EigenValue =   83343.

Loc 1 : Element nodal  values at beam < circular > < elset = ASSEMBLY_PART-1-
1__PICKEDSET2 > from source 1 : Bottom, (fraction = -1.0) ( Average criteria = 75%, Not
averaged across region boundaries )
Loc 2 : Element nodal  values at beam < circular > < elset = ASSEMBLY_PART-1-
1__PICKEDSET2 > from source 1 : Top, (fraction = 1.0) ( Average criteria = 75%, Not
averaged across region boundaries )

Field Output reported at element nodes for region: PART-1-1.Region_1
   Computation algorithm: EXTRAPOLATE_COMPUTE_AVERAGE
```

Element Label	Node Label	E.Max. Prin @Loc 1	E.Max. Prin @Loc 2	S.Max. Prin @Loc 1	S.Max. Prin @Loc 2
1	1	0.	33.52E-03	0.	6.705E+06
1	5	0.	64.52E-03	0.	12.90E+06
2	5	0.	64.52E-03	0.	12.90E+06
2	6	0.	119.3E-03	0.	23.85E+06
3	6	0.	119.3E-03	0.	23.85E+06
3	7	0.	155.9E-03	0.	31.19E+06
4	7	0.	155.9E-03	0.	31.19E+06
4	8	0.	169.0E-03	0.	33.79E+06
5	8	0.	169.0E-03	0.	33.79E+06
5	9	0.	156.4E-03	0.	31.28E+06
6	9	0.	156.4E-03	0.	31.28E+06
6	10	0.	120.1E-03	0.	24.02E+06
7	10	0.	120.1E-03	0.	24.02E+06
7	11	0.	65.64E-03	0.	13.13E+06
8	11	0.	65.64E-03	0.	13.13E+06
8	12	16.16E-03	17.37E-03	3.233E+06	3.475E+06
9	12	16.16E-03	17.37E-03	3.233E+06	3.475E+06
9	13	63.41E-03	0.	12.68E+06	0.
10	2	88.64E-03	0.	17.73E+06	0.
10	13	63.41E-03	0.	12.68E+06	0.
21	2	88.64E-03	0.	17.73E+06	0.
21	23	75.91E-03	0.	15.18E+06	0.
22	23	75.91E-03	0.	15.18E+06	0.
22	24	62.15E-03	0.	12.43E+06	0.
23	24	62.15E-03	0.	12.43E+06	0.
23	25	48.39E-03	0.	9.678E+06	0.
24	25	48.39E-03	0.	9.678E+06	0.
24	26	34.64E-03	0.	6.927E+06	0.
25	26	34.64E-03	0.	6.927E+06	0.
25	27	20.89E-03	0.	4.177E+06	0.
26	27	20.89E-03	0.	4.177E+06	0.
26	28	7.136E-03	0.	1.427E+06	0.
27	28	7.136E-03	0.	1.427E+06	0.
27	29	130.9E-06	4.248E-03	26.19E+03	849.6E+03
28	29	130.9E-06	4.248E-03	26.19E+03	849.6E+03
28	30	0.	15.37E-03	0.	3.074E+06
29	30	0.	15.37E-03	0.	3.074E+06
29	31	0.	29.12E-03	0.	5.824E+06
30	4	0.	36.00E-03	0.	7.199E+06
30	31	0.	29.12E-03	0.	5.824E+06
Minimum		0.	0.	0.	0.
At Element		30	27	30	27
Node		4	28	4	28
Maximum		88.64E-03	169.0E-03	17.73E+06	33.79E+06
At Element		21	5	10	4
Node		2	8	2	8

Field Output reported at element nodes for region: PART-1-1.Region_2

Element Label	Node Label	E.Max. Prin @Loc 1	E.Max. Prin @Loc 2	S.Max. Prin @Loc 1	S.Max. Prin @Loc 2
11	2	43.87E-03	0.	8.774E+06	0.
11	14	53.32E-03	0.	10.66E+06	0.
12	14	53.32E-03	0.	10.66E+06	0.
12	15	67.59E-03	0.	13.52E+06	0.
13	15	67.59E-03	0.	13.52E+06	0.
13	16	71.90E-03	0.	14.38E+06	0.
14	16	71.90E-03	0.	14.38E+06	0.
14	17	65.58E-03	0.	13.12E+06	0.
15	17	65.58E-03	0.	13.12E+06	0.
15	18	49.59E-03	0.	9.918E+06	0.
16	18	49.59E-03	0.	9.918E+06	0.
16	19	26.35E-03	0.	5.270E+06	0.
17	19	26.35E-03	0.	5.270E+06	0.
17	20	6.651E-03	8.803E-03	1.330E+06	1.761E+06
18	20	6.651E-03	8.803E-03	1.330E+06	1.761E+06
18	21	0.	30.33E-03	0.	6.066E+06
19	21	0.	30.33E-03	0.	6.066E+06
19	22	0.	52.65E-03	0.	10.53E+06
20	3	0.	62.24E-03	0.	12.45E+06
20	22	0.	52.65E-03	0.	10.53E+06
Minimum		0.	0.	0.	0.
At Element		20	17	20	17
Node		3	19	3	19
Maximum		71.90E-03	62.24E-03	14.38E+06	12.45E+06
At Element		13	20	14	20
Node		16	3	16	3

****

ODB: D:/Temp/deg3.odb
Frame: Mode 1: EigenValue = 83059.

Field Output reported at element nodes for region: PART-1-1.Region_1
Computation algorithm: EXTRAPOLATE_COMPUTE_AVERAGE

Element Label	Node Label	E.Max. Prin @Loc 1	E.Max. Prin @Loc 2	S.Max. Prin @Loc 1	S.Max. Prin @Loc 2
1	1	0.	33.41E-03	0.	6.682E+06
1	5	0.	64.30E-03	0.	12.86E+06
2	5	0.	64.30E-03	0.	12.86E+06
2	6	0.	118.9E-03	0.	23.78E+06
3	6	0.	118.9E-03	0.	23.78E+06
3	7	0.	155.5E-03	0.	31.11E+06
4	7	0.	155.5E-03	0.	31.11E+06
4	8	0.	168.7E-03	0.	33.74E+06
5	8	0.	168.7E-03	0.	33.74E+06
5	9	0.	156.3E-03	0.	31.27E+06
6	9	0.	156.3E-03	0.	31.27E+06
6	10	0.	120.4E-03	0.	24.08E+06
7	10	0.	120.4E-03	0.	24.08E+06
7	11	0.	66.26E-03	0.	13.25E+06
8	11	0.	66.26E-03	0.	13.25E+06
8	12	15.65E-03	17.77E-03	3.130E+06	3.553E+06
9	12	15.65E-03	17.77E-03	3.130E+06	3.553E+06
9	13	62.35E-03	0.	12.47E+06	0.
10	2	87.84E-03	0.	17.57E+06	0.
10	13	62.35E-03	0.	12.47E+06	0.
21	2	87.84E-03	0.	17.57E+06	0.
21	23	75.99E-03	0.	15.20E+06	0.
22	23	75.99E-03	0.	15.20E+06	0.
22	24	63.14E-03	0.	12.63E+06	0.
23	24	63.14E-03	0.	12.63E+06	0.
23	25	49.79E-03	0.	9.958E+06	0.
24	25	49.79E-03	0.	9.958E+06	0.
24	26	36.03E-03	0.	7.207E+06	0.

25	26	36.03E-03	0.	7.207E+06	0.
25	27	21.98E-03	0.	4.396E+06	0.
26	27	21.98E-03	0.	4.396E+06	0.
26	28	7.734E-03	0.	1.547E+06	0.
27	28	7.734E-03	0.	1.547E+06	0.
27	29	289.0E-06	4.467E-03	57.79E+03	893.3E+03
28	29	289.0E-06	4.467E-03	57.79E+03	893.3E+03
28	30	0.	16.06E-03	0.	3.211E+06
29	30	0.	16.06E-03	0.	3.211E+06
29	31	0.	30.20E-03	0.	6.041E+06
30	4	0.	37.23E-03	0.	7.446E+06
30	31	0.	30.20E-03	0.	6.041E+06
Minimum		0.	0.	0.	0.
At Element		30	27	30	27
Node		4	28	4	28
Maximum		87.84E-03	168.7E-03	17.57E+06	33.74E+06
At Element		10	5	10	4
Node		2	8	2	8

Field Output reported at element nodes for region: PART-1-1.Region_2

Element Label	Node Label	E.Max. Prin @Loc 1	E.Max. Prin @Loc 2	S.Max. Prin @Loc 1	S.Max. Prin @Loc 2
11	2	44.23E-03	0.	8.845E+06	0.
11	14	53.77E-03	0.	10.75E+06	0.
12	14	53.77E-03	0.	10.75E+06	0.
12	15	68.19E-03	0.	13.64E+06	0.
13	15	68.19E-03	0.	13.64E+06	0.
13	16	72.54E-03	0.	14.51E+06	0.
14	16	72.54E-03	0.	14.51E+06	0.
14	17	66.15E-03	0.	13.23E+06	0.
15	17	66.15E-03	0.	13.23E+06	0.
15	18	50.00E-03	0.	10.00E+06	0.
16	18	50.00E-03	0.	10.00E+06	0.
16	19	26.52E-03	0.	5.305E+06	0.
17	19	26.52E-03	0.	5.305E+06	0.
17	20	6.670E-03	8.867E-03	1.334E+06	1.773E+06
18	20	6.670E-03	8.867E-03	1.334E+06	1.773E+06
18	21	0.	30.59E-03	0.	6.117E+06
19	21	0.	30.59E-03	0.	6.117E+06
19	22	0.	53.12E-03	0.	10.62E+06
20	3	0.	62.80E-03	0.	12.56E+06
20	22	0.	53.12E-03	0.	10.62E+06
Minimum		0.	0.	0.	0.
At Element		20	17	20	17
Node		3	19	3	19
Maximum		72.54E-03	62.80E-03	14.51E+06	12.56E+06
At Element		14	20	13	20
Node		16	3	16	3

****

ODB: D:/Temp/deg5.odb
Frame: Mode 1: EigenValue = 82823.

Field Output reported at element nodes for region: PART-1-1.Region_1
Computation algorithm: EXTRAPOLATE_COMPUTE_AVERAGE

Element Label	Node Label	E.Max. Prin @Loc 1	E.Max. Prin @Loc 2	S.Max. Prin @Loc 1	S.Max. Prin @Loc 2
1	1	0.	33.3160E-03	0.	6.66321E+06
1	5	0.	64.1281E-03	0.	12.8256E+06
2	5	0.	64.1281E-03	0.	12.8256E+06
2	6	0.	118.602E-03	0.	23.7205E+06
3	6	0.	118.602E-03	0.	23.7205E+06
3	7	0.	155.213E-03	0.	31.0426E+06
4	7	0.	155.213E-03	0.	31.0426E+06
4	8	0.	168.446E-03	0.	33.6892E+06

5	8	0.	168.446E-03	0.	33.6892E+06
5	9	0.	156.308E-03	0.	31.2615E+06
6	9	0.	156.308E-03	0.	31.2615E+06
6	10	0.	120.627E-03	0.	24.1253E+06
7	10	0.	120.627E-03	0.	24.1253E+06
7	11	0.	66.7772E-03	0.	13.3554E+06
8	11	0.	66.7772E-03	0.	13.3554E+06
8	12	15.2267E-03	18.0931E-03	3.04535E+06	3.61861E+06
9	12	15.2267E-03	18.0931E-03	3.04535E+06	3.61861E+06
9	13	61.4763E-03	0.	12.2953E+06	0.
10	2	87.2763E-03	0.	17.4553E+06	0.
10	13	61.4763E-03	0.	12.2953E+06	0.
21	2	87.2763E-03	0.	17.4553E+06	0.
21	23	76.1642E-03	0.	15.2328E+06	0.
22	23	76.1642E-03	0.	15.2328E+06	0.
22	24	63.9200E-03	0.	12.7840E+06	0.
23	24	63.9200E-03	0.	12.7840E+06	0.
23	25	50.8262E-03	0.	10.1652E+06	0.
24	25	50.8262E-03	0.	10.1652E+06	0.
24	26	37.0504E-03	0.	7.41008E+06	0.
25	26	37.0504E-03	0.	7.41008E+06	0.
25	27	22.7689E-03	0.	4.55379E+06	0.
26	27	22.7689E-03	0.	4.55379E+06	0.
26	28	8.16467E-03	0.	1.63293E+06	0.
27	28	8.16467E-03	0.	1.63293E+06	0.
27	29	402.516E-06	4.62418E-03	80.5033E+03	924.837E+03
28	29	402.516E-06	4.62418E-03	80.5033E+03	924.837E+03
28	30	0.	16.5536E-03	0.	3.31073E+06
29	30	0.	16.5536E-03	0.	3.31073E+06
29	31	0.	30.9958E-03	0.	6.19916E+06
30	4	0.	38.1327E-03	0.	7.62653E+06
30	31	0.	30.9958E-03	0.	6.19916E+06

Minimum	0.	0.	0.	
At Element	30	27	30	27
Node	4	28	4	28
Maximum	87.2763E-03	168.446E-03	17.4553E+06	33.6892E+06
At Element	21	4	10	4
Node	2	8	2	8
Total	846.553E-03	1.91218	169.311E+06	382.437E+06

Field Output reported at element nodes for region: PART-1-1.Region_2

Element Label	Node Label	E.Max. Prin @Loc 1	E.Max. Prin @Loc 2	S.Max. Prin @Loc 1	S.Max. Prin @Loc 2
11	2	44.2436E-03	0.	8.84873E+06	0.
11	14	53.9358E-03	0.	10.7872E+06	0.
12	14	53.9358E-03	0.	10.7872E+06	0.
12	15	68.6063E-03	0.	13.7213E+06	0.
13	15	68.6063E-03	0.	13.7213E+06	0.
13	16	73.0950E-03	0.	14.619E+06	0.
14	16	73.0950E-03	0.	14.619E+06	0.
14	17	66.7214E-03	0.	13.3443E+06	0.
15	17	66.7214E-03	0.	13.3443E+06	0.
15	18	50.4516E-03	0.	10.0903E+06	0.
16	18	50.4516E-03	0.	10.0903E+06	0.
16	19	26.7515E-03	0.	5.35030E+06	0.
17	19	26.7515E-03	0.	5.35030E+06	0.
17	20	6.71875E-03	8.92788E-03	1.34375E+06	1.78558E+06
18	20	6.71875E-03	8.92788E-03	1.34375E+06	1.78558E+06
18	21	0.	30.8350E-03	0.	6.16701E+06
19	21	0.	30.8350E-03	0.	6.16701E+06
19	22	0.	53.5815E-03	0.	10.7163E+06
20	3	0.	63.3486E-03	0.	12.6697E+06
20	22	0.	53.5815E-03	0.	10.7163E+06

Minimum	0.	0.	0.	0.
At Element	20	17	20	17
Node	3	19	3	19

Maximum	73.095E-03	63.3486E-03	14.619E+06	12.6697E+06
At Element	14	20	14	20
Node	16	3	16	3
Total	736.804E-03	250.037E-03	147.361E+06	50.0075E+06

****

ODB: D:/Temp/deg7.odb
Frame: Mode 1: EigenValue = 82531.

Field Output reported at element nodes for region: PART-1-1.Region_1
Computation algorithm: EXTRAPOLATE_COMPUTE_AVERAGE

Element Label	Node Label	E.Max. Prin @Loc 1	E.Max. Prin @Loc 2	S.Max. Prin @Loc 1	S.Max. Prin @Loc 2
1	1	0.	33.20E-03	0.	6.640E+06
1	5	0.	63.91E-03	0.	12.78E+06
2	5	0.	63.91E-03	0.	12.78E+06
2	6	0.	118.2E-03	0.	23.65E+06
3	6	0.	118.2E-03	0.	23.65E+06
3	7	0.	154.8E-03	0.	30.96E+06
4	7	0.	154.8E-03	0.	30.96E+06
4	8	0.	168.2E-03	0.	33.63E+06
5	8	0.	168.2E-03	0.	33.63E+06
5	9	0.	156.3E-03	0.	31.25E+06
6	9	0.	156.3E-03	0.	31.25E+06
6	10	0.	120.9E-03	0.	24.18E+06
7	10	0.	120.9E-03	0.	24.18E+06
7	11	0.	67.41E-03	0.	13.48E+06
8	11	0.	67.41E-03	0.	13.48E+06
8	12	14.70E-03	18.50E-03	2.940E+06	3.699E+06
9	12	14.70E-03	18.50E-03	2.940E+06	3.699E+06
9	13	60.39E-03	0.	12.08E+06	0.
10	2	86.65E-03	0.	17.33E+06	0.
10	13	60.39E-03	0.	12.08E+06	0.
21	2	86.65E-03	0.	17.33E+06	0.
21	23	76.45E-03	0.	15.29E+06	0.
22	23	76.45E-03	0.	15.29E+06	0.
22	24	64.84E-03	0.	12.97E+06	0.
23	24	64.84E-03	0.	12.97E+06	0.
23	25	52.02E-03	0.	10.40E+06	0.
24	25	52.02E-03	0.	10.40E+06	0.
24	26	38.21E-03	0.	7.642E+06	0.
25	26	38.21E-03	0.	7.642E+06	0.
25	27	23.67E-03	0.	4.733E+06	0.
26	27	23.67E-03	0.	4.733E+06	0.
26	28	8.652E-03	0.	1.730E+06	0.
27	28	8.652E-03	0.	1.730E+06	0.
27	29	530.8E-06	4.802E-03	106.2E+03	960.4E+03
28	29	530.8E-06	4.802E-03	106.2E+03	960.4E+03
28	30	0.	17.12E-03	0.	3.423E+06
29	30	0.	17.12E-03	0.	3.423E+06
29	31	0.	31.90E-03	0.	6.380E+06
30	4	0.	39.17E-03	0.	7.834E+06
30	31	0.	31.90E-03	0.	6.380E+06
Minimum		0.	0.	0.	0.
At Element		30	27	30	27
Node		4	28	4	28
Maximum		86.65E-03	168.2E-03	17.33E+06	33.63E+06
At Element		10	5	21	4
Node		2	8	2	8

Field Output reported at element nodes for region: PART-1-1.Region_2

Element Label	Node Label	E.Max. Prin @Loc 1	E.Max. Prin @Loc 2	S.Max. Prin @Loc 1	S.Max. Prin @Loc 2
11	2	44.08E-03	0.	8.815E+06	0.
11	14	53.99E-03	0.	10.80E+06	0.

12	14	53.99E-03	0.	10.80E+06	0.
12	15	69.06E-03	0.	13.81E+06	0.
13	15	69.06E-03	0.	13.81E+06	0.
13	16	73.80E-03	0.	14.76E+06	0.
14	16	73.80E-03	0.	14.76E+06	0.
14	17	67.48E-03	0.	13.50E+06	0.
15	17	67.48E-03	0.	13.50E+06	0.
15	18	51.08E-03	0.	10.22E+06	0.
16	18	51.08E-03	0.	10.22E+06	0.
16	19	27.09E-03	0.	5.419E+06	0.
17	19	27.09E-03	0.	5.419E+06	0.
17	20	6.803E-03	9.009E-03	1.361E+06	1.802E+06
18	20	6.803E-03	9.009E-03	1.361E+06	1.802E+06
18	21	0.	31.17E-03	0.	6.234E+06
19	21	0.	31.17E-03	0.	6.234E+06
19	22	0.	54.20E-03	0.	10.84E+06
20	3	0.	64.07E-03	0.	12.81E+06
20	22	0.	54.20E-03	0.	10.84E+06
Minimum		0.	0.	0.	0.
At Element		20	17	20	17
Node		3	19	3	19
Maximum		73.80E-03	64.07E-03	14.76E+06	12.82E+06
At Element		13	20	13	20
Node		16	3	16	3

****

ODB: D:/Temp/deg9.odb
Frame: Mode 1: EigenValue = 82195.

Field Output reported at element nodes for region: PART-1-1.Region_1
Computation algorithm: EXTRAPOLATE_COMPUTE_AVERAGE

Element Label	Node Label	E.Max. Prin @Loc 1	E.Max. Prin @Loc 2	S.Max. Prin @Loc 1	S.Max. Prin @Loc 2
1	1	0.	33.06E-03	0.	6.613E+06
1	5	0.	63.66E-03	0.	12.73E+06
2	5	0.	63.66E-03	0.	12.73E+06
2	6	0.	117.8E-03	0.	23.56E+06
3	6	0.	117.8E-03	0.	23.56E+06
3	7	0.	154.3E-03	0.	30.87E+06
4	7	0.	154.3E-03	0.	30.87E+06
4	8	0.	167.8E-03	0.	33.56E+06
5	8	0.	167.8E-03	0.	33.56E+06
5	9	0.	156.2E-03	0.	31.24E+06
6	9	0.	156.2E-03	0.	31.24E+06
6	10	0.	121.2E-03	0.	24.25E+06
7	10	0.	121.2E-03	0.	24.25E+06
7	11	0.	68.14E-03	0.	13.63E+06
8	11	0.	68.14E-03	0.	13.63E+06
8	12	14.10E-03	18.96E-03	2.820E+06	3.792E+06
9	12	14.10E-03	18.96E-03	2.820E+06	3.792E+06
9	13	59.14E-03	0.	11.83E+06	0.
10	2	85.99E-03	0.	17.20E+06	0.
10	13	59.14E-03	0.	11.83E+06	0.
21	2	85.99E-03	0.	17.20E+06	0.
21	23	76.84E-03	0.	15.37E+06	0.
22	23	76.84E-03	0.	15.37E+06	0.
22	24	65.87E-03	0.	13.17E+06	0.
23	24	65.87E-03	0.	13.17E+06	0.
23	25	53.31E-03	0.	10.66E+06	0.
24	25	53.31E-03	0.	10.66E+06	0.
24	26	39.45E-03	0.	7.890E+06	0.
25	26	39.45E-03	0.	7.890E+06	0.
25	27	24.63E-03	0.	4.925E+06	0.
26	27	24.63E-03	0.	4.925E+06	0.
26	28	9.174E-03	0.	1.835E+06	0.
27	28	9.174E-03	0.	1.835E+06	0.
27	29	667.8E-06	4.992E-03	133.6E+03	998.4E+03
28	29	667.8E-06	4.992E-03	133.6E+03	998.4E+03

28	30	0.	17.72E-03	0.	3.544E+06
29	30	0.	17.72E-03	0.	3.544E+06
29	31	0.	32.87E-03	0.	6.575E+06
30	4	0.	40.29E-03	0.	8.058E+06
30	31	0.	32.87E-03	0.	6.575E+06
Minimum		0.	0.	0.	0.
At Element		30	27	30	27
Node		4	28	4	28
Maximum		85.99E-03	167.8E-03	17.20E+06	33.56E+06
At Element		21	5	21	4
Node		2	8	2	8

Field Output reported at element nodes for region: PART-1-1.Region_2

Element Label	Node Label	E.Max. Prin @Loc 1	E.Max. Prin @Loc 2	S.Max. Prin @Loc 1	S.Max. Prin @Loc 2
11	2	43.72E-03	0.	8.743E+06	0.
11	14	53.94E-03	0.	10.79E+06	0.
12	14	53.94E-03	0.	10.79E+06	0.
12	15	69.54E-03	0.	13.91E+06	0.
13	15	69.54E-03	0.	13.91E+06	0.
13	16	74.62E-03	0.	14.92E+06	0.
14	16	74.62E-03	0.	14.92E+06	0.
14	17	68.42E-03	0.	13.68E+06	0.
15	17	68.42E-03	0.	13.68E+06	0.
15	18	51.87E-03	0.	10.37E+06	0.
16	18	51.87E-03	0.	10.37E+06	0.
16	19	27.54E-03	0.	5.509E+06	0.
17	19	27.54E-03	0.	5.509E+06	0.
17	20	6.920E-03	9.108E-03	1.384E+06	1.822E+06
18	20	6.920E-03	9.108E-03	1.384E+06	1.822E+06
18	21	0.	31.58E-03	0.	6.316E+06
19	21	0.	31.58E-03	0.	6.316E+06
19	22	0.	54.95E-03	0.	10.99E+06
20	3	0.	64.96E-03	0.	12.99E+06
20	22	0.	54.95E-03	0.	10.99E+06
Minimum		0.	0.	0.	0.
At Element		20	17	20	17
Node		3	19	3	19
Maximum		74.62E-03	64.96E-03	14.92E+06	12.99E+06
At Element		14	20	14	20
Node		16	3	16	3

****

ODB: D:/Temp/deg15.odb
Frame: Mode 1: EigenValue = 80849.

Field Output reported at element nodes for region: PART-1-1.Region_1
Computation algorithm: EXTRAPOLATE_COMPUTE_AVERAGE

Element Label	Node Label	E.Max. Prin @Loc 1	E.Max. Prin @Loc 2	S.Max. Prin @Loc 1	S.Max. Prin @Loc 2
1	1	0.	32.45E-03	0.	6.489E+06
1	5	0.	62.51E-03	0.	12.50E+06
2	5	0.	62.51E-03	0.	12.50E+06
2	6	0.	115.8E-03	0.	23.17E+06
3	6	0.	115.8E-03	0.	23.17E+06
3	7	0.	152.1E-03	0.	30.42E+06
4	7	0.	152.1E-03	0.	30.42E+06
4	8	0.	166.0E-03	0.	33.21E+06
5	8	0.	166.0E-03	0.	33.21E+06
5	9	0.	155.5E-03	0.	31.11E+06
6	9	0.	155.5E-03	0.	31.11E+06
6	10	0.	122.2E-03	0.	24.43E+06
7	10	0.	122.2E-03	0.	24.43E+06
7	11	0.	70.83E-03	0.	14.17E+06
8	11	0.	70.83E-03	0.	14.17E+06

8	12	11.66E-03	20.74E-03	2.332E+06	4.148E+06
9	12	11.66E-03	20.74E-03	2.332E+06	4.148E+06
9	13	54.01E-03	0.	10.80E+06	0.
10	2	83.48E-03	0.	16.70E+06	0.
10	13	54.01E-03	0.	10.80E+06	0.
21	2	83.48E-03	0.	16.70E+06	0.
21	23	78.54E-03	0.	15.71E+06	0.
22	23	78.54E-03	0.	15.71E+06	0.
22	24	69.60E-03	0.	13.92E+06	0.
23	24	69.60E-03	0.	13.92E+06	0.
23	25	57.88E-03	0.	11.58E+06	0.
24	25	57.88E-03	0.	11.58E+06	0.
24	26	43.83E-03	0.	8.766E+06	0.
25	26	43.83E-03	0.	8.766E+06	0.
25	27	28.01E-03	0.	5.602E+06	0.
26	27	28.01E-03	0.	5.602E+06	0.
26	28	11.02E-03	0.	2.204E+06	0.
27	28	11.02E-03	0.	2.204E+06	0.
27	29	1.157E-03	5.653E-03	231.4E+03	1.131E+06
28	29	1.157E-03	5.653E-03	231.4E+03	1.131E+06
28	30	0.	19.84E-03	0.	3.967E+06
29	30	0.	19.84E-03	0.	3.967E+06
29	31	0.	36.31E-03	0.	7.262E+06
30	4	0.	44.25E-03	0.	8.850E+06
30	31	0.	36.31E-03	0.	7.262E+06
Minimum		0.	0.	0.	0.
At Element		30	27	30	27
Node		4	28	4	28
Maximum		83.48E-03	166.0E-03	16.70E+06	33.21E+06
At Element		21	5	21	4
Node		2	8	2	8

Field Output reported at element nodes for region: PART-1-1.Region_2

Element Label	Node Label	E.Max. Prin @Loc 1	E.Max. Prin @Loc 2	S.Max. Prin @Loc 1	S.Max. Prin @Loc 2
11	2	41.22E-03	0.	8.245E+06	0.
11	14	52.84E-03	0.	10.57E+06	0.
12	14	52.84E-03	0.	10.57E+06	0.
12	15	70.97E-03	0.	14.19E+06	0.
13	15	70.97E-03	0.	14.19E+06	0.
13	16	77.84E-03	0.	15.57E+06	0.
14	16	77.84E-03	0.	15.57E+06	0.
14	17	72.33E-03	0.	14.47E+06	0.
15	17	72.33E-03	0.	14.47E+06	0.
15	18	55.34E-03	0.	11.07E+06	0.
16	18	55.34E-03	0.	11.07E+06	0.
16	19	29.61E-03	0.	5.922E+06	0.
17	19	29.61E-03	0.	5.922E+06	0.
17	20	7.507E-03	9.509E-03	1.501E+06	1.902E+06
18	20	7.507E-03	9.509E-03	1.501E+06	1.902E+06
18	21	0.	33.29E-03	0.	6.659E+06
19	21	0.	33.29E-03	0.	6.659E+06
19	22	0.	58.10E-03	0.	11.62E+06
20	3	0.	68.64E-03	0.	13.73E+06
20	22	0.	58.10E-03	0.	11.62E+06
Minimum		0.	0.	0.	0.
At Element		20	17	20	17
Node		3	19	3	19
Maximum		77.84E-03	68.64E-03	15.57E+06	13.73E+06
At Element		13	20	13	20
Node		16	3	16	3